



MARMARA UNIVERSITY
FACULTY OF ENGINEERING



Computerized Multibody Analysis of Structural Behaviours Resulting from Dynamic Conditions of Linear Vibrating Feeders and Design Improvements

EFEKAN ŞENCAN, YAKUP TANER TAŞDELEN

GRADUATION PROJECT REPORT

Department of Mechanical Engineering

Supervisor

Prof. Dr. Paşa YAYLA

ISTANBUL, 2024



MARMARA UNIVERSITY
FACULTY OF ENGINEERING



**Computerized Multibody Analysis of Structural Behaviours Resulting
from Dynamic Conditions of Linear Vibrating Feeders and Design
Improvements**
Efekan ŞENCAN
Yakup Taner TAŞDELEN

June, 2024, Istanbul

**SUBMITTED TO THE DEPARTMENT OF MECHANICAL ENGINEERING IN PARTIAL
FULFILLMENT OF THE REQUIREMENTS FOR THE DEGREE**

**OF
BACHELOR OF SCIENCE
AT
MARMARA UNIVERSITY**

The authors hereby grant Marmara University permission to reproduce and to distribute publicly paper and electronic copies of this document in whole or in part and declare that the prepared document does not in any way include copying of previous work on the subject or the use of ideas, concepts, words, or structures regarding the subject without appropriate acknowledgement of the source material.

Signature of Author(s) **Efekan ŞENCAN** **Yakup Taner TAŞDELEN**

Department of Mechanical Engineering

Certified by **Prof.Dr. Paşa YAYLA**
Project Supervisor, Department of Mechanical Engineering

Accepted by **Prof.Dr. Bülent EKİCİ**

Head of the Department of Mechanical Engineering

ACKNOWLEDGEMENTS

We would like to extend our sincere thanks to our advisor Prof. Dr. Paşa YAYLA for enabling the realization of this study. His guidance and advice have directed us at every stage of our thesis. His insights and mentorship have contributed to the development of our critical thinking skills and have improved our methods for solving complex engineering problems. Additionally, we would like to express our gratitude to the committee members for permitting our defence and for their thoughtful comments and suggestions.

We thank Özge GÜLER, the Research and Development Manager at Burçelik Bursa Çelik Döküm Sanayi A.Ş., for her continuous support and collaboration.

Furthermore, we would like to thank TÜBİTAK for providing financial support and materials for our project within the scope of the 2209-A University Student Research Projects Support Program.

CONTENTS

ACKNOWLEDGEMENTS	iii
CONTENTS	iv
ÖZET	vi
ABSTRACT	vii
SYMBOLS	viii
ABBREVIATIONS	ix
LIST OF FIGURES	x
LIST OF TABLE	xiv
1 INTRODUCTION.....	1
1.1 Background	1
1.2 Problem Statement	1
1.3 Literature Review.....	2
1.3.1 Vibratory Feeder.....	2
1.3.2 CAD of Vibratory Feeder	4
1.3.3 Static Analysis of Vibratory Feeder.....	5
1.3.4 Modal Analysis of Vibratory Feeder	6
1.3.5 Mathematical Background	7
1.3.6 Transient Structural Analysis of Vibratory Feeder	9
1.3.7 Fatigue Life Analysis of Vibratory Feeder	9
1.4 Scope of Research	11
2 Practical Investigation.....	12
2.1 CAE Software	12
2.2 Selecting ANSYS	14

2.3	Geometry Cleaning	14
3	Analysis.....	16
3.1	Analysis of First Feeder	16
3.1.1	Static Analysis	18
3.1.2	Modal Analysis.....	27
3.1.3	Transient Structural Analysis	30
3.1.4	Fatigue Life Analysis	37
3.1.5	Effect of Meshing Process on Analysis	38
3.2	Analysis of Second Feeder.....	39
3.2.1	Static Analysis	41
3.2.2	Modal Analysis.....	47
3.2.3	Transient Structural Analysis	49
3.2.4	Fatigue Life Analysis	53
3.2.5	Effect of Feeder Meshing and Convergence Study on Analysis	54
4	Result and Discussion	55
4.1	Conclusion of Thesis	55
4.2	Recommendations for Future Works.....	60
4.3	Evaluation of Current Work from MUDEK Perspective	61
4.3.1	Economic Analysis.....	61
4.3.2	Real-Life Conditions	62
	REFERENCES.....	63
	APPENDICES.....	66

ÖZET

Titreşimli besleyiciler, malzeme taşıma uygulamalarında yaygın olarak kullanılmaktadır ve malzeme transferini kolaylaştırarak birçok endüstride kritik bir rol oynamaktadır. Bu makale, statik ve dinamik aşamalardaki stres değişimlerini ayırtırmayı hedefleyen deneysel bir araştırmayı ele almaktadır.

Bu araştırma makalesi, belirli bir titreşimli besleyici tipinin stres ve deformasyon davranışlarını sonlu elemanlar yöntemi ile yorgunluk oluşumlarını tespit ederek ve yorulma bölgelerini analiz ederek potansiyel kırılmaları önceden engellemekte ve tasarımcılara önemli bilgiler sunmaktadır. Ayrıca, bu makale titreşimli besleyici teknolojisinin temel prensiplerini, tasarıminının önemi ve tasarım sırasında dikkat edilmesi gereken gerilme ve yıgılma bölgelerini tespitini kolaylaştırılmasına olanak sağlamaktadır.

ABSTRACT

Vibratory feeders play a vital role in facilitating the transfer of materials in numerous industries. Achieving the ideal material flow rate is dependent on the efficient operation of the feeder. This thesis addresses an experimental investigation aimed at distinguishing stress variations experienced during static and dynamic phases. The vibrating feeder and the loads applied to it were examined using the ANSYS software.

Vibratory feeders are widely used in material handling applications across various industries. This thesis examines the stress and deformation problems of a specific type of vibratory feeder. Additionally, it elucidates the theory behind vibratory feeder technology and underscores the importance of its design.

The finite element method detects these fatigue issues and analyses fatigue zones, preventing potential fractures and providing insights to shape and strengthen our design.

SYMBOLS

<u>Symbol</u>	<u>Name</u>	<u>Unit</u>
A	Area	m^2
C	Damping coefficient	$\text{kg}\cdot\text{m}^{-1}\cdot\text{s}^{-1}$
C_{eq}	Equivalent damping coefficient	$\text{kg}\cdot\text{m}^{-1}\cdot\text{s}^{-1}$
F	Force	$\text{kg}\cdot\text{m}\cdot\text{s}^{-2}$
$f(t)$	Force as a function of time	$\text{kg}\cdot\text{m}\cdot\text{s}^{-2}$
G	Shear modulus	$\text{kg}\cdot\text{m}^{-1}\cdot\text{s}^{-2}$
k	Stiffness coefficient	$\text{kg}\cdot\text{s}^{-2}$
l	Stretched spring length	m
l_0	Unstretched spring length	m
Δl	Change in length	m
m	Mass	Kg
x	Displacement	m
γ	Shear strain	
$\Delta\gamma$	Change in shear strain	
E	Young's modulus	$\text{kg}\cdot\text{m}^{-1}\cdot\text{s}^{-2}$
ϵ	Strain	
$\Delta\epsilon$	Change in strain	
σ	Stress	$\text{kg}\cdot\text{m}^{-1}\cdot\text{s}^{-2}$
$\Delta\sigma$	Change in stress	$\text{kg}\cdot\text{m}^{-1}\cdot\text{s}^{-2}$
r	Shear stress	$\text{kg}\cdot\text{m}^{-1}\cdot\text{s}^{-2}$
Δr	Change in shear stress	$\text{kg}\cdot\text{m}^{-1}\cdot\text{s}^{-2}$
ω_F	Operating frequency	$\text{rad}\cdot\text{s}^{-1}$

ABBREVIATIONS

FEA: Finite Element Analysis

FEM: Finite Element Method

SQP: Sequential Quadratic Programming

SDOF: Single Degree of Freedom

LIST OF FIGURES

Figure 1.1:Optimization process	3
Figure 1.2: Dynamic design process of a vibrating screen	4
Figure 1.3: The system dynamics of vibrating feeder (Chandravanshi, 2015)	8
Figure 1.4: Vibratory feeder (Singh,2022)	9
Figure 2.1: CAE software's tree	13
Figure 2.2: ANSYS working principle (McMilan,2011)	14
Figure 3.1: Opening SpaceClaim on ANSYS Workbench	16
Figure 3.2: Isometric view of first feeder.....	16
Figure 3.3: Top view of first feeder.....	17
Figure 3.4: Left view of first feeder	17
Figure 3.5: Bottom view of first feeder.....	17
Figure 3.6: Grilles before removing bolted connections.....	18
Figure 3.7: Grilles after removing bolted connections.....	18
Figure 3.8: The appearance of the springs in the data sent by BURÇELIK.	19
Figure 3.9: New image of springs created with ANSYS.....	19
Figure 3.10: Test report of springs of BURÇELIK	19
Figure 3.11: Display of changed springs on the draft in ANSYS and display of the detail tab.	20
Figure 3.12: Protective elements used only to prevent any damage during transportation. (green coloured parts).....	20
Figure 3.13: After removing protective elements.....	20
Figure 3.14: Bottom side of feeder before removing vibro motors	21
Figure 3.15: Bottom side of feeder after removing vibro motors	21
Figure 3.16: Properties of material.....	21

Figure 3.17: Properties of feeder.....	22
Figure 3.18: Example of contact controlling.....	22
Figure 3.19: Details about one of the contact.....	23
Figure 3.20: Ideal mesh view of vibrating feeder	23
Figure 3.21: Details of mesh	23
Figure 3.22: Local mesh.....	24
Figure 3.23: Example of local mesh (multizone)	24
Figure 3.24: Boundary conditions of feeder.....	25
Figure 3.25: Fixed supports of feeder	25
Figure 3.26: Static analysis - total deformation	26
Figure 3.27: Static analysis - equivalent (von-mises) stress	27
Figure 3.28: Static analysis – spring probe	27
Figure 3.29: Technical data of vibro motor - 1.....	30
Figure 3.30: Technical data of vibro motor – 2	31
Figure 3.31: Exciting force (centrifugal force) directions at four special moments. Respectively (left to right), reverse and inward direction, same direction and forward, reverse and outward, same direction and backwards (Ningning Xu et al., 2021)	31
Figure 3.32: Boundary conditions of transient structural analysis	32
Figure 3.33: Result of transient structural analysis (equivalent stress)	35
Figure 3.34: Result of transient structural – fatigue tool (life).....	38
Figure 3.35: Graph of maximum stress (von-misses) vs number of nodes.....	38
Figure 3.36: Isometric view of second feeder.	39
Figure 3.37: Top view of second feeder.	39
Figure 3.38: Left view of second feeder.....	40
Figure 3.39: Bottom view of second feeder.	40

Figure 3.40: Illustration of the support that has been added.	40
Figure 3.41: Reinforced version of the intermediate circular part.	41
Figure 3.42: Display of geometric and structural changes made on feeder 2.	42
Figure 3.43: Sample contact control for the second feeder.	42
Figure 3.44: Ideal mesh view of vibrating feeder.....	43
Figure 3.45: Details of 'mesh' of second vibrating feeder.	43
Figure 3.46: Details of 'multi-zone 4.'	44
Figure 3.47: Boundary conditions of second feeder	44
Figure 3.48: Fixed support is shown of second feeder.	45
Figure 3.49: Static analysis of second feeder- total deformation.	46
Figure 3.50: Static analysis of second feeder -equivalent (von-Mises) stress.....	46
Figure 3.51: Static analysis of second feeder - spring probe	47
Figure 3.52: Boundary conditions of transient structural analysis for second feeder.	50
Figure 3.53: Result of transient structural analysis for second feeder (equivalent stress-time:0.165 s).....	51
Figure 3.54: Result of transient structural – fatigue tool (life).....	53
Figure 3.55: Graph of maximum stress (von-misses) vs number of nodes.....	54
Figure 4.1: Broken area of the first feeder	55
Figure 4.2: Max stress values in the fractured area (first feeder on the left, second feeder on the right).	56
Figure 4.3: Details of 'fatigue tool.'	58
Figure 4.4: S-N diagram.....	58
Figure 4.5: Fatigue life result values in the fractured area (first feeder on the left, second feeder on the right).	59
Figure 4.6: Project schematic of both feeders	60

Figure A1: Quality certificate of springs	66
Figure A2: Technical drawing of spring	67
Figure A3: Experiment report of springs.....	68
Figure A4: Technical data of vibro motor	69
Figure A5: Technical data of vibro motor	70
Figure A6: Technical data of vibro motor	71
Figure A7: Technical data of vibro motor	72

LIST OF TABLE

Table 3.1: Modal analysis.....	28
Table 3.2: Tabular data of force 6.....	32
Table 3.3: Tabular data of force 7 (force 8 have same tabular data but opposite direction)	33
Table 3.4: Result of transient structural analysis (equivalent stress)	35
Table 3.5: Modal analysis of second feeder.	48
Table 3.6: Result of transient structural analysis.....	51

1 INTRODUCTION

This study, which focuses on vibrating feeders, is divided into four main portions. This study provides a thorough assessment of the issue by comparing different literature studies. The first portion provides information about feeder models, optimization, and operation, with an emphasis on the research's aim. The first chapter gives guidance for the study by providing the groundwork for future chapters. Furthermore, the first chapter discusses the FEM method's influence on research, as well as the possibilities and limitations of simulation's role in mistake detection. In the second phase, computer-aided engineering software was compared, and the best one was chosen. The third part explains the findings of the nutritional analyses and shows the adjustments made to the analyses. The analysis results are also compared in this section. The final portion discusses the economic and manufacturing benefits, as well as the study's findings.

1.1 Background

In industrial and mining operations, vibrating feeders are critical for material processing. It employs vibration to "feed" material to a process or machine. Key components are a vibratory drive unit, vibratory feeder bowl, amplitude controller, and inline feeder and track. However, excessive vibration can cause vibratory feeders to malfunction, reducing their performance and dependability.

1.2 Problem Statement

Recently, there has been an extensive effort to improve the efficiency and geometry of vibratory feeders. This increased focus displays a clear desire to improve performance. Despite numerous attempts to optimize vibratory feeders, additional study is needed to investigate the possibilities of using a feeder model to offer insights into its performance and help in the detection of defects or damages. This study gap opens up a great opportunity for future discovery and analysis.

1.3 Literature Review

The literature study is organized into seven sub-topics covering various branches of vibratory feeders. This part gives a thorough grasp of the issue and contrasts previous and current publications.

The first topic covers the design, operation, and optimization of feeders. It also introduces the FEM approach and its use in feeders, which will be covered in greater detail later in the thesis. This chapter establishes a firm basis for the subsequent chapters by detailing the technique and its functioning. The second study topic illustrates the significance of the Finite Element Method (FEM) model in the thesis and discusses Computer-Aided Design .The third study subject depicts the static analysis of vibrating feeders. The other research topic represents the static analysis of vibrating feeders. The fifth study subject displays the modal analysis of vibrating feeders. The final two research subjects show the transient structural analysis and fatigue life analysis of vibrating feeders.

1.3.1 Vibratory Feeder

This chapter discusses vibratory feeders, focusing on the important components necessary for R&D. The topics addressed include error identification, modelling approaches, and the vibrating feeder optimization process.

The primary process for designing vibrating screens begins with simulating the feeder using Finite Element Method (FEM) software. Running the feeder modelling in a FEM environment allows for parameter changes without the need to create a new feeder for each design iteration. Building a FEM model is a cost-effective and straightforward replacement for establishing settings in a real feeder. The process for creating a FEM model for the feeder may be used to improve material handling efficiency as well as to simulate defects in vibrating feeders. The following FEA analysis types are being used: static analysis, modal analysis, harmonic analysis, temporal dynamic analysis, spectrum analysis, buckling analysis, and open dynamic analysis (Ramatsetse et al., 2017).

Full research was carried out utilizing ANSYS, a cutting-edge engineering analysis program that included modal and harmonic response analysis. These thorough analyses produced an abundance of dynamic data. Among the crucial insights revealed were natural frequencies, complicated mode forms, and stress and strain distribution across the structure. This innovative study has cleared the door for a new understanding of the vibrating feeder's behaviour.

Optimization is a mathematical strategy for determining the lowest or greatest values of given functions while taking into account a set of constraints or criteria. When it comes to design, optimizing machine components is a critical step that leads to high-quality goods while reducing costs. This method is commonly used to improve vibrating feeder designs, optimize frequency, and increase productivity (Csizmadia et al., 2011; Wang et al., 2012), resulting in smooth and efficient operation. The steps of optimization shown are in Figure 1.1.

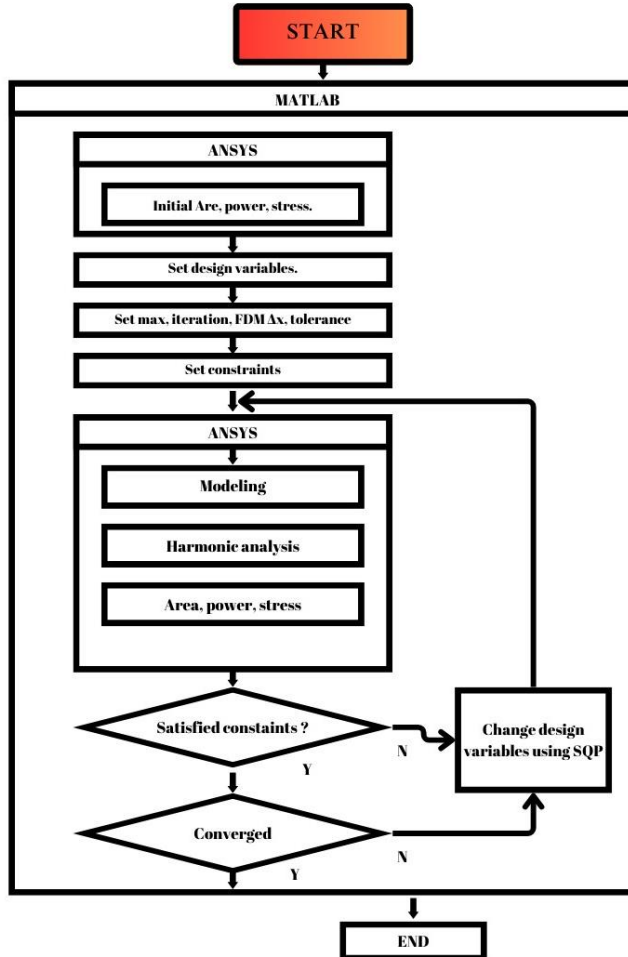


Figure 1.1: Optimization process

Optimizing vibratory feeders is simple: increase profitability ('Vibration Analysis of Vibrating Screens', 2012). Several ways are used to improve the efficiency of vibratory feeders, including lowering energy consumption, increasing output, reducing downtime, and simplifying maintenance. Yue-Min et al. (2009) found that adjusting the size of the stiffeners on the side plate while accounting for different frequency limits improved the dependability of vibrating screens. This modification lowered the weight of the side plates, resulting in an increase in natural frequencies, thereby shifting them away from the operational frequency. Production expenses have dropped as the screen's weight has decreased. Moving the natural frequency

further from the operational frequency also enhanced resonance avoidance, which reduced the risk of screen damage. Manufacturing expenses were decreased by lowering the weight of the screen. Furthermore, shifting the natural frequency away from the operational frequency increased resonance avoidance, reducing possible screen damage.

1.3.2 CAD of Vibratory Feeder

CAD techniques offer significant advantages in the design and optimization of vibratory feeders. Finite Element Analysis (FEA) has emerged as a powerful tool for simulating the structural and dynamic behaviour of feeder components under various operating conditions (Wang et al., 2019). FEA allows engineers to predict stresses, displacements, and natural frequencies, facilitating the identification of potential design flaws and optimization opportunities.

In addition to FEA, Multibody Dynamics (MBD) simulations have gained traction in the field of vibratory feeder design. MBD enables the modelling of complex interactions between moving parts, such as the feeder tray, springs, and excitors, providing insights into system performance and efficiency (Li & Zhang, 2021).

The vibrating screens have had a fast development in the last 30 years, so they require a higher standard design with the equipment's upsizing. Compared to conventional static design, the dynamic design method can reveal the distribution of the dynamic stress in the main structure exactly and ensure the rationality of structure design. The goal of the dynamic design for the large vibrating screens was to make it work more reliably and more long and to maintain the economic and technical indexes during normal operation at the same time. The process of the dynamic design was shown in Figure 1.2 (Zhang, Y. L., Liu, X. P., & Hou, C. L., 2015).

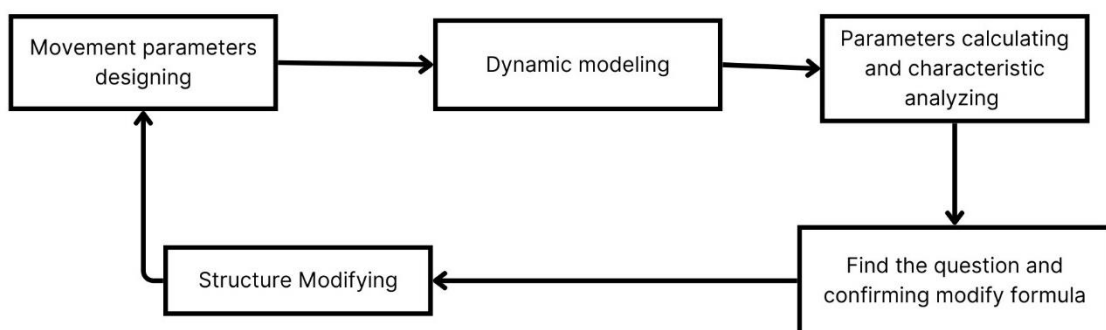


Figure 1.2: Dynamic design process of a vibrating screen

Despite significant advancements, several challenges persist in the field of CAD for vibratory feeders. Accurately modelling complex material behaviour, accounting for nonlinearities, and integrating real-time control algorithms remain areas of active research. Furthermore, there is a growing interest in leveraging emerging technologies, such as artificial intelligence and additive manufacturing, to enhance the design and manufacturing processes of vibratory feeders.

In conclusion, the literature reviewed underscores the importance of CAD techniques in the design and optimization of vibratory feeders. Through advanced simulation tools and optimization strategies, engineers can develop robust and efficient feeder systems tailored to specific application requirements. Continued research efforts are essential to address existing challenges and unlock new opportunities for innovation in this field.

1.3.3 Static Analysis of Vibratory Feeder

Static analysis involves studying the behaviour of vibratory feeders under static loading conditions, typically focuses on aspects such as structural integrity, deflection, stress distribution, and material deformation. By analysing these factors, engineers can assess the mechanical performance and safety of feeder components.

Analytical methods play a fundamental role in the static analysis, offering insights into the behaviour of vibratory feeders without the need for complex simulations. Classical engineering principles, such as beam theory and finite element methods, are often employed to derive analytical expressions for stress, deflection, and natural frequency (Ramatsetse, B., Mpofu, K., & Makinde, O., 2017). These analytical models serve as valuable tools for preliminary design and theoretical validation.

Finite Element Analysis (FEA) has emerged as a powerful tool for simulating the static behaviour of vibratory feeders in detail. FEA enables engineers to model complex geometries, material properties, and loading conditions with high fidelity, allowing for accurate prediction of stress, displacement, and deformation (Guo, N. Q., Liu, W., & Huang, W. P., 2012). Parametric studies within FEA frameworks facilitate sensitivity analysis, identifying critical design parameters and optimization opportunities.

Properly defining boundary conditions and constraints is critical for obtaining meaningful results in static analysis. In vibratory feeder systems, boundary conditions may include fixed supports, contact interfaces, and external loads applied to feeder trays and structural components (Rumiche, F., Noriega, A., Lean, P., & Fosca, C., 2020). Careful consideration of

these boundary conditions ensures realistic simulation of operational scenarios and enhances the validity of static analysis results.

Despite significant advancements, several challenges persist in the static analysis of vibratory feeders. Integrating realistic material models, accounting for geometric nonlinearities, and addressing the effects of dynamic loading on static behaviour remain areas of ongoing research (He, W. F., & Xian, A. M., 2013). Furthermore, there is a growing interest in exploring advanced simulation techniques, such as coupled multi-physics simulations, to capture the coupled effects of static and dynamic loading in vibratory feeder systems.

In conclusion, the literature reviewed highlights the importance of static analysis in optimizing the design and performance of vibratory feeders. Analytical methods and finite element simulations provide valuable insights into the structural integrity and mechanical behaviour of feeder components under static loading conditions. Continued research efforts are essential to address existing challenges and advance the state-of-the-art in static analysis techniques for vibratory feeders.

1.3.4 Modal Analysis of Vibratory Feeder

The modal analysis involves the study of vibratory feeder dynamics under dynamic loading conditions, focusing on resonant frequencies, mode shapes, and damping characteristics (Zhang, L. W., Yin, Z. J., Chen, B., Tang, Z. C., & Tian, Z. 2010)). By characterizing these dynamic properties, engineers can optimize feeder design and mitigate resonance-related issues.

Experimental modal analysis (EMA) is a widely used technique for characterizing the dynamic behaviour of vibratory feeders through physical testing (Chandravanshi, M. L., & Mukhopadhyay, A. K., 2015)). EMA provides valuable insights into natural frequencies and mode shapes, facilitating the validation of numerical models and informing design decisions.

Finite Element Analysis (FEA) offers a powerful approach to modal analysis, enabling engineers to simulate feeder dynamics numerically (Peng, C. Y., & Su, R. H., 2011). FEA allows for investigating various design parameters and operating conditions, providing insights into vibration behaviour and structural response.

Recent studies have focused on analysing variations in vibration behaviour due to changes in feeder components. Chandravanshi and Mukhopadhyay (2017) investigated the impact of

helical spring stiffness on feeder vibration using FEM and EMA methods, highlighting the influence of spring parameters on natural frequencies and mode shapes.

Design optimization is crucial for enhancing feeder performance and efficiency. Zhu, Wang, and Dong (2012) proposed a self-synchronous shaker with balanced elliptical motion, demonstrating improved performance through innovative design features. The proposed shaker design achieved enhanced conveying efficiency and reduced energy consumption by optimising motion characteristics, such as amplitude and frequency.

Finite Element Analysis (FEA) techniques have been applied to diagnose issues in vibratory feeder units. Oraon, Chandravanshi, and Bajpai (2019) utilized FEA to perform diagnostic checks on vibratory feeder units, identifying potential structural weaknesses and recommending design modifications for improved reliability and performance.

Despite significant advancements, challenges remain in the modal analysis of vibratory feeders. Addressing nonlinearities, integrating advanced material models, and enhancing experimental techniques are areas for future research. Furthermore, there is a need for comprehensive validation of numerical models to ensure accurate prediction of feeder dynamics under diverse operating conditions.

In conclusion, modal analysis is a valuable tool for optimizing the design and performance of vibratory feeders. Incorporating recent research findings, such as the impact of spring stiffness on vibration behaviour and innovative design solutions, enhances our understanding of feeder dynamics and informs future developments in this field.

1.3.5 Mathematical Background

The vibratory feeder mathematical model is vital for reflecting the system's behaviour and dynamics. The model encapsulates the vibrating feeder's essential features and gives a mathematical knowledge of its operation, including forced vibration in the Single Degree of Freedom (SDOF) system. Including crucial components like the chute, support structure, coil springs, and engine layout improves the model's authenticity. These components are required for the feeder to function and are essential in determining its behaviour. The device also stands out for its use of a sinusoidal external force to produce vibration. This sort of stimulation is commonly utilized in vibratory feeders and effectively achieves the desired feeding effects. This mathematical model is crucial because it fully models the vibrating feeder system,

including key components, an angled trough, and sinusoidal excitation. Given these considerations, the model is an effective tool for studying and enhancing the performance of vibratory feeders in a variety of applications. The system dynamics of the vibrating feeder are shown in Figure 1.3.

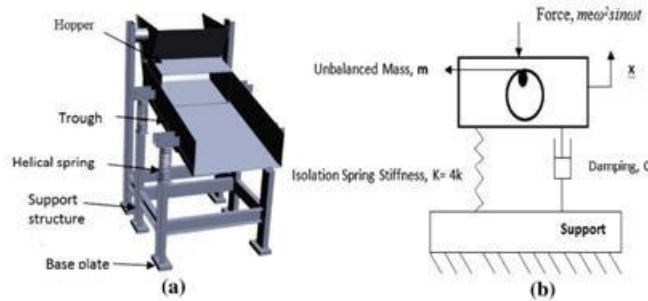


Figure 1.3: The system dynamics of vibrating feeder (Chandravanshi, 2015)

The exciting sinusoidal force may be expressed as $F_o \sin \omega t$, where F_o represents the magnitude of the external excitation force. The equation for force vibration is as follows.

$$M \frac{d^2x}{dt^2} + c \frac{dx}{dt} + Kx = F \sin \omega t$$

Here, M denotes the mass of the trough, which includes the vibratory motor. The inclusion of the vibratory motor in the mass calculation separates this model by accounting for the motor's added weight and dynamics.

K denotes the combined stiffness of the four helical springs on which the trough is installed. The use of helical springs as the supporting mechanism adds uniqueness to the model, as it affects the overall stiffness and response of the system.

K represents the combined stiffness of the four helical springs on which the trough is placed. The inclusion of helical springs as the supporting mechanism adds originality to the model by influencing the overall stiffness and reactivity of the system.

By incorporating these parameters - the mass of the trough including the vibratory motor, the combined stiffness of the helical springs, and the system's damping characteristics - the model captures the specific attributes of the vibratory feeder under consideration, making it unique in its representation and characterization of the system's dynamics.

The springs are first modelled with a completely elastic behaviour (Childs, 2004), with the longitudinal and transversal stiffness given by:

$$D_E \nabla^4 w(x, y, t) + [\rho + m_c \delta(x - u) \delta(y - v)] \frac{\partial^2 w}{\partial t^2} = 0$$

where $D_E = E_Y/(12(1-v^2))$ is the bending stiffness. 3-D system is shown in Figure 1.4 (Singh,2022)

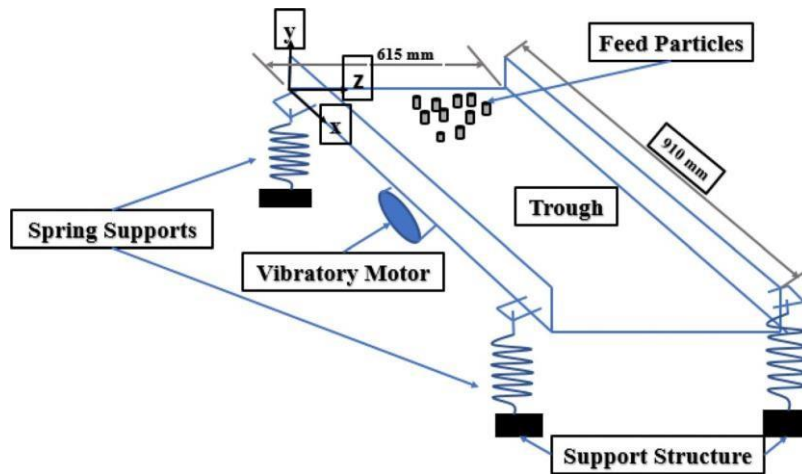


Figure 1.4: Vibratory feeder (Singh,2022)

1.3.6 Transient Structural Analysis of Vibratory Feeder

The transient structural analysis focuses on studying the time-varying behaviour of vibratory feeders under dynamic loading conditions. This analysis is crucial for assessing the structural integrity, dynamic response, and fatigue life of feeder components during start-up, shutdown, and transient operation (Wang & Lin, 2021). Understanding transient behaviour enables engineers to optimize feeder design and mitigate structural failures.

In conclusion, transient structural analysis is essential for optimizing the design and performance of vibratory feeders under dynamic loading conditions. Incorporating recent research findings, such as structural optimization based on inertia release, enhances our understanding of feeder transient behaviour and informs future developments in this field. Continued research efforts are essential to address existing challenges and advance the state-of-the-art in transient structural analysis techniques for vibratory feeders.

1.3.7 Fatigue Life Analysis of Vibratory Feeder

Fatigue life analysis is essential for assessing the structural integrity and durability of vibratory feeders, subjected to cyclic loading during operation. Understanding the fatigue behaviour of these systems is critical for preventing premature failures and ensuring reliable performance.

This literature review provides an overview of research concerning the fatigue life analysis of vibratory feeders, incorporating recent studies and emphasizing key findings, methodologies, and areas for further investigation.

Fatigue life analysis involves predicting the lifespan of vibratory feeders under cyclic loading conditions, considering factors such as material properties, stress concentrations, and operational parameters. By evaluating fatigue damage accumulation, engineers can identify critical components, optimize design features, and implement maintenance strategies to prolong feeder service life.

Finite Element Analysis (FEA) is a powerful tool for conducting fatigue life analysis of vibratory feeders, enabling engineers to simulate cyclic loading and assess structural response (Wang et al., 2010). FEA allows for the prediction of stress distribution, fatigue crack initiation, and propagation, facilitating the estimation of component lifespan and the identification of fatigue-prone regions.

Recent studies have investigated fatigue life analysis in various types of vibrating equipment, providing valuable insights into structural behaviour and failure mechanisms. Hou, Fang, and Zeng (2012) conducted finite element analysis of a dual-frequency vibrating screen, highlighting the importance of stress concentration analysis and fatigue life prediction in optimizing screen design and enhancing reliability.

Wang, Y. Y., Fu, X. H., Guo, T. T., Chen, L., and Mao, H. Q. (2010) explored the fatigue life analysis of a large-scale liner vibration screener based on ANSYS. Their study emphasized the significance of accurately modelling material properties, loading conditions, and boundary constraints for reliable fatigue life predictions. By integrating FEA with experimental validation, the authors provided valuable insights into fatigue failure mechanisms and proposed design improvements to extend the screener's service life.

In conclusion, fatigue life analysis is a critical aspect of vibratory feeder design and optimization, ensuring structural reliability and longevity. By integrating finite element analysis with experimental validation, engineers can accurately predict fatigue damage accumulation, identify critical failure modes, and implement proactive maintenance strategies to enhance feeder performance and durability.

1.4 Scope of Research

In this important document, we carry out an extensive study with a knockout machine serving as the main focus of attention. We wish to perform an extensive evaluation on the vibratory feeder, looking at stress distribution and deformation under static and dynamic loads. Specifically, during high-intensity loads, the vibrating feeder experiences intense vibrations, which increases the risk of fatigue failure. Due to its exclusive shape and structure, current design methodologies need to be modified in order to accurately quantify the resulting stress levels.

2 Practical Investigation

Studies were carried out on regional ruptures resulting from the static and dynamic states of the feeder in order to collect information about the strength and deformations under force. These measurements were made to test the load capacity of the relevant machine and to calculate its life. Determining the maximum voltage acting on the machine without experiencing any durability problems and supporting this with computerized analysis.

Vibrational equipment structures must be extremely strong since they are subjected to enormous dynamic forces, and poor design can result in early failure. Metal fatigue, caused by continual dynamic loading and finally leading to cracking and catastrophic failure under high pressures, requires a full understanding of the vibratory system and the loads it transfers to its supporting structure. Specifically, the forces generated by a vibratory feeder provide a substantial problem, necessitating an unusually strong support structure capable of withstanding dynamic stresses that exceed static values (McMilan, 2011).

This section of the thesis is organized into two sub-titles. The first section describes how and why the ideal program for fatigue, cracking, and stress analysis was chosen. The second section discusses the importance of the basic preparations made at the start of the analysis in this program, as well as what has been done in general.

2.1 CAE Software

Computer-Aided Engineering (CAE) is a complete technique that uses computer software to simplify engineering analytical duties. Its major objective is to simulate and assess the behaviour of engineering designs and systems prior to actual construction. CAE software provides a variety of analysis techniques, including structural, thermal, and fluid dynamics.

Engineers utilize CAE to construct virtual prototypes of items or systems and test them under simulated operational circumstances. This enables the comparison of various design possibilities, the detection of possible concerns, and the refining of designs to improve performance, reliability, and efficiency.

CAE software frequently interfaces smoothly with Computer Aided Design (CAD) software, allowing engineers to easily move geometry data from CAD models to CAE simulations. This

integration speeds the design process and guarantees that simulations are based on correct geometry.

The advantages of CAE include decreased development time and cost by eliminating the need for physical prototypes, increased product quality and dependability through early identification and resolution of design flaws, and the opportunity to investigate a broader variety of design choices.

CAE finds applications in a variety of sectors, including automotive, aircraft, civil engineering, electronics, and manufacturing. It plays an important role in the design and development of cars, aeroplanes, consumer electronics, industrial machinery, and other products. Overall, CAE is a strong tool that allows engineers to improve product design, optimize performance, and quickly implement novel ideas. When considering factors such as the number of elements or nodes it can handle, maximum model size, and any limitations on the geometry or meshing capabilities, ANSYS is the best choice among them. CAE software's tree is shown in Figure 2.1.

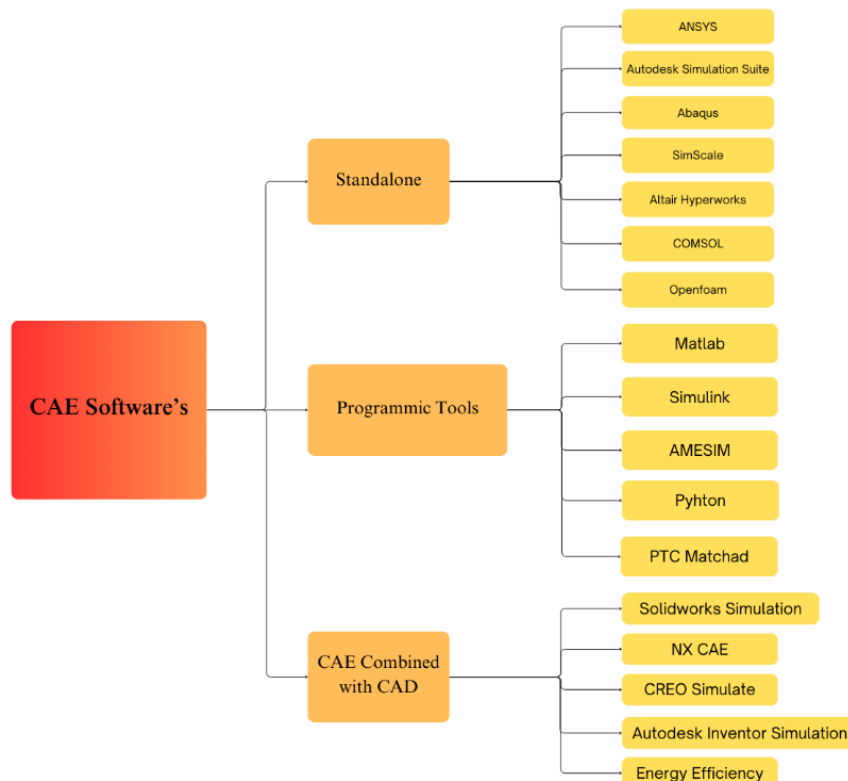


Figure 2.1: CAE software's tree

2.2 Selecting ANSYS

ANSYS is a software for designing mechanical products and analysing civil structures. It addresses problems utilizing computer-based numerical methods. It is ANSYS Inc.'s finite element analysis software. It is often used in business to analyse solutions. It can solve a wide range of difficulties. It helps with the engineering and development of complex, highly nonlinear, large models. It is used to excite computer models of structures, electronics, or machine components in order to analyse strength, elasticity, and temperature. The ANSYS Workbench system is utilized for the vast bulk of its stimulation. It also develops data management and backup software. The working principle of ANSYS is shown in Figure 2.2.

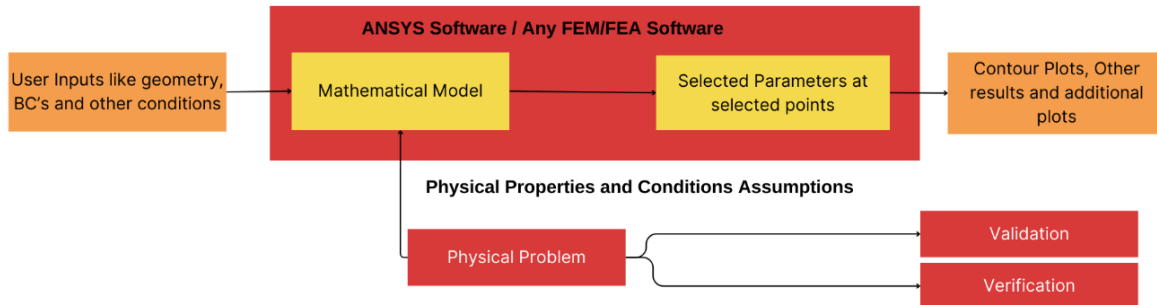


Figure 2.2: ANSYS working principle (McMilan, 2011)

The primary advantages of adopting ANSYS in this model are that it accurately executes complex simulations, optimizes many characteristics such as geometry boundary conditions, and can import and run models from multiple CAD applications. Furthermore, ANSYS offers powerful meshing tools that allow users to generate high-quality models for accurate simulations. It supports structured, unstructured, and hybrid meshing approaches, as well as automatic mesh adaptation for increased accuracy and efficiency. This allows us to manually pick the mesh that is most suited to the parts, improving the solution's dependability.

2.3 Geometry Cleaning

When using ANSYS or any other CAE tool, geometry cleaning and import are crucial steps in the analysis process. Clean and exact geometry gives reliable and valid analytical results, whilst proper import ensures that the model is appropriately represented. These procedures increase computing efficiency, allow for accurate boundary condition application, simplify simulation setup, and improve result interpretation. When geometry is not cleaned prior to analysis, it becomes difficult to create a mesh. Mesh algorithms rely on clearly defined and connected

surfaces, edges, and vertices. Unclean geometry can lead to improperly formed parts, the use of several element types, or even complete mesh generation failure. As a result, accuracy may suffer, convergence may be harder to achieve, or analysis may need more computing power. Finding computers capable of managing the resulting complex and time-consuming mesh is also challenging.

The analysis part includes geometry cleaning and other analysis preparations performed before each analysis in the model.

3 Analysis

BURCELİK designed two feeder designs using CAD software. The rationale for having two is that there were some issues when the first feeder was manufactured and shipped to the company's client. Therefore, the second design was created with small changes based on customer input. The issues were resolved in the second design. The main purpose is to do extensive static and dynamic evaluations using two ANSYS feeds.

The two feeder designs were sent as files with .stp extension. First, these .stp files were opened with the help of the SpaceClaim service of ANSYS.

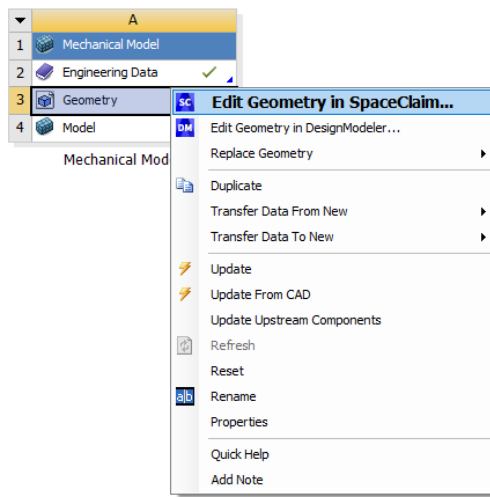


Figure 3.1: Opening SpaceClaim on ANSYS Workbench

3.1 Analysis of First Feeder

First, the first feeder design was revealed on the SpaceClaim service. Views of the feeder shown in Figure 3.2, Figure 3.3, Figure 3.4 and Figure 3.5.

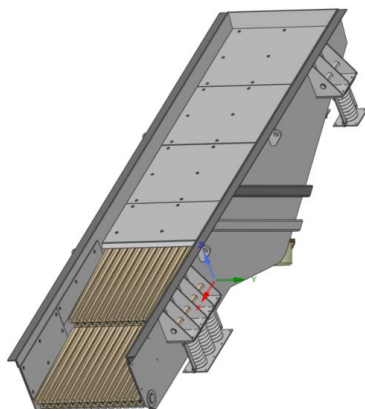


Figure 3.2: Isometric view of first feeder

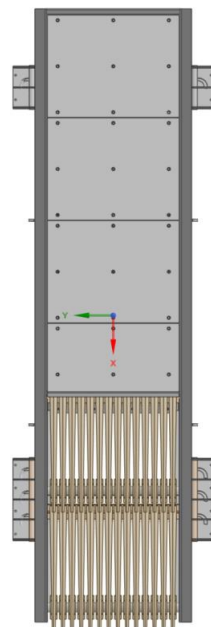


Figure 3.3: Top view of first feeder

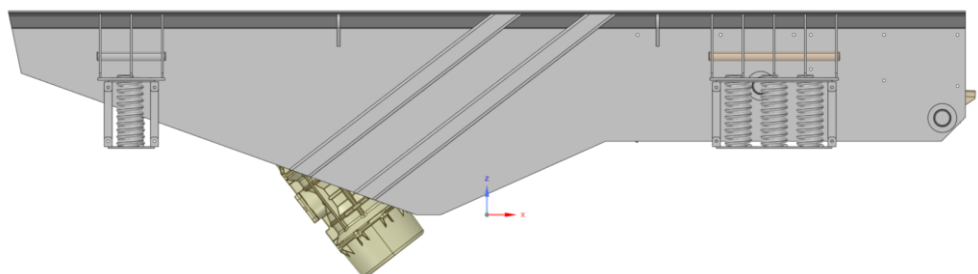


Figure 3.4: Left view of first feeder

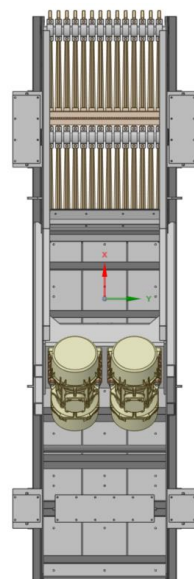


Figure 3.5: Bottom view of first feeder

3.1.1 Static Analysis

3.1.1.1 Preparations for Static Analysis

In order for stress assessments to be made accurately in both feeder configurations, some preparations had to be made. The preparations of both feeders are the same. It will be useful to compare the differences in the results under the same boundary conditions.

To ensure that the mesh procedure was completed accurately and without mistakes, a technique known as geometry cleaning was initially undertaken. The minimization of elements that may impact the meshing process is critical in this procedure known as geometry cleaning. As a first step in geometry, all bolt connections on the geometry were removed. The refinement shown in Figure 3.6 and Figure 3.7.

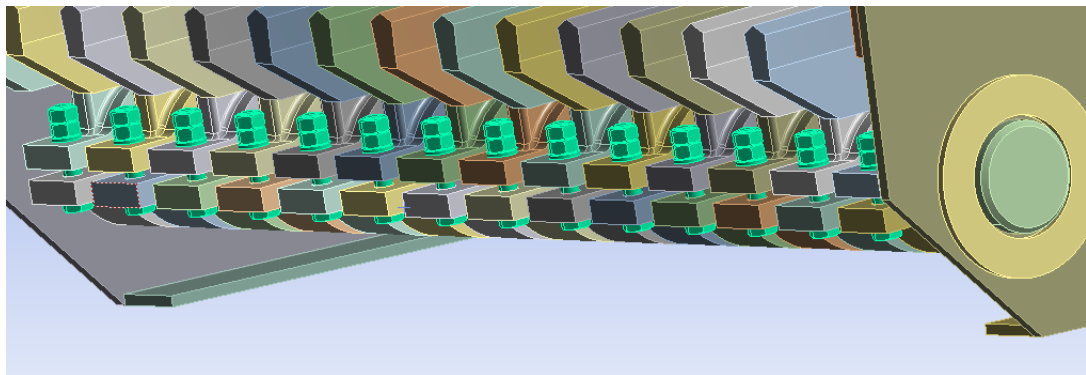


Figure 3.6: Grilles before removing bolted connections

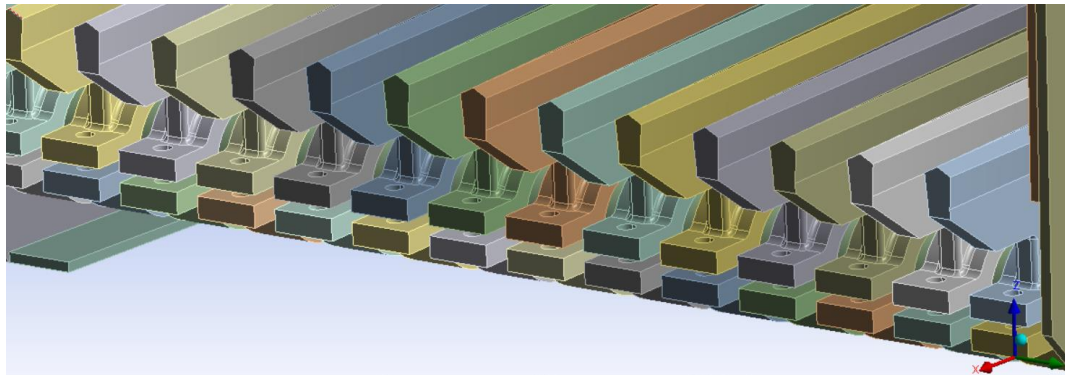


Figure 3.7: Grilles after removing bolted connections

The next step was to remove the springs on CAD and add springs via ANSYS so that we could enter the spring constant of the springs. This step is shown in Figure 3.8 and Figure 3.9

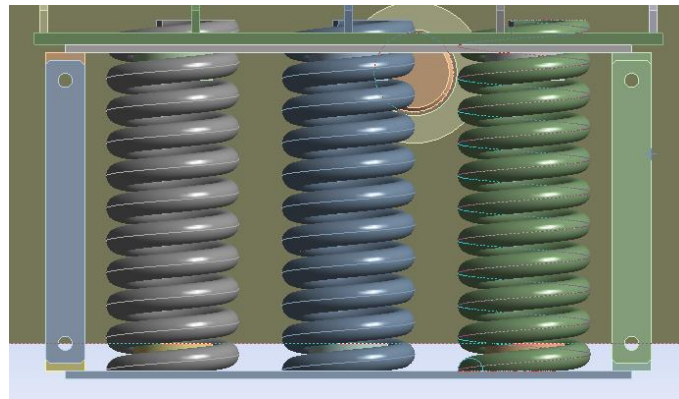


Figure 3.8: The appearance of the springs in the data sent by BURÇELIK.

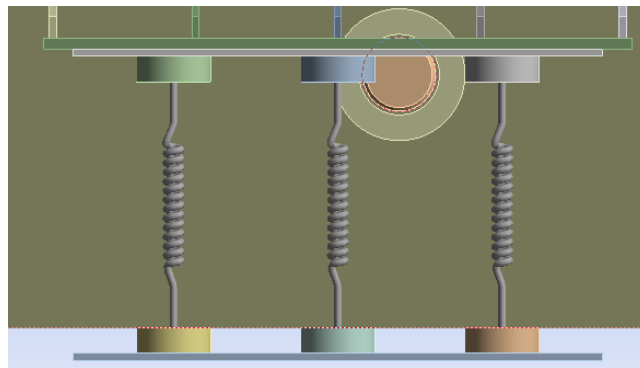


Figure 3.9: New image of springs created with ANSYS.

The data obtained from the tests carried out for the springs sent by BURÇELIK were entered into the necessary values on ANSYS is shown in Figure 3.10, Figure 3.11 and Figure A3. In addition, quality certificate and technical drawing of spring are shown in Figure A1 and Figure A2.

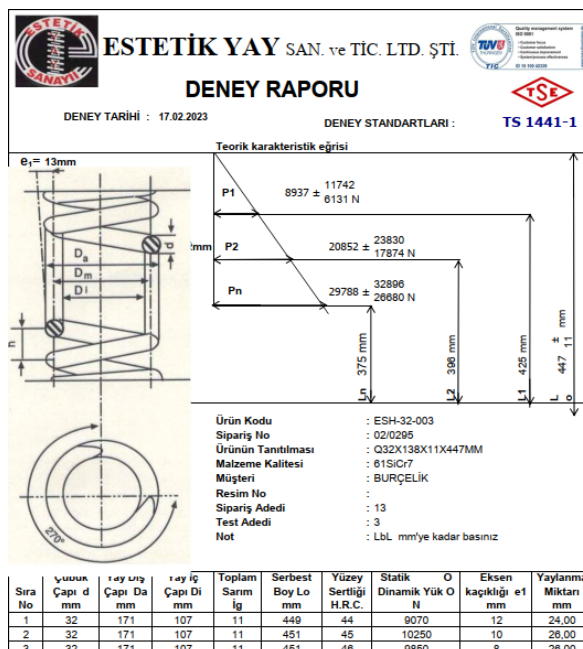


Figure 3.10: Test report of springs of BURÇELIK

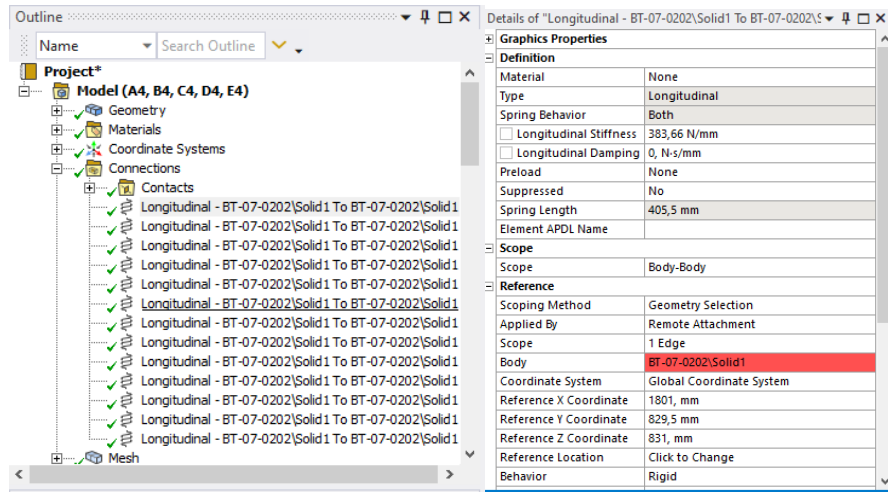


Figure 3.11: Display of changed springs on the draft in ANSYS and display of the detail tab.

A third change is the removal of the protective elements in the design, which were used only to prevent any damage during transportation. This removing process is shown in Figure 3.12 and Figure 3.13.

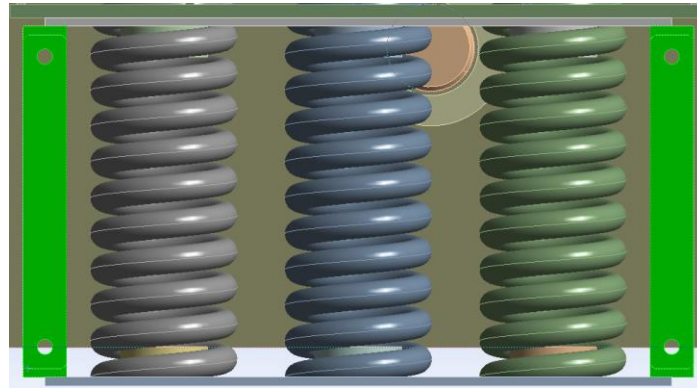


Figure 3.12: Protective elements used only to prevent any damage during transportation.
(green coloured parts)

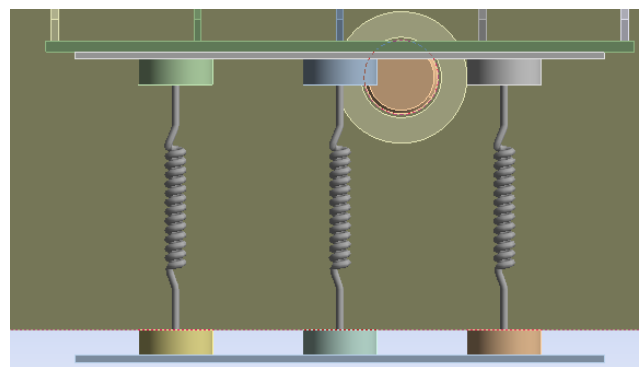


Figure 3.13: After removing protective elements.

Fourthly, vibro motors, which were present in the design and caused difficulties in the construction of the mesh, were removed. These changes are shown in Figure 3.14 and Figure 3.15.

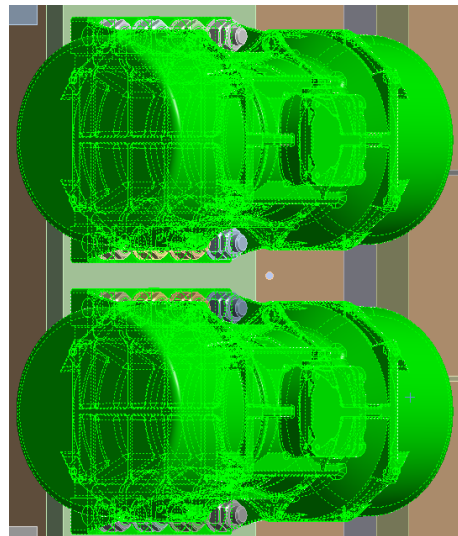


Figure 3.14: Bottom side of feeder before removing vibro motors

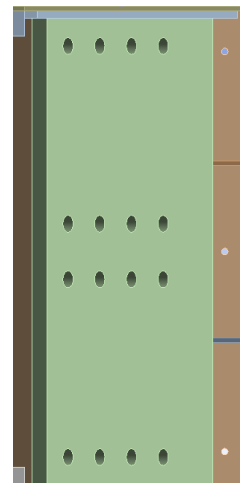


Figure 3.15: Bottom side of feeder after removing vibro motors

Finally, since the materials of the feeder are generally cast, its total weight is calculated as 21 tons. Since structural steel was chosen as the material in Ansys, the weight of the feeder is 5 tons. To correct this situation, the density of the material used was changed. The engineering data is shown in Figure 3.16 and Details of Geometry is shown in Figure 3.17.

Outline of Schematic A2, B2, C2, D2, E2: Engineering Data					
	A	B	C	D	E
1	Contents of Engineering Data				
2	Material				
3	Structural Steel				
	Fatigue Data at zero mean stress comes from 1998 ASME BPV Code, Section 8, Div 2, Table 5-110.1				
	Click here to add a new material				
Properties of Outline Row 3: Structural Steel					
	A	B	C	D	E
1	Property	Value	Unit	☒	☒
2	Material Field Variables	Table		☒	☒
3	Density	27978	kg m ⁻³	☒	☒
4	Isotropic Secant Coefficient of Thermal Expansion			☒	☒
6	Isotropic Elasticity			☒	☒
12	Strain-Life Parameters			☒	☒
20	S-N Curve	Tabular		☒	☒
24	Tensile Yield Strength	2,3E+08	Pa	☒	☒
25	Compressive Yield Strength	2,3E+08	Pa	☒	☒
26	Tensile Ultimate Strength	4,6E+08	Pa	☒	☒
27	Compressive Ultimate Strength	0	Pa	☒	☒

Figure 3.16: Properties of material

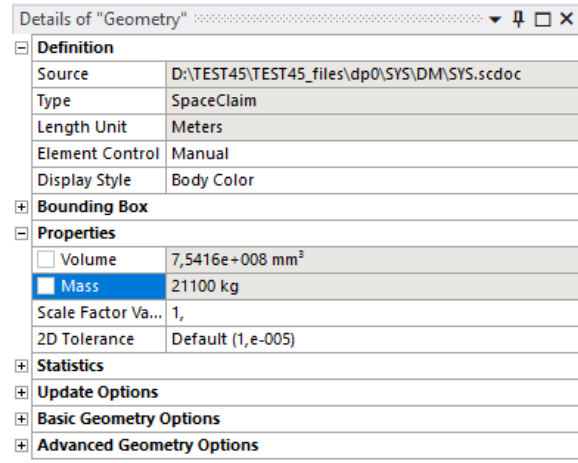


Figure 3.17: Properties of feeder

Following this step, the contacts were controlled, which was the final operation required to ensure the Mesh operation was proper. All contacts were created and verified one by one using the Contact Tool option in the Connections page. If this is not done, ANSYS recognizes each part independently and returns analysis findings as if they were independent of one another. As a result of the changes made 509 contacts for the first feeder. An example of this situation is shown in Figure 3.18 and Figure 3.19.

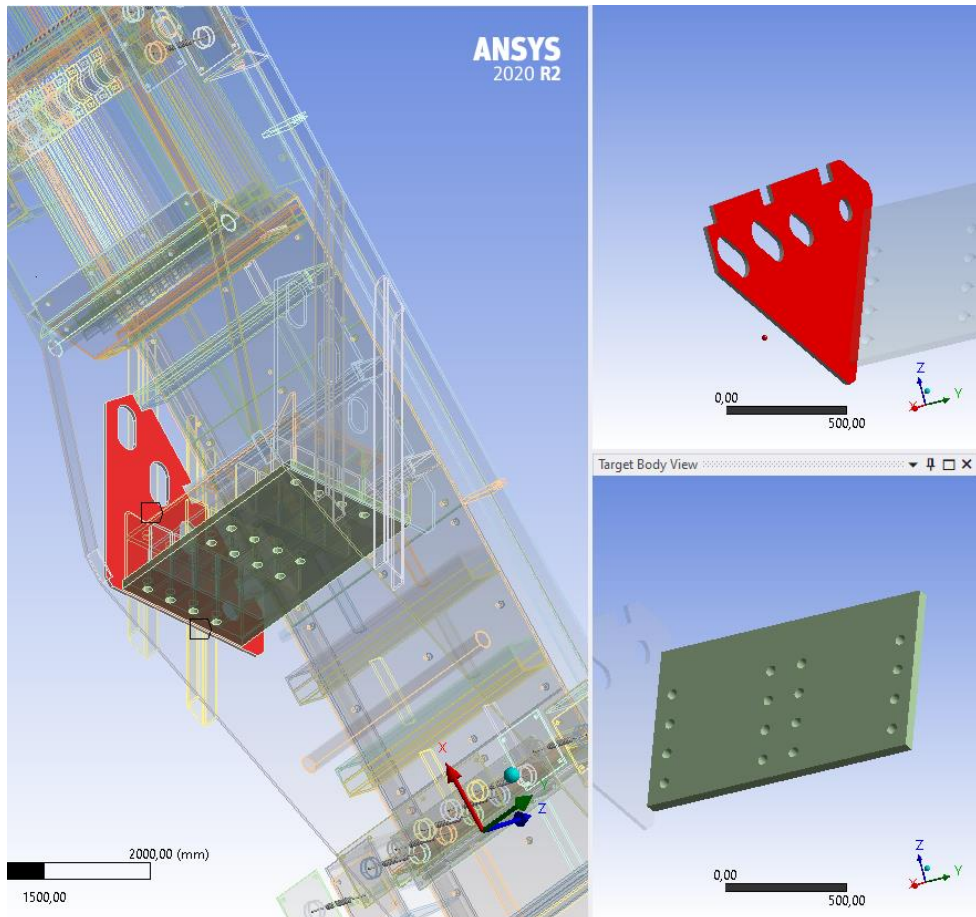


Figure 3.18: Example of contact controlling

Details of "Bonded - BT-07-1201\Solid1 To BT-07-1204\Solid1"	
Scope	
Scoping Method	Geometry Selection
Contact	1 Face
Target	1 Face
Contact Bodies	BT-07-1201\Solid1
Target Bodies	BT-07-1204\Solid1
Protected	No
Definition	
Type	Bonded
Scope Mode	Automatic
Behavior	Program Controlled
Trim Contact	Program Controlled
Trim Tolerance	16,623 mm
Suppressed	No
Advanced	
Formulation	Program Controlled
Small Sliding	Program Controlled
Detection Method	Program Controlled
Penetration Tolerance	Program Controlled
Elastic Slip Tolerance	Program Controlled
Normal Stiffness	Program Controlled
Update Stiffness	Program Controlled
Pinball Region	Program Controlled
Geometric Modification	

Figure 3.19: Details about one of the contact

After contact conditions are assigned, mesh operations are performed to generate a mesh that accurately captures the geometry and contact interfaces of the system. This meshing process ensures that the simulation accurately represents the physical behaviour of the system under study. The mesh study is shown in Figure 3.20 and Figure 3.21.

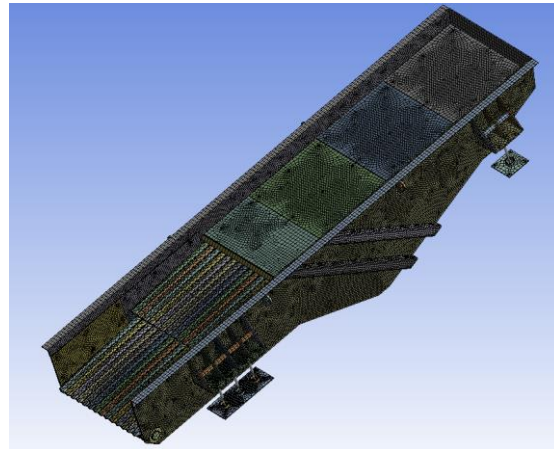


Figure 3.20: Ideal mesh view of vibrating feeder

Display	Display Style	Use Geometry Setting
Defaults		
Physics Preference	Mechanical	
Element Order	Program Controlled	
<input type="checkbox"/> Element Size	40, mm	
Sizing		
Use Adaptive Siz...	No	
<input type="checkbox"/> Growth Rate	Default (1,85)	
<input type="checkbox"/> Max Size	Default (80, mm)	
Mesh Defeaturing	Yes	
<input type="checkbox"/> Defeature Size	Default (0,2 mm)	
Capture Curvature	No	
Capture Proximity	No	
Bounding Box Di...	6649,3 mm	
Average Surface ...	8279,7 mm ²	
Minimum Edge L...	1,3509e-002 mm	
Quality		
<input type="checkbox"/> Check Mesh Qua...		Yes, Errors
Error Limits		Aggressive Mechanical
<input type="checkbox"/> Target Quality	0,5	
Smoothing		High
Mesh Metric		Skewness
<input type="checkbox"/> Min	1,3057e-010	
<input type="checkbox"/> Max	0,99173	
<input type="checkbox"/> Average	0,32858	
<input type="checkbox"/> Standard Devi...	0,26405	
Inflation		
Advanced		
Statistics		
<input type="checkbox"/> Nodes	833886	
<input type="checkbox"/> Elements	166857	

Figure 3.21: Details of mesh

As seen in Figure 3.22, local mesh methods were used when creating the mesh. As seen in Figure 3.23 an example of multi-zone mesh is shown.

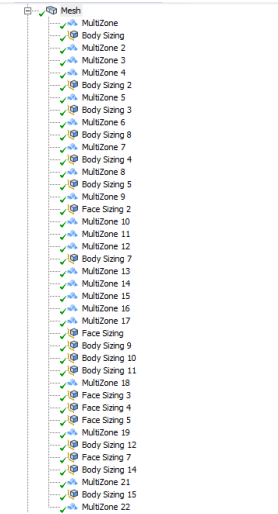


Figure 3.22: Local mesh

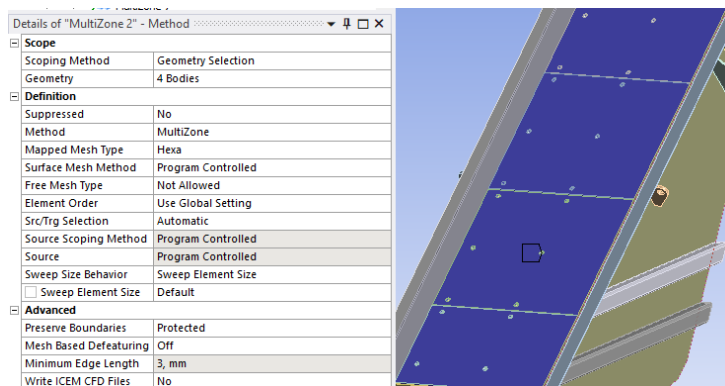


Figure 3.23: Example of local mesh (multizone)

Following the meshing process, final preparations for the static analysis began. First, a force of 1000 N was applied to each plate in accordance with the company's specifications. This 1000 N was dispersed equally across the tiered grilles in front of the feeders. Each layer had 14 grids, hence the force applied to each grid was 71.43 N. Then, fixed supports were installed. In addition, standard earth gravity was applied to the -Z direction. These Situations are shown in Figure 3.24 and Figure 3.25.

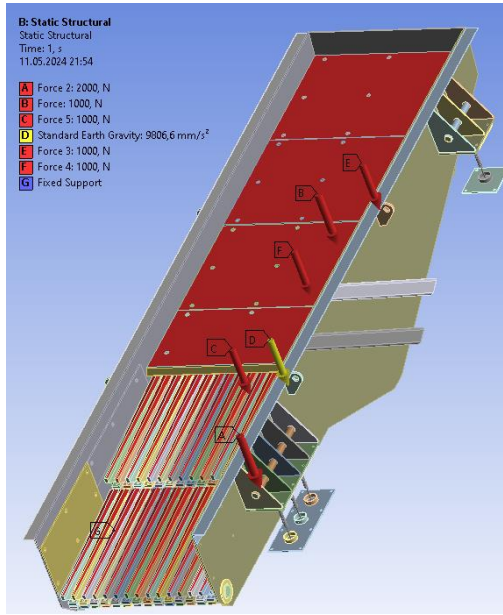


Figure 3.24: Boundary conditions of feeder

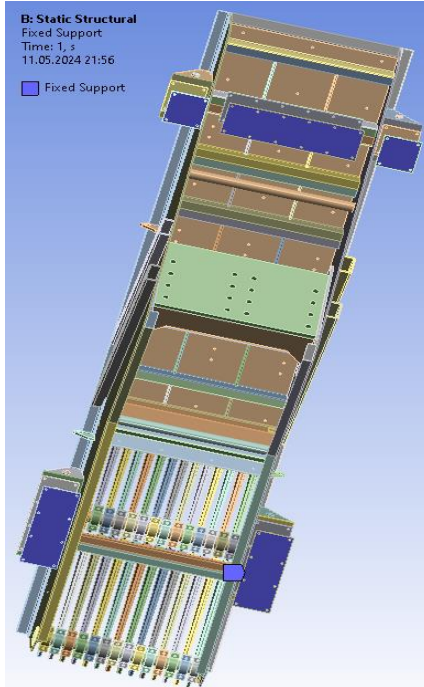


Figure 3.25: Fixed supports of feeder

3.1.1.2 Result of Static Analysis

Several key results were obtained in the static analysis conducted using ANSYS, including total deformation, equivalent (von-Mises) stress, and spring probe data.

Total deformation provides information about how much the structure deforms under the applied loads, offering a comprehensive view of displacement across the structure due to the applied forces. This metric is crucial for assessing structural deflection or movement under load,

aiding in determining if the deformation is within acceptable limits. in Figure 3.26 the Total Deformation for the first feeder are presented in the figure below. The deformation scale on the left side of the picture displays the colour and amount of distortion in millimetres. The maximum deformation was 49,557 mm. The minimum deformation was 0 mm.

Equivalent (von-Mises) Stress measures the stress state within the structure, considering all principal stresses (normal and shear stresses). This value helps engineers evaluate potential structural failure based on a single scalar value. By comparing von-Mises stress to the material's yield strength, engineers can assess if the structure operates within safe limits or is at risk of failure. In Figure 3.27 the Equivalent (von-Mises) Stress analysis result is the final analysis result for the initial feeder. The investigation yielded the maximum Equivalent (von-Mises) Stress of 595.11 MPa. The lowest equivalent (von-Mises) stress is 0.00014889 MPa.

Spring Probe Data shown in Figure 3.28 typically refers to results obtained from analysing the behaviour of spring elements or connections within the structure. This data includes information such as spring forces, displacements, or stresses. It is particularly relevant for assemblies or systems with components exhibiting spring-like behaviour, aiding in understanding how these components contribute to the structure's overall behaviour and ensuring they function as intended.

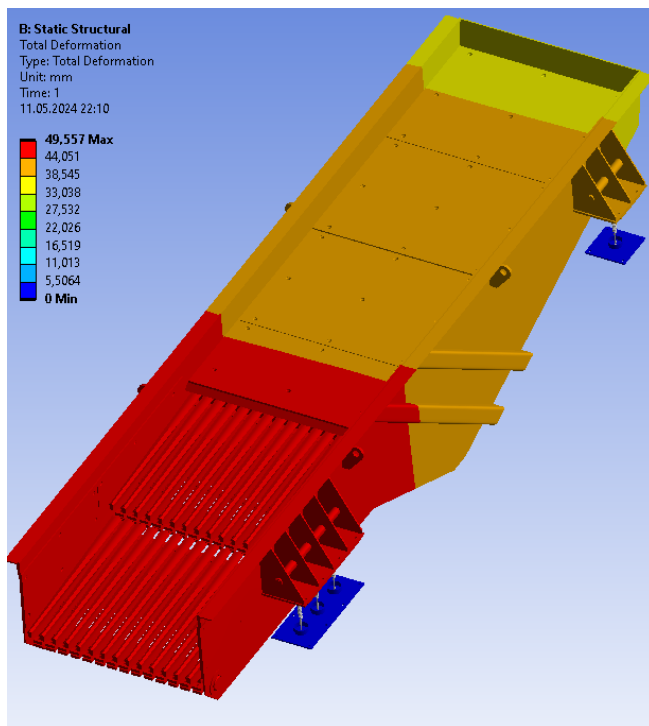


Figure 3.26: Static analysis - total deformation

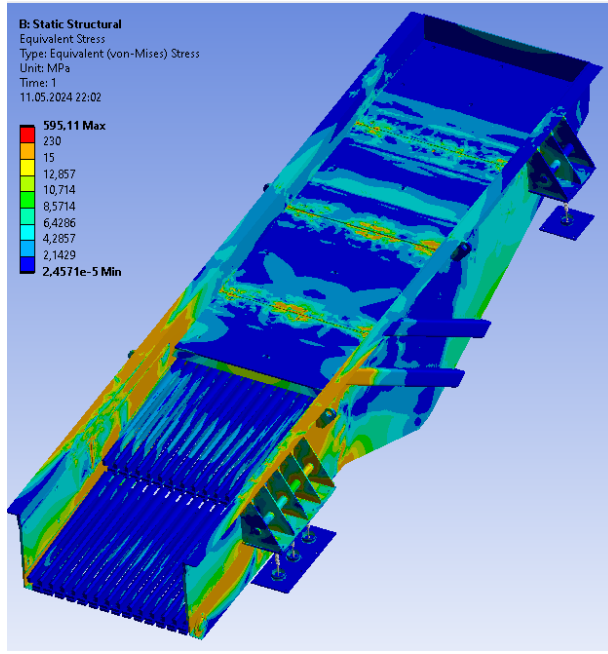


Figure 3.27: Static analysis - equivalent (von-mises) stress

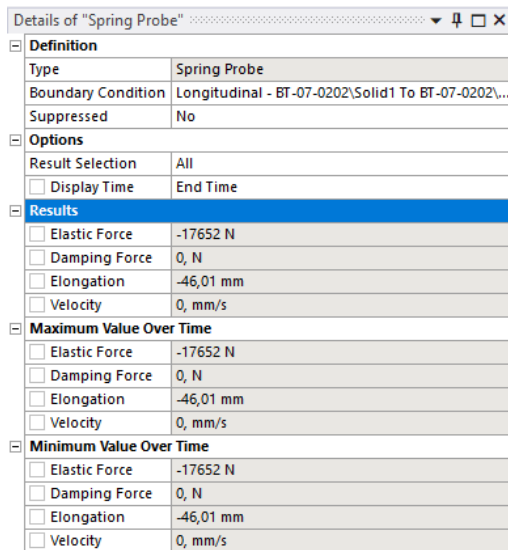


Figure 3.28: Static analysis – spring probe

3.1.2 Modal Analysis

Ten modes were identified in the modal analysis conducted using ANSYS. Modal analysis is a technique for determining the natural frequencies and mode shapes of a structure or system.

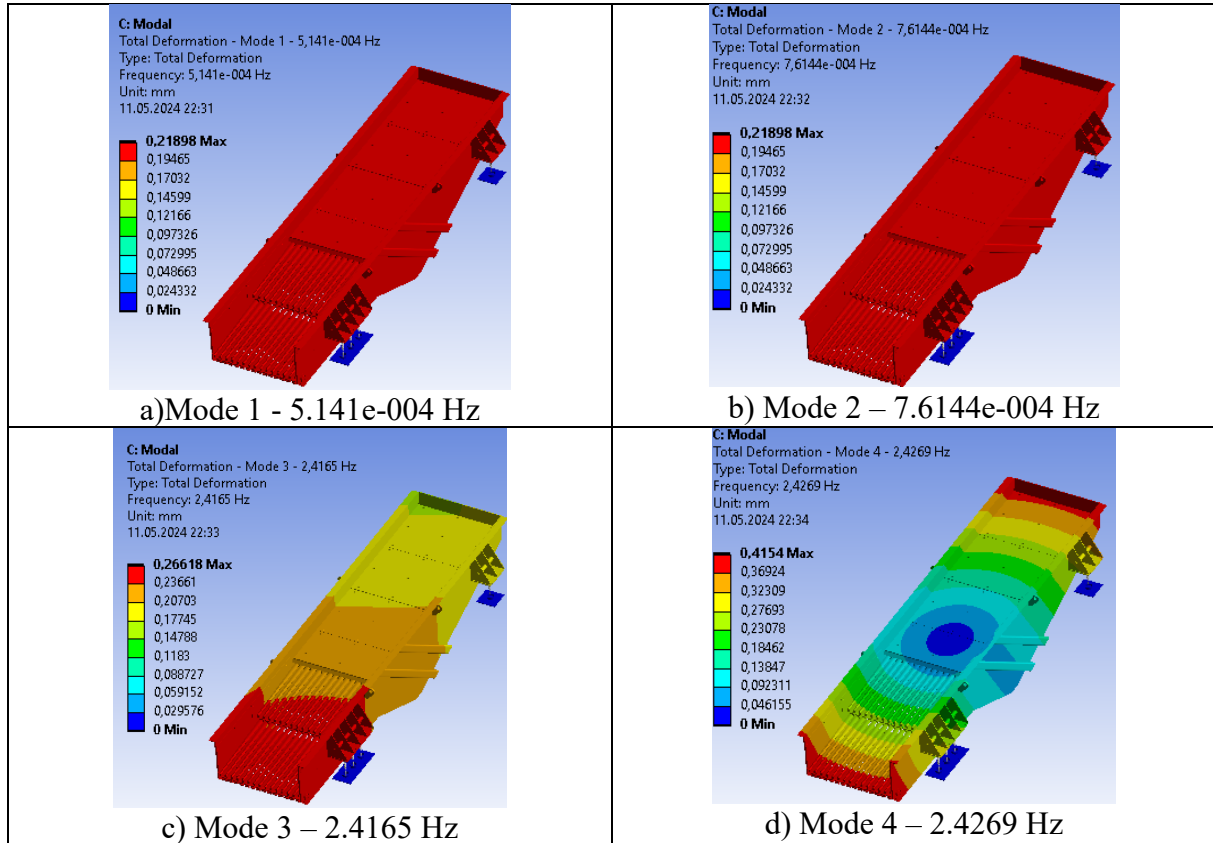
The natural frequencies correspond to the rates at which the structure tends to oscillate when subjected to dynamic loading, expressed in Hertz (Hz). Lower frequencies typically indicate larger-scale, global deformations, while higher frequencies correspond to smaller, more localized vibrations.

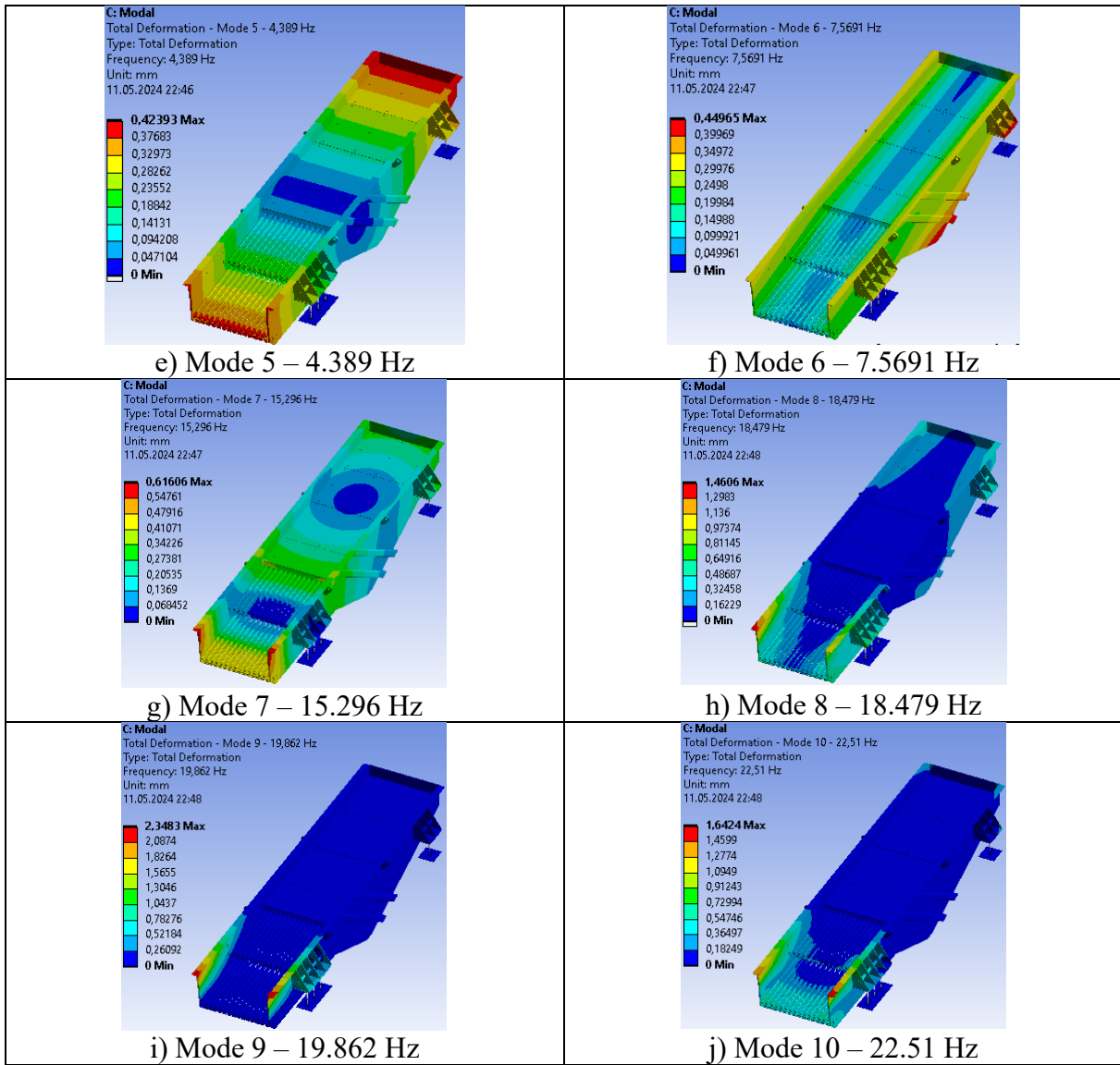
For each natural frequency, there is a corresponding mode shape, which describes the pattern of deformation or vibration exhibited by the structure. Mode shapes provide insight into how different parts of the structure move relative to each other at a specific frequency.

Damping ratios quantify the amount of energy dissipated in each mode over time. Higher damping ratios indicate greater energy dissipation and faster decay of vibrations, leading to shorter transient responses.

Identifying resonance frequencies is crucial for avoiding potentially damaging vibrations and ensuring the system's structural integrity. In modal analysis, boundary conditions are shown in Figure 3.25. The results are shown in Table 3.1.

Table 3.1: Modal analysis





The mode forms produced for the typical vibratory feeder at their natural frequencies are presented below in Table 3.1, indicating that these are roughly the depiction of mode shapes of the separate vibratory feeder components. Mode 1 occurs at the natural frequency of 5.141e-004 Hz. For mode 2 at the natural frequency of 7.614E-04 Hz. Now, Mode 3 occurs at the natural frequency of 2.416 Hz. At mode 4, with a natural frequency of 2.427 Hz. For mode 5 with a natural frequency of 4.389 Hz. At mode 6, occurs at the natural frequency of 7.569 Hz. Mode 7 occurs at the natural frequency of 15.30 Hz. At mode 8, with a natural frequency of 18.48 Hz. For mode 9 at the natural frequency of 19.86 Hz. At mode 10, it occurs at the natural frequency of 22.51 Hz. (Sanjay Oraon et al., 2019)

3.1.3 Transient Structural Analysis

Several key results were obtained from the transient structural study performed with ANSYS, revealing how the structure responds to dynamic loads over time.

The study provides information on the structure's response over time, including changes in displacement, velocity, acceleration, stress, and other response variables. Understanding the time history response helps to analyse the structure's dynamic behaviour and ability to handle transient stresses.

The stress distribution throughout the structure over time is presented, which aids in comparing stress levels to allowed limits and detecting crucial places where structural collapse might occur. This insight is critical for improving designs and preserving structural integrity during transient stress circumstances.

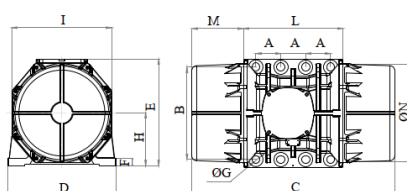
In this part, some dynamic forces are added into boundary conditions with static forces. Vibro motor makes dynamic forces, which are called centrifugal forces. The force data is given by BURÇELIK shown in Figure 3.29, Figure 3.30, Figure A4, Figure A5, Figure A6 and Figure A7.



MVE 19500/1E-105A0 [EE619500A5A08A0000]

3 PH - 6 kutup - 1000 d/d - 380-415 V [Delta] - 50 Hz

Çalışma momenti [Kg*cm]	Vibratör çekicileri [Kg*cm]	Santrifüj kuvveti [Kg]	Nominal voltaj [V]	Giriş gücü [kW]	Akım [A]	Güç faktörü	Ia/in
3.632	1.816	20.285	380-415 [Delta]	11,96	Δ 24	0,72	5,4



*Technical drawings are illustrative purposes only, please refer to 2D/3D drawings available on "FINDER" app.

Contact us for more information.

TÜM EBATLAR [mm]													
Ağırlık [Kg]	A	B	G	Delik sayısı	C	D	E	F	H	I	L	M	N
768	140	480	45	8	1.060	570	542	48	268	510	560	250	490

Figure 3.29: Technical data of vibro motor - I

RPM	Model	MECHANICAL SPECIFICATIONS				ELECTRICAL SPECIFICATIONS				
		Centrifugal Force		Static Moment *	Weight	Nominal Voltage	Maximal Current	Connector Type	Maximal Power	
		Type/rpm	KG	N	kgmm	KG	V	A	Wye	kW
T R I P H A S E	50 Hz	MVE 50/1	53	520	47,5	10	400	0,30	Y	0,12
		MVE 100/1	105	1030	94	11	400	0,30	Y	0,12
		MVE 200/1	187	1834	167,5	19	400	0,65	Y	0,15
		MVE 300/1	318	3120	284,5	26	400	0,67	Y	0,25
		MVE 500/1*	513	5033	459,5	34	400	1,22	Y	0,55
		MVE 800/1	767	7524	687	60	400	1,42	Y	0,75
		MVE 1100/1	1048	10281	938,5	78	400	1,42	Y	0,75
		MVE 1500/1	1590	15598	1424	84	400	1,80	Y	0,9
		MVE 1600/1	1673	16412	1498	90	400	2,40	Y	0,9
		MVE 2100/1	2083	20434	1865,5	105	400	3,00	Y	1,5
		MVE 2200/1	2239	21965	2005	107	400	3,00	Y	1,5
		MVE 2600/1	2610	25604	2337	146,5	400	4,10	Y	1,96
		MVE 3000/1	3017	29597	2701,5	155	400	4,50	Y	2,2
		MVE 3700/1	3797	37249	3512,5	159	400	4,50	Y	2,2
		MVE 3800/1	3799	37268	3402	216	400	5,50	Y	2,5
		MVE 4700/1	4681	45921	4191,5	220	400	6,50	Y	3,2
		MVE 5200/1*	5228	51287	4682	236	400	6,50	Y	3,2
		MVE 6500/1	6506	63824	5826	288	400	7,76	Y	4,3
		MVE 8000/1*	8018	78657	7180	309	400	12,60	Y	5,5
		MVE 9000/1*	8936	87662	8002	322	400	13,20	Y	6,2
		MVE 10000/1*	9986	97963	8942	374	400	14,00	Y	6,1
		MVE 11400/1	11485	112668	10284,5	404	400	13,00	Y	6,4
		MVE 13000/1*	12904	126588	11555	411	400	17,20	Y	8
		MVE 12000/1	12580	123410	11265	522	400	15,00	Y	8
		MVE 15000/1	14706	144266	13170	672	400	18,00	Y	10,1
		MVE 17500/1	17980	176384	16100	744	400	21,00	Y	11,9
		MVE 19500/1	20285	198996	18160	768	400	24,00	V	12
		MVE 22000/1	22711	222795	20335	916	400	28,00	Y	13,9
		MVE 25000/1	25532	250469	22860	994	400	28,00	Y	13,9

Figure 3.30: Technical data of vibro motor – 2

Figure 3.31 depicts four moments that correspond to distinct orientations of the exciting force of the vibrating feeder. The dotted arrow indicates the direction of material movement, whereas the line arrow depicts the direction of the exciting force. These four instances represent the vibrating feeder's maximum amplitude and speed, respectively. When the direction of the exciting force was consistent and forward, the material force nearly reached its maximum. The exciting force's reverse inward and reverse outward orientations matched the maximal pressure and pulling force. Thus, these four moments might indicate the vibrating feeder's limit conditions throughout the reciprocating vibration operation (Ningning Xu et al., 2021)

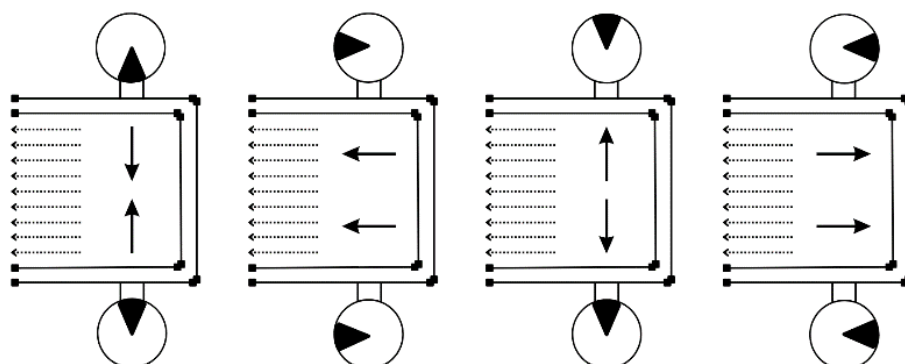


Figure 3.31: Exciting force (centrifugal force) directions at four special moments. Respectively (left to right), reverse and inward direction, same direction and forward, reverse and outward, same direction and backwards (Ningning Xu et al., 2021)

Boundary Conditions are shown in Figure 3.32. Static Forces are Force, Force 2, Force 3, Force 4, Force 5. Dynamic Forces are Force 6, Force 7, Force 8. Force 6 is applying upward and downward forces. Force 7 and Force 8 are applying right and left side forces. In addition, Force 7 and Force 8 are opposing forces. Numerical data of all dynamic forces are given in the Table 3.2 and Table 3.3.

Since the vibro motor operates at 50 Hz, the dynamic forces time-force relationship was distributed in tabular data according to 50 Hz and transferred to ANSYS.

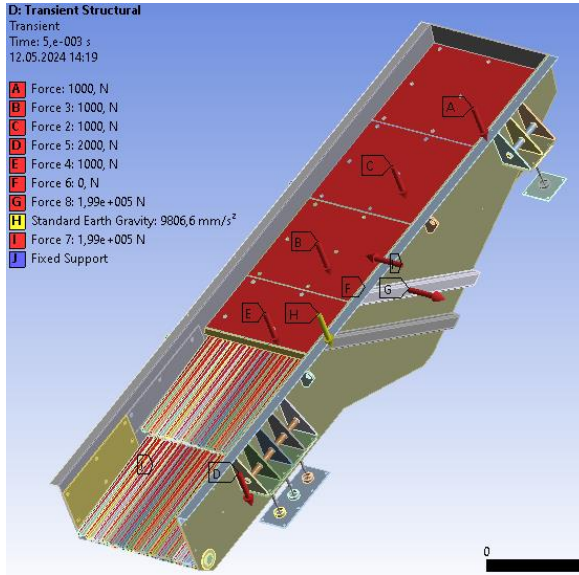


Figure 3.32: Boundary conditions of transient structural analysis

Table 3.2: Tabular data of force 6

Time [s]	Force [N]	Time [s]	Force [N]	Time [s]	Force [N]	Time [s]	Force [N]
0	0	0,25	3,98E+05	0,5	-3,98E+05	0,75	3,98E+05
5,00E-03	0	0,255	0	0,505	0	0,755	0
1,00E-02	3,98E+05	0,26	-3,98E+05	0,51	3,98E+05	0,76	-3,98E+05
1,50E-02	0	0,265	0	0,515	0	0,765	0
2,00E-02	-3,98E+05	0,27	3,98E+05	0,52	-3,98E+05	0,77	3,98E+05
2,50E-02	0	0,275	0	0,525	0	0,775	0
3,00E-02	3,98E+05	0,28	-3,98E+05	0,53	3,98E+05	0,78	-3,98E+05
3,50E-02	0	0,285	0	0,535	0	0,785	0
4,00E-02	-3,98E+05	0,29	3,98E+05	0,54	-3,98E+05	0,79	3,98E+05
4,50E-02	0	0,295	0	0,545	0	0,795	0
5,00E-02	3,98E+05	0,3	-3,98E+05	0,55	3,98E+05	0,8	-3,98E+05
5,50E-02	0	0,305	0	0,555	0	0,805	0
6,00E-02	-3,98E+05	0,31	3,98E+05	0,56	-3,98E+05	0,81	3,98E+05
6,50E-02	0	0,315	0	0,565	0	0,815	0
7,00E-02	3,98E+05	0,32	-3,98E+05	0,57	3,98E+05	0,82	-3,98E+05
7,50E-02	0	0,325	0	0,575	0	0,825	0
8,00E-02	-3,98E+05	0,33	3,98E+05	0,58	-3,98E+05	0,83	3,98E+05
8,50E-02	0	0,335	0	0,585	0	0,835	0
9,00E-02	3,98E+05	0,34	-3,98E+05	0,59	3,98E+05	0,84	-3,98E+05

9,50E-02	0	0,345	0	0,595	0	0,845	0
0,1	-3,98E+05	0,35	3,98E+05	0,6	-3,98E+05	0,85	3,98E+05
0,105	0	0,355	0	0,605	0	0,855	0
0,11	3,98E+05	0,36	-3,98E+05	0,61	3,98E+05	0,86	-3,98E+05
0,115	0	0,365	0	0,615	0	0,865	0
0,12	-3,98E+05	0,37	3,98E+05	0,62	-3,98E+05	0,87	3,98E+05
0,125	0	0,375	0	0,625	0	0,875	0
0,13	3,98E+05	0,38	-3,98E+05	0,63	3,98E+05	0,88	-3,98E+05
0,135	0	0,385	0	0,635	0	0,885	0
0,14	-3,98E+05	0,39	3,98E+05	0,64	-3,98E+05	0,89	3,98E+05
0,145	0	0,395	0	0,645	0	0,895	0
0,15	3,98E+05	0,4	-3,98E+05	0,65	3,98E+05	0,9	-3,98E+05
0,155	0	0,405	0	0,655	0	0,905	0
0,16	-3,98E+05	0,41	3,98E+05	0,66	-3,98E+05	0,91	3,98E+05
0,165	0	0,415	0	0,665	0	0,915	0
0,17	3,98E+05	0,42	-3,98E+05	0,67	3,98E+05	0,92	-3,98E+05
0,175	0	0,425	0	0,675	0	0,925	0
0,18	-3,98E+05	0,43	3,98E+05	0,68	-3,98E+05	0,93	3,98E+05
0,185	0	0,435	0	0,685	0	0,935	0
0,19	3,98E+05	0,44	-3,98E+05	0,69	3,98E+05	0,94	-3,98E+05
0,195	0	0,445	0	0,695	0	0,945	0
0,2	-3,98E+05	0,45	3,98E+05	0,7	-3,98E+05	0,95	3,98E+05
0,205	0	0,455	0	0,705	0	0,955	0
0,21	3,98E+05	0,46	-3,98E+05	0,71	3,98E+05	0,96	-3,98E+05
0,215	0	0,465	0	0,715	0	0,965	0
0,22	-3,98E+05	0,47	3,98E+05	0,72	-3,98E+05	0,97	3,98E+05
0,225	0	0,475	0	0,725	0	0,975	0
0,23	3,98E+05	0,48	-3,98E+05	0,73	3,98E+05	0,98	-3,98E+05
0,235	0	0,485	0	0,735	0	0,985	0
0,24	-3,98E+05	0,49	3,98E+05	0,74	-3,98E+05	0,99	3,98E+05
0,245	0	0,495	0	0,745	0	0,995	0
						1	-3,98E+05

Table 3.3: Tabular data of force 7 (force 8 have same tabular data but opposite direction)

Time[s]	Force[N]	Time[s]	Force[N]	Time[s]	Force[N]	Time[s]	Force[N]
0	0	0,25	0	0,5	0	0,75	0
5,00E-03	1,99E+05	0,255	-1,99E+05	0,505	1,99E+05	0,755	-1,99E+05
1,00E-02	0	0,26	0	0,51	0	0,76	0
1,50E-02	-1,99E+05	0,265	1,99E+05	0,515	-1,99E+05	0,765	1,99E+05
2,00E-02	0	0,27	0	0,52	0	0,77	0
2,50E-02	1,99E+05	0,275	-1,99E+05	0,525	1,99E+05	0,775	-1,99E+05
3,00E-02	0	0,28	0	0,53	0	0,78	0
3,50E-02	-1,99E+05	0,285	1,99E+05	0,535	-1,99E+05	0,785	1,99E+05
4,00E-02	0	0,29	0	0,54	0	0,79	0
4,50E-02	1,99E+05	0,295	-1,99E+05	0,545	1,99E+05	0,795	-1,99E+05
5,00E-02	0	0,3	0	0,55	0	0,8	0
5,50E-02	-1,99E+05	0,305	1,99E+05	0,555	-1,99E+05	0,805	1,99E+05
6,00E-02	0	0,31	0	0,56	0	0,81	0
6,50E-02	1,99E+05	0,315	-1,99E+05	0,565	1,99E+05	0,815	-1,99E+05
7,00E-02	0	0,32	0	0,57	0	0,82	0
7,50E-02	-1,99E+05	0,325	1,99E+05	0,575	-1,99E+05	0,825	1,99E+05
8,00E-02	0	0,33	0	0,58	0	0,83	0

8,50E-02	1,99E+05	0,335	-1,99E+05	0,585	1,99E+05	0,835	-1,99E+05
9,00E-02	0	0,34	0	0,59	0	0,84	0
9,50E-02	-1,99E+05	0,345	1,99E+05	0,595	-1,99E+05	0,845	1,99E+05
0,1	0	0,35	0	0,6	0	0,85	0
0,105	1,99E+05	0,355	-1,99E+05	0,605	1,99E+05	0,855	-1,99E+05
0,11	0	0,36	0	0,61	0	0,86	0
0,115	-1,99E+05	0,365	1,99E+05	0,615	-1,99E+05	0,865	1,99E+05
0,12	0	0,37	0	0,62	0	0,87	0
0,125	1,99E+05	0,375	-1,99E+05	0,625	1,99E+05	0,875	-1,99E+05
0,13	0	0,38	0	0,63	0	0,88	0
0,135	-1,99E+05	0,385	1,99E+05	0,635	-1,99E+05	0,885	1,99E+05
0,14	0	0,39	0	0,64	0	0,89	0
0,145	1,99E+05	0,395	-1,99E+05	0,645	1,99E+05	0,895	-1,99E+05
0,15	0	0,4	0	0,65	0	0,9	0
0,155	-1,99E+05	0,405	1,99E+05	0,655	-1,99E+05	0,905	1,99E+05
0,16	0	0,41	0	0,66	0	0,91	0
0,165	1,99E+05	0,415	-1,99E+05	0,665	1,99E+05	0,915	-1,99E+05
0,17	0	0,42	0	0,67	0	0,92	0
0,175	-1,99E+05	0,425	1,99E+05	0,675	-1,99E+05	0,925	1,99E+05
0,18	0	0,43	0	0,68	0	0,93	0
0,185	1,99E+05	0,435	-1,99E+05	0,685	1,99E+05	0,935	-1,99E+05
0,19	0	0,44	0	0,69	0	0,94	0
0,195	-1,99E+05	0,445	1,99E+05	0,695	-1,99E+05	0,945	1,99E+05
0,2	0	0,45	0	0,7	0	0,95	0
0,205	1,99E+05	0,455	-1,99E+05	0,705	1,99E+05	0,955	-1,99E+05
0,21	0	0,46	0	0,71	0	0,96	0
0,215	-1,99E+05	0,465	1,99E+05	0,715	-1,99E+05	0,965	1,99E+05
0,22	0	0,47	0	0,72	0	0,97	0
0,225	1,99E+05	0,475	-1,99E+05	0,725	1,99E+05	0,975	-1,99E+05
0,23	0	0,48	0	0,73	0	0,98	0
0,235	-1,99E+05	0,485	1,99E+05	0,735	-1,99E+05	0,985	1,99E+05
0,24	0	0,49	0	0,74	0	0,99	0
0,245	1,99E+05	0,495	-1,99E+05	0,745	1,99E+05	0,995	-1,99E+05
						1	0

As a result of the analysis, a 200-step equivalent stress result table was created. As a result, the highest stress value for maximum values is 1541.4 MPa, and the lowest stress value is 80.306 MPa. For minimum values, the highest stress value is 4.6156e-005 MPa, and the lowest stress value is 3.1879e-007 MPa. For the average stress value, the largest value is 16.919 MPa, and the smallest value is 0.98827 MPa. In addition, as a result of the analysis, it was observed that the springs changed 40 mm forward and backward, and 90 mm upward and downward, with the resulting movements.

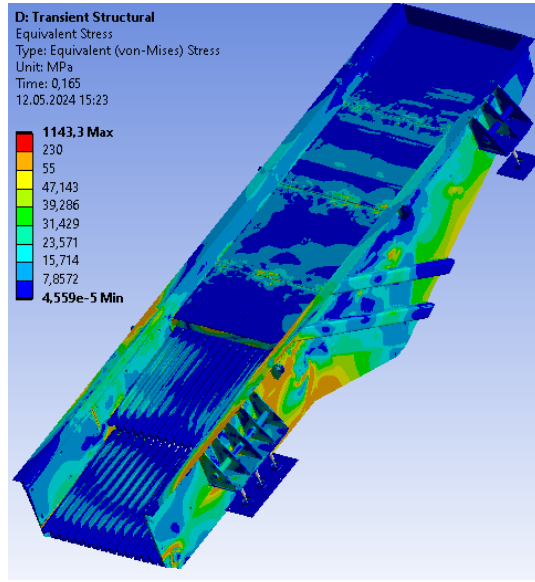


Figure 3.33: Result of transient structural analysis (equivalent stress)

The visual seen in Figure 3.33 is 0.165 s for the second feeder is the stress value per second, which is 1143,3 MPa.

Table 3.4 shows the results of the transient structural analysis performed for the second feeder.

Table 3.4: Result of transient structural analysis (equivalent stress)

Time[s]	Minimum [Mpa]	Maximum [Mpa]	Average[Mpa]	Time[s]	Minimum [Mpa]	Maximum [Mpa]	Average[Mpa]
5,00E-03	1,80E-06	80,306	0,98827	0,505	2,28E-05	512,85	10,226
1,00E-02	2,74E-06	143,39	2,8645	0,51	2,23E-05	656,59	8,5298
1,50E-02	2,84E-06	226,29	3,5299	0,515	2,25E-05	789,58	10,393
2,00E-02	3,71E-06	197,05	4,9677	0,52	2,35E-05	561,73	7,9127
2,50E-02	3,54E-06	295,11	4,6822	0,525	2,54E-05	617,76	11,174
3,00E-02	3,52E-06	259,15	6,809	0,53	2,72E-05	761,22	9,9136
3,50E-02	4,03E-06	302,91	5,5745	0,535	2,96E-05	891,53	11,165
4,00E-02	2,44E-06	309,39	7,0846	0,54	3,23E-05	649,58	8,7493
4,50E-02	2,13E-06	356,08	6,8145	0,545	3,50E-05	823,2	11,873
5,00E-02	6,22E-06	427,41	7,2899	0,55	3,81E-05	968,48	11,291
5,50E-02	1,11E-05	410,81	7,5834	0,555	4,13E-05	971,25	12,326
6,00E-02	9,10E-06	469	6,4748	0,56	4,29E-05	847,8	10,041
6,50E-02	9,90E-06	586,31	8,1606	0,565	4,33E-05	1004,4	13,095
7,00E-02	1,28E-05	514,37	7,5483	0,57	4,40E-05	1113,5	12,355
7,50E-02	1,83E-05	551,95	8,4995	0,575	4,47E-05	1169,8	13,224
8,00E-02	1,90E-05	518,76	6,5245	0,58	4,56E-05	932,82	11,074
8,50E-02	2,12E-05	572,91	8,7314	0,585	4,62E-05	1075	14,187
9,00E-02	2,23E-05	616,79	8,0333	0,59	4,60E-05	1204,3	13,581
9,50E-02	2,25E-05	915,5	9,5603	0,595	4,59E-05	1293,4	14,284
0,1	2,24E-05	567,78	7,2272	0,6	4,58E-05	1044,9	12,086
0,105	2,29E-05	550,17	9,3008	0,605	4,57E-05	1128,2	14,981
0,11	2,43E-05	587,59	8,6717	0,61	4,56E-05	1275,9	14,194
0,115	2,60E-05	969,58	9,5851	0,615	4,52E-05	1464,1	15,111
0,12	2,80E-05	880,04	8,3386	0,62	4,49E-05	1245,6	13,1
0,125	3,09E-05	664,39	10,662	0,625	4,49E-05	1138,4	15,944
0,13	3,42E-05	772,06	10,487	0,63	4,48E-05	1384,5	15,055
0,135	3,75E-05	993,36	11,027	0,635	4,48E-05	1487	15,479
0,14	4,10E-05	897,83	9,6141	0,64	4,49E-05	1216,8	13,315
0,145	4,28E-05	981,13	12,491	0,645	4,53E-05	1148,3	16,02
0,15	4,33E-05	1071,2	11,905	0,65	4,56E-05	1295,6	15,116
0,155	4,40E-05	1028,5	13,087	0,655	4,58E-05	1360,7	15,516
0,16	4,47E-05	1032,3	11,611	0,66	4,58E-05	1069,2	13,09
0,165	4,56E-05	1143,3	14,974	0,665	4,59E-05	1136,1	15,65

0,17	4,61E-05	1161,4	14,326	0,67	4,61E-05	1238,8	14,393
0,175	4,59E-05	1259,1	14,856	0,675	4,59E-05	1230	15,028
0,18	4,58E-05	1074,6	12,881	0,68	4,50E-05	971,73	12,347
0,185	4,58E-05	1250,1	16,127	0,685	4,41E-05	1038,8	14,895
0,19	4,57E-05	1288,8	15,903	0,69	4,34E-05	1094,4	13,747
0,195	4,52E-05	1385,9	16,394	0,695	4,29E-05	1073,4	14,049
0,2	4,48E-05	1123,3	13,337	0,7	4,12E-05	848,74	11,052
0,205	4,47E-05	1273	16,573	0,705	3,77E-05	930,01	13,293
0,21	4,46E-05	1361,5	15,505	0,71	3,44E-05	978,6	11,759
0,215	4,44E-05	1541,4	16,919	0,715	3,14E-05	840,6	12,48
0,22	4,44E-05	1253,3	13,672	0,72	2,87E-05	688,12	9,3421
0,225	4,46E-05	1110,3	16,757	0,725	2,65E-05	733,13	11,645
0,23	4,49E-05	1338,9	15,668	0,73	2,47E-05	696,62	9,7389
0,235	4,51E-05	1531,1	16,652	0,735	2,30E-05	790,76	10,705
0,24	4,55E-05	1280,3	13,513	0,74	2,24E-05	503,57	7,4931
0,245	4,58E-05	1050,4	16,186	0,745	2,27E-05	545,17	10,058
0,25	4,59E-05	1184	14,452	0,75	2,22E-05	544,43	8,0352
0,255	4,60E-05	1305,1	15,334	0,755	2,03E-05	601,16	9,391
0,26	4,60E-05	1104,1	12,682	0,76	1,85E-05	395,78	6,2327
0,265	4,51E-05	1065,9	14,96	0,765	1,60E-05	515,03	8,9822
0,27	4,42E-05	1068	13,047	0,77	1,02E-05	344,32	6,7434
0,275	4,35E-05	980,66	13,533	0,775	9,08E-06	421,4	8,8094
0,28	4,29E-05	894,83	10,771	0,78	9,99E-06	389,76	6,195
0,285	4,09E-05	983,68	13,322	0,785	6,25E-06	488,4	9,0249
0,29	3,75E-05	954,9	11,85	0,79	1,22E-06	366,98	6,9457
0,295	3,42E-05	893,53	12,15	0,795	5,13E-06	402	9,0829
0,3	3,09E-05	657,21	8,9081	0,8	3,26E-06	393,73	6,7561
0,305	2,80E-05	806,03	11,583	0,805	2,87E-06	404,35	9,4375
0,31	2,59E-05	834,2	9,4975	0,81	4,13E-07	391,7	7,101
0,315	2,40E-05	713,51	10,593	0,815	1,28E-06	422,99	9,5956
0,32	2,27E-05	484,2	7,0119	0,82	5,92E-06	349,61	7,0995
0,325	2,24E-05	628,46	9,8975	0,825	6,83E-06	433,17	9,6009
0,33	2,28E-05	572,94	8,038	0,83	7,97E-06	398,56	7,2079
0,335	2,22E-05	624,52	9,2995	0,835	7,93E-06	462,13	9,5048
0,34	2,03E-05	341,29	5,8453	0,84	6,44E-06	371,92	7,062
0,345	1,85E-05	475,93	9,0019	0,845	4,50E-06	411,19	9,3149
0,35	1,47E-05	400,21	6,6208	0,85	1,58E-06	386,31	6,8483
0,355	9,93E-06	517,52	9,1263	0,855	3,85E-06	413,61	8,9106
0,36	9,16E-06	370,02	5,9543	0,86	3,50E-06	369,76	6,1479
0,365	1,01E-05	513,79	9,1156	0,865	4,59E-06	425,75	8,6263
0,37	6,27E-06	340,47	6,421	0,87	1,70E-06	369,19	5,9925
0,375	2,11E-06	432,39	9,1374	0,875	5,67E-06	399,94	8,5475
0,38	1,63E-06	389,28	6,3962	0,88	7,58E-06	392,63	5,8784
0,385	3,39E-06	477,59	9,1439	0,885	9,55E-06	519,13	8,9064
0,39	3,53E-06	356,47	6,7234	0,89	9,08E-06	363,52	7,0703
0,395	2,91E-06	379,36	8,8527	0,895	1,18E-05	525,19	9,3481
0,4	2,79E-06	374,72	6,4061	0,9	1,81E-05	391,83	6,8003
0,405	4,82E-07	372,4	8,8077	0,905	1,86E-05	498,93	9,8362
0,41	4,45E-06	377,01	6,3536	0,91	2,07E-05	560,17	8,3243
0,415	4,32E-06	434,77	8,7659	0,915	2,23E-05	689,62	10,277
0,42	3,19E-07	341,85	6,3112	0,92	2,26E-05	454,78	7,7741
0,425	2,78E-06	434,76	8,6061	0,925	2,24E-05	560,97	10,877
0,43	3,97E-06	404,63	6,4338	0,93	2,30E-05	657,09	9,6357
0,435	2,74E-06	436,69	8,7003	0,935	2,46E-05	762,97	11,417
0,44	3,11E-06	382,6	6,2982	0,94	2,63E-05	576,76	8,9438
0,445	3,69E-06	403,9	8,6713	0,945	2,83E-05	751,22	12,006
0,45	4,66E-06	392,69	6,3143	0,95	3,08E-05	879,37	11,26
0,455	2,07E-06	407,47	8,8103	0,955	3,37E-05	925,57	12,627
0,46	6,22E-06	359,35	5,9158	0,96	3,68E-05	752,58	10,18
0,465	8,91E-06	484,15	9,011	0,965	3,99E-05	906,29	13,237
0,47	9,64E-06	355,43	6,7462	0,97	4,27E-05	1018,5	12,303
0,475	9,12E-06	437,08	9,2286	0,975	4,31E-05	1091,6	13,372
0,48	1,23E-05	389,66	6,6358	0,98	4,37E-05	900,38	11,077
0,485	1,75E-05	535,28	9,471	0,985	4,44E-05	1046,2	14,052
0,49	1,85E-05	445,02	7,9757	0,99	4,52E-05	1158,4	13,26
0,495	1,99E-05	622,82	9,9471	0,995	4,61E-05	1208,1	13,929
0,5	2,22E-05	453,72	7,1977	1	4,61E-05	996,53	11,693

3.1.4 Fatigue Life Analysis

Several key findings were obtained from the fatigue life study using ANSYS, revealing structural durability and lifespan under cyclic stress conditions.

The major conclusion is an estimate of the structure's projected lifespan under cyclic loads. Engineers calculate how many loading cycles the structure can sustain before failing due to fatigue, which aids in determining its durability and dependability.

Fatigue life analysis also shows how fatigue damage builds up over time, such as tracking fatigue cracks, propagation rates, and critical fracture diameters. Understanding this helps to detect probable failure mechanisms and optimize structural designs.

Critical areas of the structure where fatigue damage is most likely to develop are identified. This allows engineers to focus on mitigation techniques like reworking components or optimizing material choices.

The distribution of stress and strain under cyclic loading circumstances is disclosed, which helps to optimize designs and ensure structural integrity during the planned service life.

Engineers compare estimated fatigue life to necessary design life to determine the structure's factor of safety against fatigue failure. This influences judgments about design specifications and fatigue mitigation strategies.

BURÇELIK said that this feeder broke down in about 1 month. In Fatigue Life Analysis, it was determined that the point where the break started was approximately 10^4 cycles. The lifespan is calculated based on the feeder operating 12 hours a day.

$$\frac{\text{cycles}}{\text{times/day}} = \frac{10^4}{12 * 60} = 13.9$$

As a result of the calculation, the feeder starts to break due to vibration on the 14th day and Life data shown in Figure 3.34

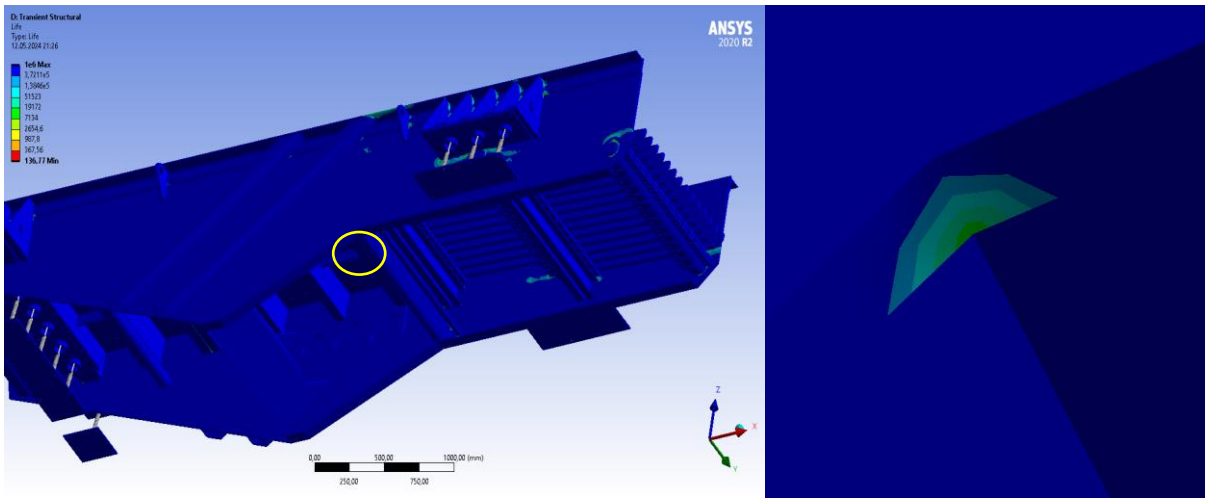


Figure 3.34: Result of transient structural – fatigue tool (life)

3.1.5 Effect of Meshing Process on Analysis

Before completing operations in 3.1.2, 3.1.3, and 3.1.4, these analyses were conducted using meshing with fewer nodes and elements. The method was further enhanced, allowing for more complex meshing. Detailed meshing produced more accurate findings. (Chandravanshi and Mukhopadhyay, 2017)

We completed the mesh process by trying 20 different mesh sizes and types, performing a static analysis and selecting the mesh type with the least number of nodes that gave the same result. The graphical data are given in Figure 3.35.

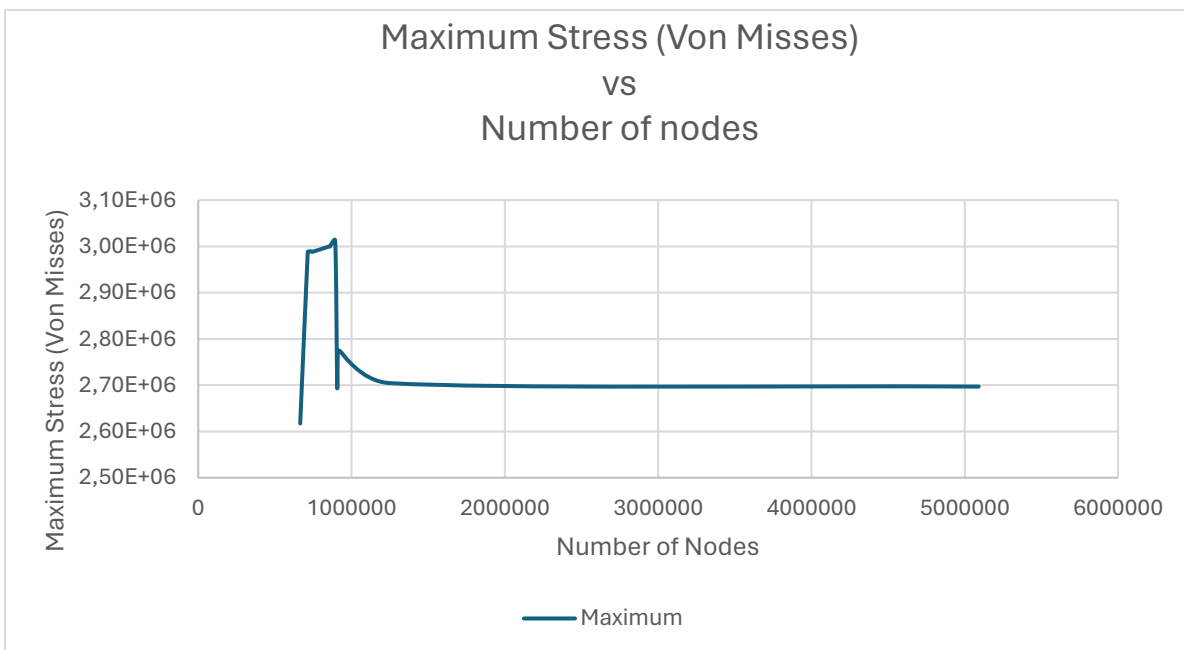


Figure 3.35: Graph of maximum stress (von-misses) vs number of nodes

The ideal number of nodes and elements we obtained with this graph is 833886 nodes, 166857 elements.

3.2 Analysis of Second Feeder

In this section, we will examine the analysis studies of the second vibrating feeder, which was optimized and strengthened with additional supports because it was deemed undesirable by BURÇELİK. First, the image of the second feeder on SpaceClaim is shown in Figure 3.36, Figure 3.37, Figure 3.38, and Figure 3.39.

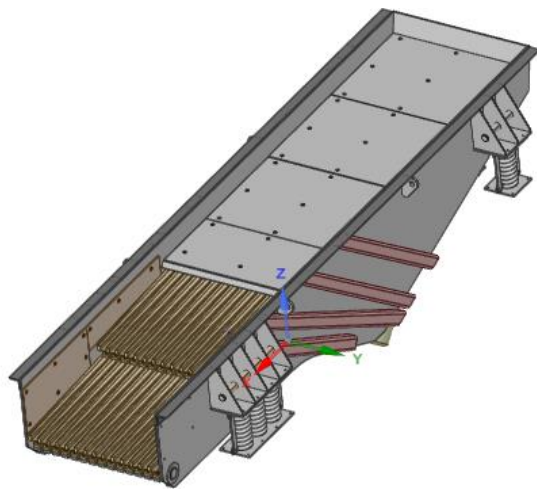


Figure 3.36: Isometric view of second feeder.

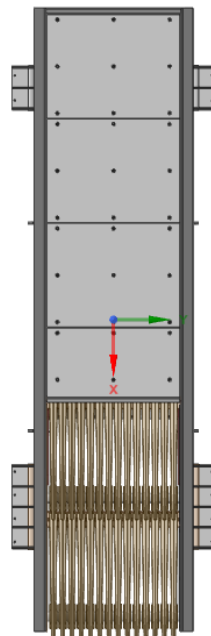


Figure 3.37: Top view of second feeder.

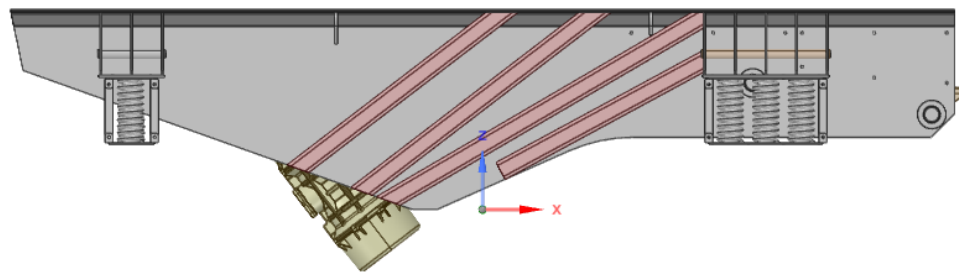


Figure 3.38: Left view of second feeder.

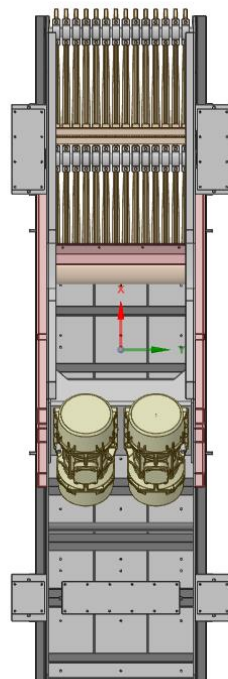


Figure 3.39: Bottom view of second feeder.

As seen in Figure 3.40, additional supports have been included in the structure to increase the strength of the object and strengthen areas that may be destroyed. In addition, fillets in the second feeder was added and shown in Figure 3.40 in orange circle.

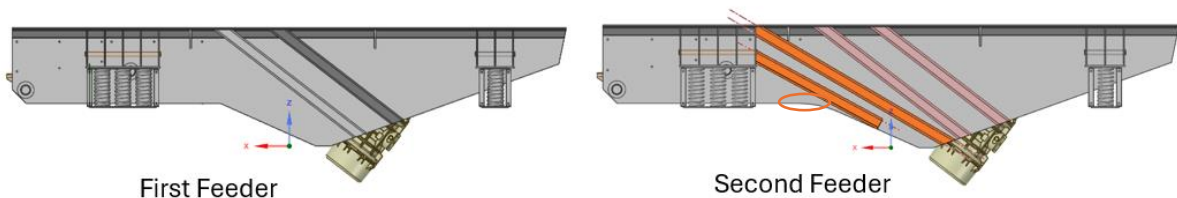


Figure 3.40: Illustration of the support that has been added.

As seen in Figure 3.41, the wall thickness of the intermediate part shown in orange was increased and the radius value was increased to strengthen the intermediate part and increase the material strength.

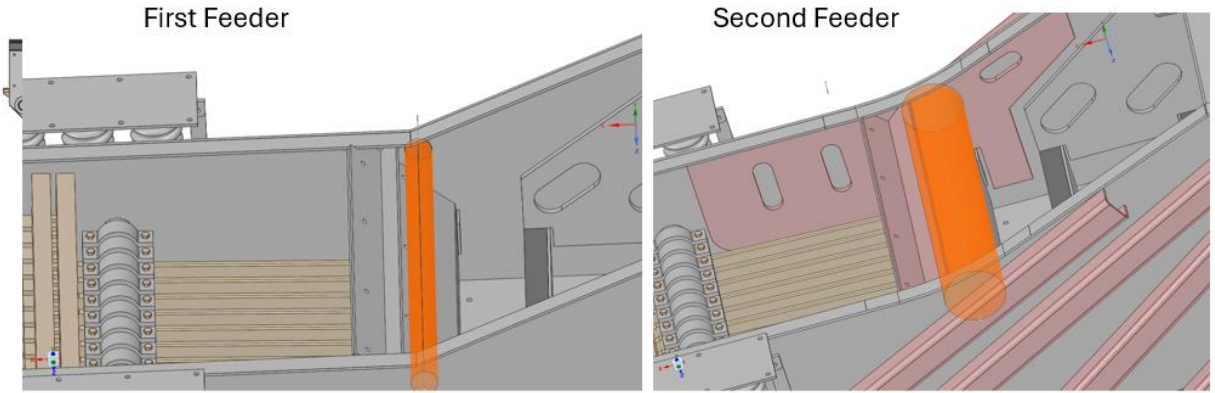


Figure 3.41: Reinforced version of the intermediate circular part.

3.2.1 Static Analysis

3.2.1.1 Preparations for Static Analysis for Second Feeder

In the second feeder configuration, preparations had to be made so that the stress assessment could be made accurately. The preparations of both feeders are the same. To compare and correctly evaluate the differences in results, the boundary conditions must be the same.

To ensure that the mesh procedure was completed correctly and without errors, a technique known as geometry cleaning was first applied. In this procedure, known as geometry cleaning, it is critical to minimize the elements that may affect the mesh creation process. As mentioned in Section 3.1.1.1, the entire preparation process was repeated for the second feeder. First, the bolts were removed, then the springs were modelled on ANSYS, the elements protecting the springs were suppressed, and finally, the density value of the material was changed. The studies carried out are indicated by the squared areas in Figure 3.42.

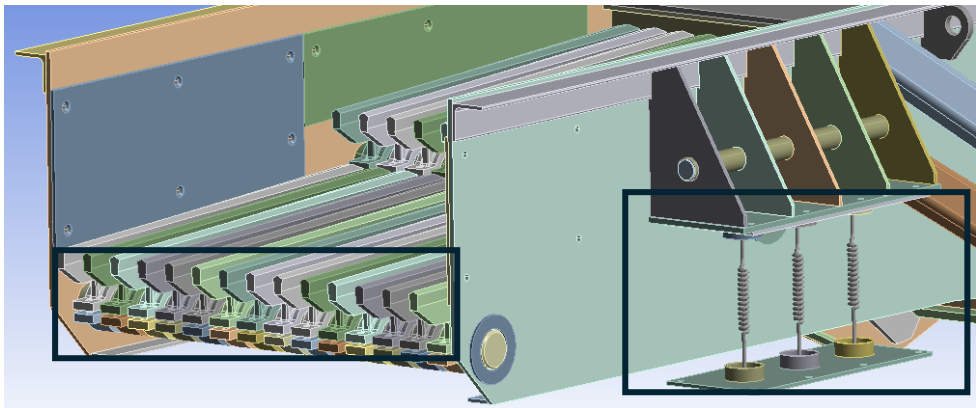


Figure 3.42: Display of geometric and structural changes made on feeder 2.

After the geometric and structural changes, the feeder contacts were checked, and the necessary adjustments were made to obtain an accurate analysis result. 712 active contacts were examined and checked. Figure 3.43 shows an example of contact control.

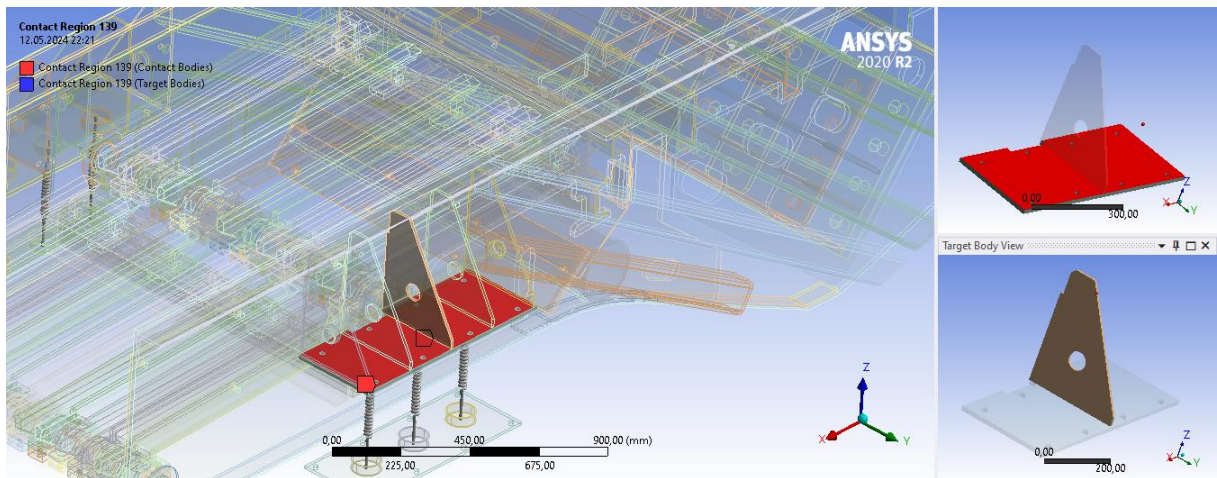


Figure 3.43: Sample contact control for the second feeder.

Mesh operations are carried out to produce a mesh that precisely represents the geometry and contact interfaces of the system after the contact conditions have been established. The simulation's correct representation of the physical behaviour of the system under study is ensured by this meshing procedure. The image seen in Figure 3.44 shows the mesh version of the device. The image seen in Figure 3.45 shows the content of the details of mesh tab. As can be seen from here, there are 556656 elements and 1623860 nodes on our geometry.

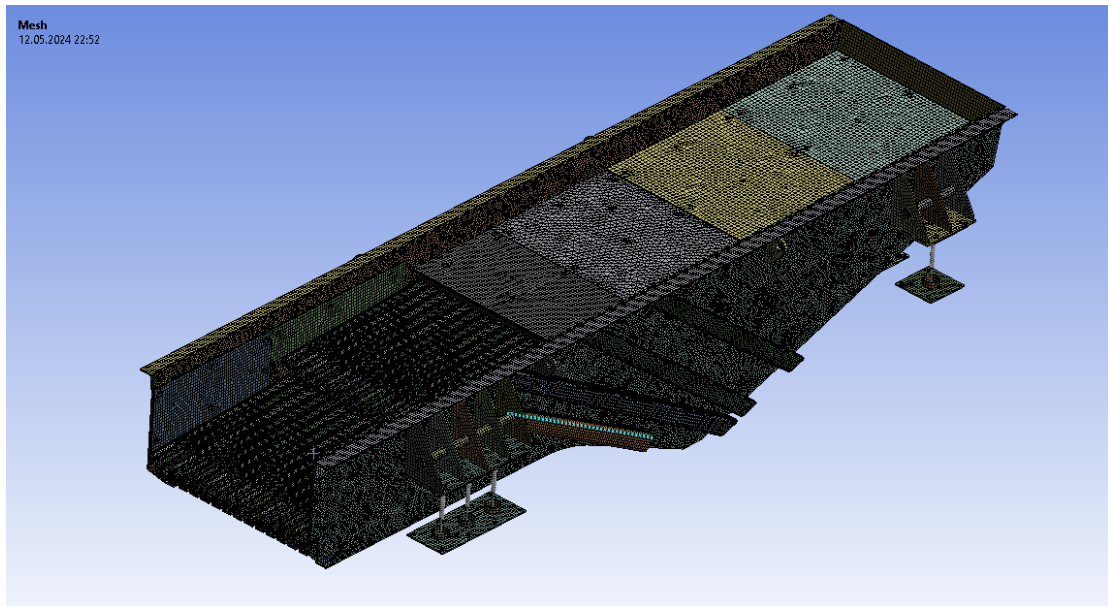


Figure 3.44: Ideal mesh view of vibrating feeder.

Details of "Mesh"	
Display	Use Geometry Setting
Display Style	Use Geometry Setting
Defaults	
Physics Preference	Mechanical
Element Order	Program Controlled
<input type="checkbox"/> Element Size	20, mm
Sizing	
Use Adaptive Siz...	No
<input type="checkbox"/> Growth Rate	Default (1,85)
<input type="checkbox"/> Max Size	Default (40, mm)
Mesh Defeaturing	Yes
<input type="checkbox"/> Defeature Size	Default (0,1 mm)
Capture Curvature	No
Capture Proximity	No
Bounding Box Di...	6651,1 mm
Average Surface ...	9616,1 mm ²
Minimum Edge L...	8,2252e-005 mm
Quality	
Check Mesh Qua...	Yes, Errors
Error Limits	Aggressive Mechanical
<input type="checkbox"/> Target Quality	0,5
Smoothing	High
Mesh Metric	None
Inflation	
Advanced	
Statistics	
<input type="checkbox"/> Nodes	1623860
<input type="checkbox"/> Elements	556656

Figure 3.45: Details of 'mesh' of second vibrating feeder.

Different local mesh techniques were used on our geometry in order to obtain high quality during the mesh work. The different techniques used are seen in Figure 3.46, and an example of the multi-zone technique is seen in Figure 3.46.

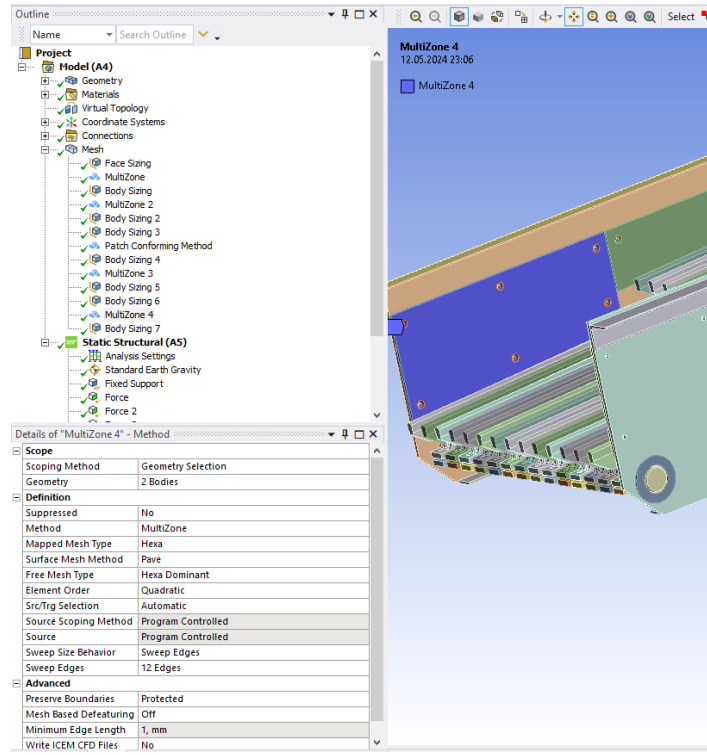


Figure 3.46: Details of 'multi-zone 4.'

As mentioned in 3.1.1.1, after the meshing process, the last steps toward static analysis were initiated. First, each plate was subjected to a force of 1000 N in compliance with the company's specifications, as mentioned in section 3.1.1.1. Then, each grid received an application of 71.43 N of force. After that, fixed supports were positioned. Standard gravity was additionally applied in the -Z direction. These situations are depicted in Figure 3.48 and Figure 3.47.

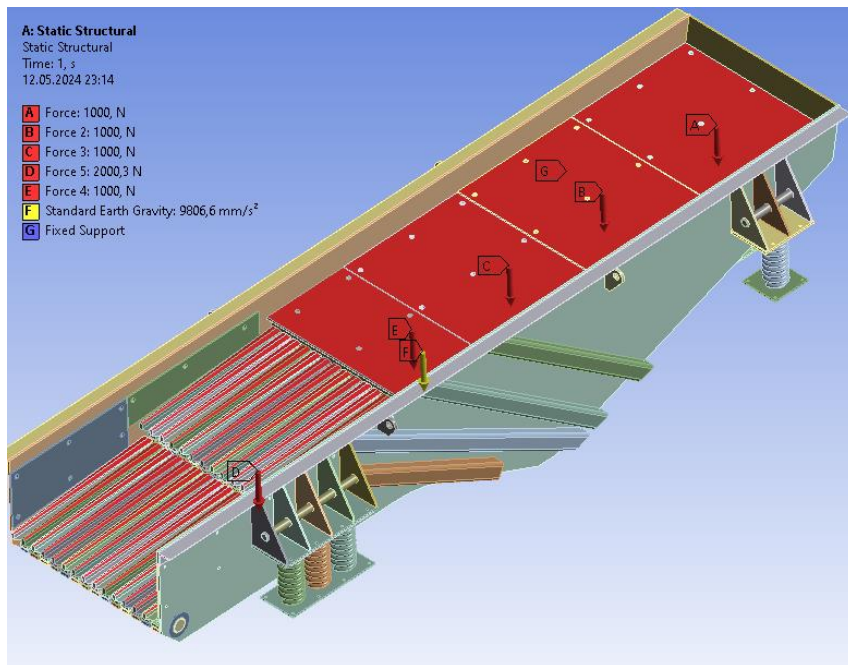


Figure 3.47: Boundary conditions of second feeder



Figure 3.48: Fixed support is shown of second feeder.

The ANSYS static analysis produced a number of significant findings, including total deformation, equivalent (Von-Mises) stress, and data from the spring probe.

Total Deformation offers a thorough understanding of the displacement along the structure because of applied forces by revealing how much the structure deforms under applied loads. This measurement is essential for evaluating the movement or deflection of the structure under load and for establishing if the deformation is within allowable bounds. The second feeder's total deformation is displayed below in Figure 3.49. The image's left deformation scale displays the hue and millimeter-level deformation. 58.395 mm was the highest deformation. There was 0 mm of lowest deformation.

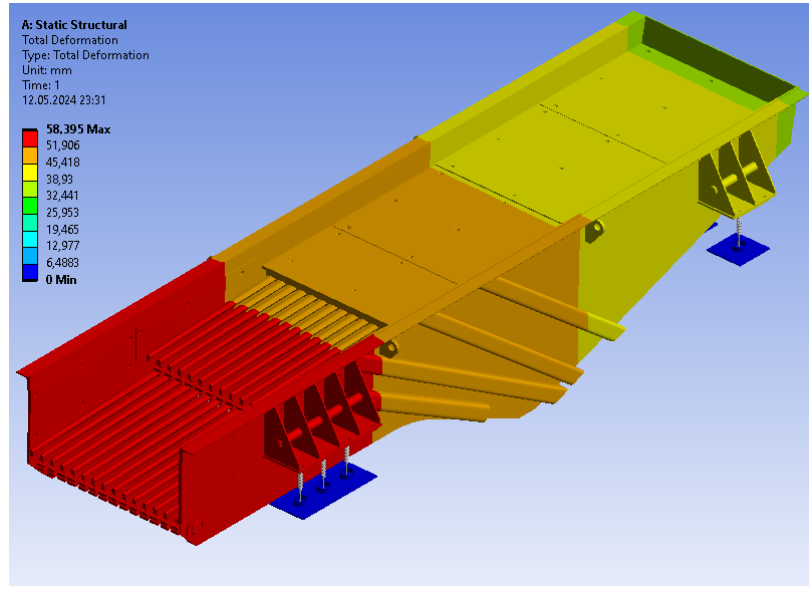


Figure 3.49: Static analysis of second feeder- total deformation.

By taking into account all primary stresses, including shear and normal stresses, equivalent (von-Mises) stress quantifies the stress condition within the structure. Based on a single scalar number, this value aids engineers in assessing possible structural failure. Engineering professionals can determine if a feeder is operating within safe bounds or is in danger of failing by comparing the von-Mises stress to the yield strength of the material. As shown in Figure 3.50 The final analysis result for the original feeder is the Equivalent (von-Mises) Stress analysis result. The greatest Equivalent (von-Mises) Stress found throughout the research was 557.74 MPa. 4.9588e-5 MPa is the lowest equivalent (von-Mises) stress.

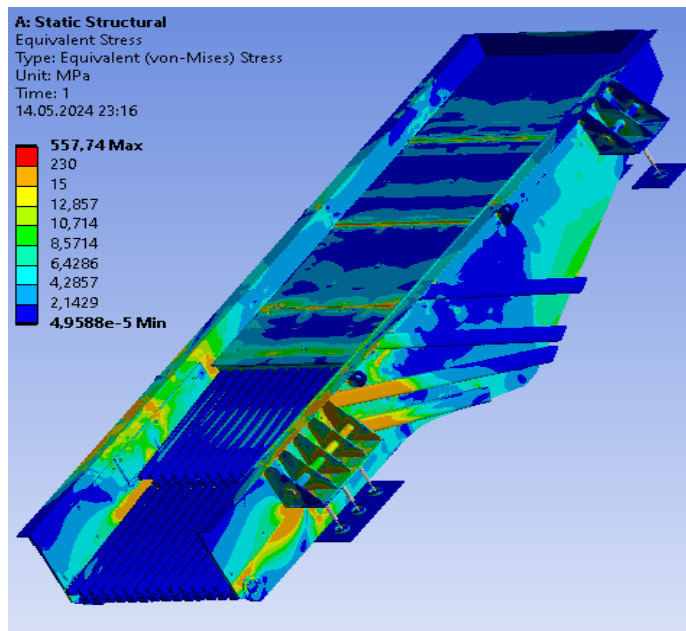


Figure 3.50: Static analysis of second feeder -equivalent (von-Mises) stress.

Spring Probe The information displayed in Figure 3.51 usually relates to findings from the examination of how spring components or connections behave inside the structure. Information like spring forces, displacements, and stresses are included in this data. It helps to understand how components that behave like springs contribute to the overall behaviour of the structure and makes sure those components work as intended. This is especially important for assemblies or systems that contain those components.

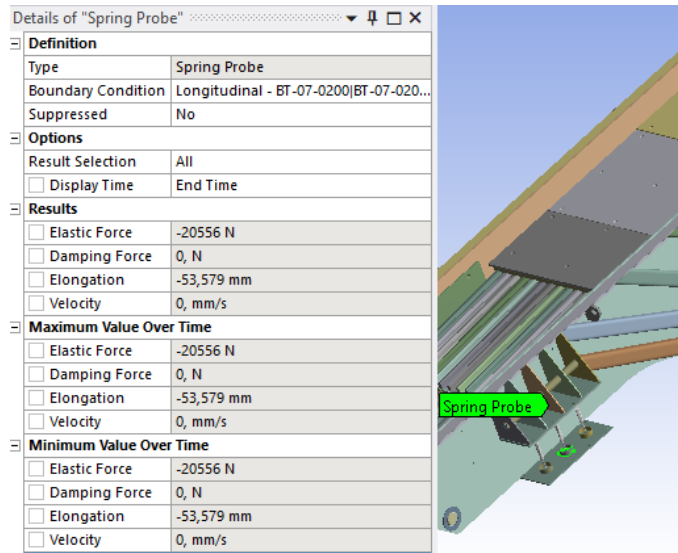


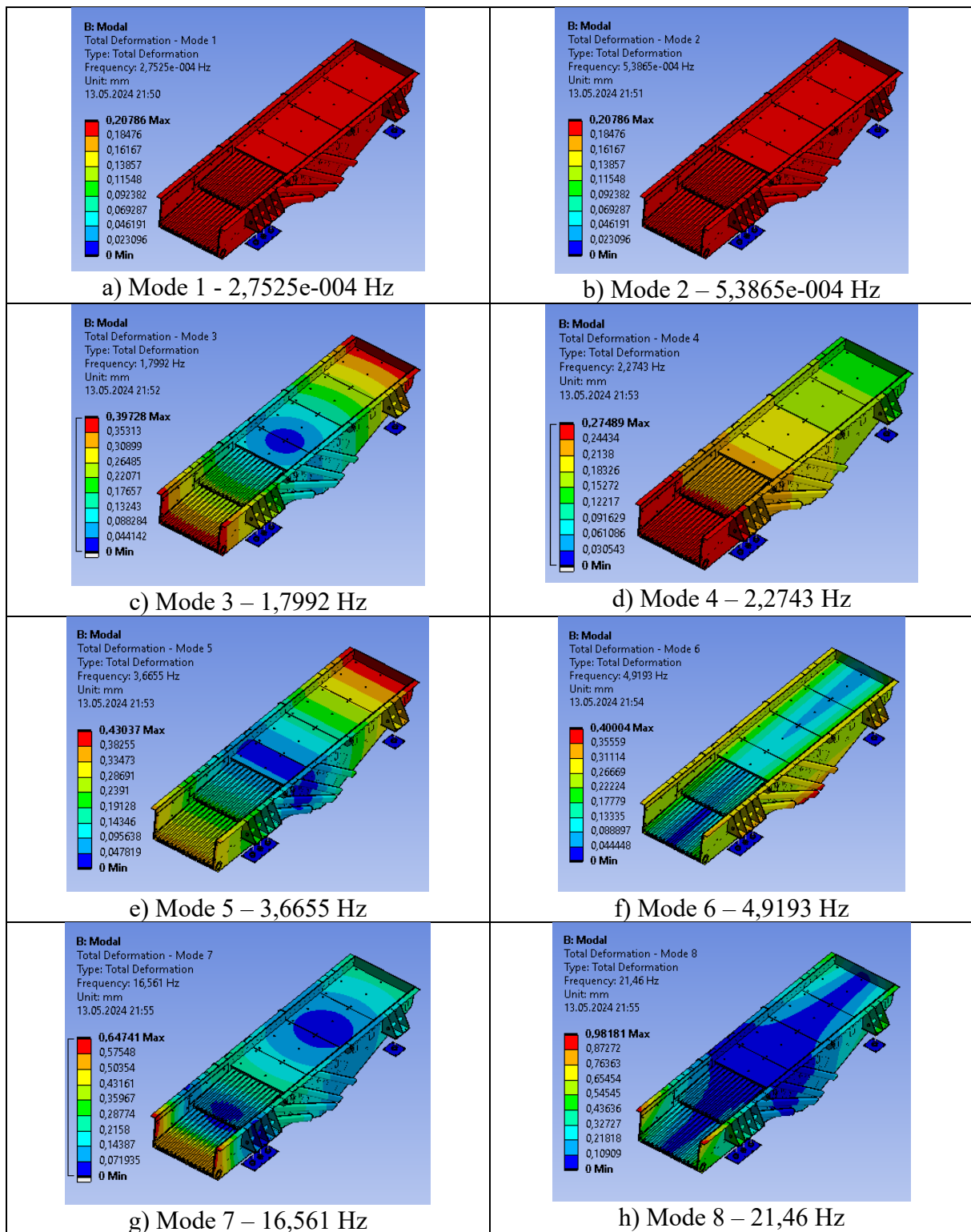
Figure 3.51: Static analysis of second feeder - spring probe

3.2.2 Modal Analysis

Modal analysis is a technique used to comprehend the dynamic reactions to nonlinear loads on a structure or system, as mentioned in 3.1.2. Finding the structures' inherent frequencies, mode shapes, and damping ratios are also part of this investigation. The vibrational frequencies of a structure under dynamic loads are represented by its natural frequencies. Establishing resonance frequencies that match natural frequency values is crucial for safeguarding the system's structural integrity and averting potentially harmful vibrations. The structure's mode forms display the vibrations at each of the natural frequencies.

In order to investigate the above-mentioned features for the second feeder, we conducted a modal analysis study on ANSYS software with a modal value of 10 for the second feeder.

Table 3.5: Modal analysis of second feeder.



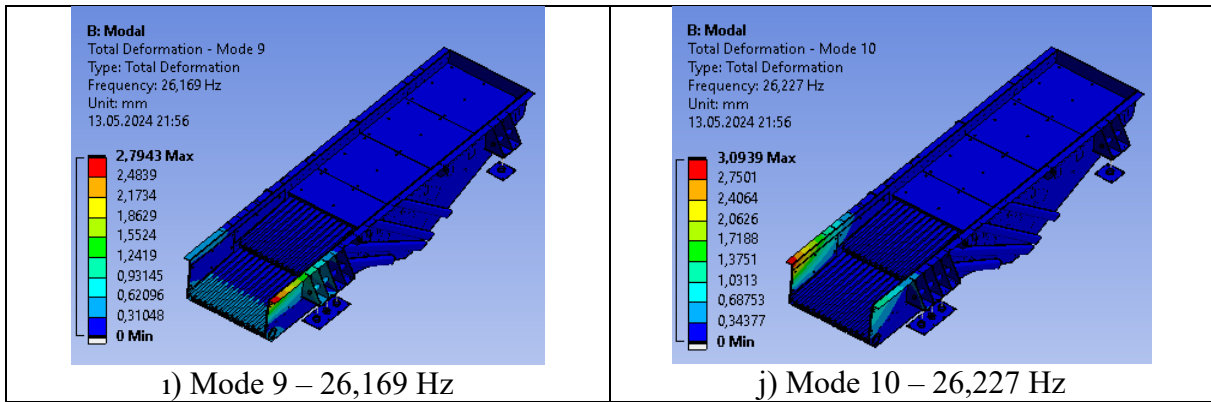


Table 3.5 shows the mode forms generated for the standard vibratory feeder at their natural frequencies. These mode forms roughly represent the mode shapes of the individual vibratory feeder components. The natural frequency of 5.141e-004 Hz is where mode 1 occurs. For mode 2 at 7.614E-04 Hz, which is the natural frequency. At 2.416 Hz, which is the normal frequency, Mode 3 now takes place. Having a natural frequency of 2.427 Hz in mode 4. Regarding mode 5, which has a 4.389 Hz natural frequency, it happens at 7.569 Hz, which is the natural frequency of mode 6. At 15.30 Hz, which is the natural frequency, mode 7 is present. At mode 8, with a natural frequency of 21.46 Hz. For mode 9 at the natural frequency of 26,169 Hz. At mode 10, it occurs at the natural frequency of 26,227 Hz. (Sanjay Oraon et al., 2019)

3.2.3 Transient Structural Analysis

Based on the objectives stated in Title 3.1.3, transient structural analysis was performed for the second feeder. In a transient structural study performed in ANSYS, we examined the dynamic behaviour of the mechanical system over time and under different loading scenarios. Through this research, we aimed to gain some understanding of the system's response to dynamic inputs.

The analysis's findings highlight important model parameters at strategic points, including displacements, velocities, accelerations, and stresses and strains. These findings explain the system's dynamic response and long-term evolution.

Additionally, the study facilitated the assessment of dynamic stresses to which the structure was subjected, pointing out possible trouble spots and directing further design revisions. By carefully evaluating these results, one can make intelligent decisions to improve the performance and structural integrity of the mechanical system.

In this section, boundary conditions, including static forces, are supported by certain dynamic forces. Centrifugal forces are dynamic forces produced by a vibromotor. BURÇELİK used the

same engine in the second feeder and provided the force data for the study shown in Figure 3.29: Technical data of vibro motor - 1, Figure 3.30: Technical data of vibro motor – 2.

Four moments are depicted in ‘Figure 3.31: Exciting force (centrifugal force) directions at four special moments. Respectively (left to right), reverse and inward direction, same direction and forward, reverse and outward, same direction and backwards (Ningning Xu et al., 2021)’, each of which represents a distinct direction of the vibrating feeder's stimulating force. The line arrow indicates the direction of the exciting force, while the dotted arrow indicates the direction of material movement. These four samples show the vibrating feeder's maximum amplitude and speed, accordingly. The material force nearly reached its maximum when the exciting force was directed consistently forward. The greatest compressive and tensile forces matched the reverse inward and reverse outward orientations of the stimulating force. Consequently, during the reciprocating vibration process, these four moments can represent the vibrating feeder's boundary conditions (Ningning Xu et al., 2021). Boundary conditions for the second feeder were defined using the work reported in this article.

Boundaries for the second feeder, as depicted in Figure 3.52. Force, Force2, Force3, Force4, and Force 5 are examples of static forces. Forces 6 through 8 are dynamic forces. Force 6 exerts both downward and upward force. Forces 7 and 8 exert forces to the left and right, respectively. All dynamic forces' numerical data are provided in the designated tables and are identical to the first feeder data in Table 3.2: Tabular data of force 6 and Table 3.3: Tabular data of force 7 (force 8 have same tabular data but opposite direction).

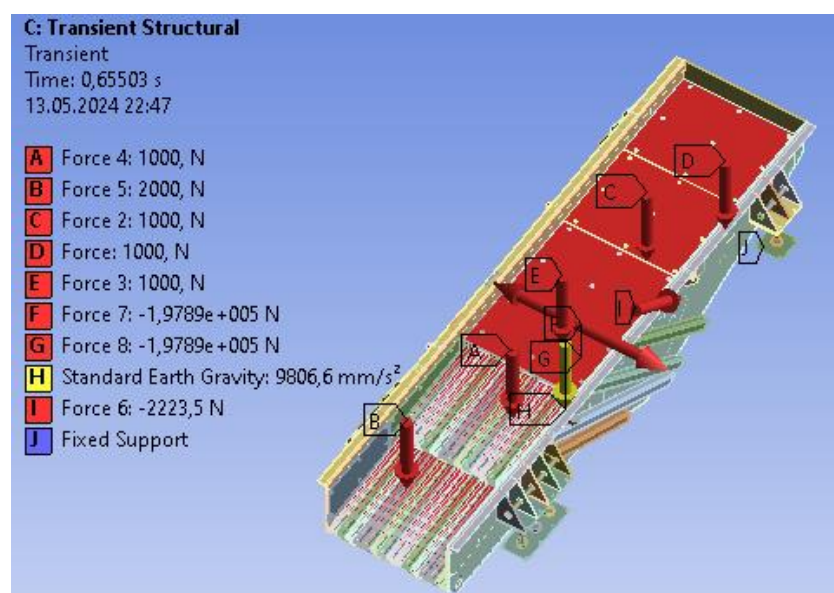


Figure 3.52: Boundary conditions of transient structural analysis for second feeder.

The dynamic forces and time-force relationship were distributed as tabular data according to 50 Hz and transmitted to ANSYS because the vibro motor in the second feeder operated at that frequency.

Based on the investigation, a 200-step equivalent stress result table was generated for the first feeder. Consequently, for maximum values, 1536.6 MPa is the greatest stress value and 107.04 MPa is the lowest stress value. 1.5582e-006 MPa is the lowest stress value and 6.1637e-005 MPa is the highest stress value for minimal values. In terms of average stress values, 14.095 MPa is the highest value and 0.93728 MPa is the lowest. Furthermore, the analysis's movements were seen to cause the springs to travel 35 mm in both directions (left and right) and 120 mm up and down.

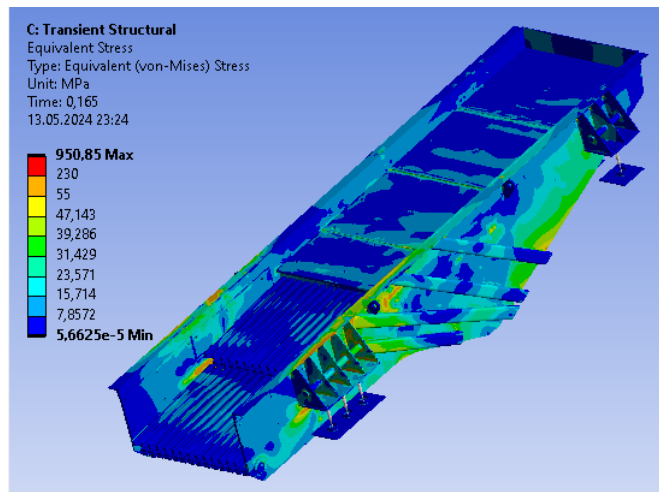


Figure 3.53: Result of transient structural analysis for second feeder (equivalent stress-time: 0.165 s)

The visual seen in Figure 3.53 is 0.165 s for the second feeder is the stress value per second, which is 950.85 MPa.

Table 3.6 shows the results of the transient structural analysis performed for the second feeder.

Table 3.6: Result of transient structural analysis

Time[s]	Minimum [MPa]	Maximum [MPa]	Average [MPa]	Time[s]	Minimum [MPa]	Maximum [MPa]	Average [MPa]
5,00E-03	1,61E-06	107,04	0,93728	0,505	2,71E-05	200,82	6,5302
1,00E-02	1,97E-06	141,76	2,5109	0,51	2,88E-05	347,69	6,7434
1,50E-02	2,93E-06	143,3	2,8186	0,515	2,95E-05	312,83	6,5066
2,00E-02	3,36E-06	249,43	4,0469	0,52	3,14E-05	429,4	6,1054
2,50E-02	7,07E-06	170,96	3,9949	0,525	3,41E-05	516,46	7,4299
3,00E-02	9,91E-06	307,69	5,5135	0,53	3,69E-05	596,79	8,1316
3,50E-02	1,36E-05	217,99	4,7391	0,535	4,13E-05	605,15	7,3872
4,00E-02	1,43E-05	295,83	6,3095	0,54	4,76E-05	724,17	6,883
4,50E-02	1,71E-05	279,92	5,8905	0,545	4,88E-05	819,29	8,6087
5,00E-02	2,43E-05	313,66	6,4866	0,55	4,83E-05	893,5	9,1789
5,50E-02	2,49E-05	289,4	6,6834	0,555	4,83E-05	900,29	8,3059
6,00E-02	2,49E-05	314,55	6,1905	0,56	4,85E-05	963,62	7,5046
6,50E-02	2,78E-05	315,43	8,1178	0,565	4,94E-05	1033,3	9,7117
7,00E-02	2,99E-05	285,46	6,2711	0,57	5,05E-05	1073	10,36
7,50E-02	3,41E-05	283,19	8,2829	0,575	5,23E-05	1063,7	9,1848

8,00E-02	3,82E-05	308,06	5,6998	0,58	5,51E-05	1135	8,2084
8,50E-02	4,40E-05	300,52	9,3046	0,585	5,57E-05	1179,7	10,58
9,00E-02	4,91E-05	323,01	6,7832	0,59	5,60E-05	1198	11,32
9,50E-02	4,83E-05	263,64	8,7793	0,595	5,64E-05	1179,5	9,8655
0,1	4,83E-05	291,48	5,5866	0,6	5,69E-05	1230	8,6583
0,105	4,89E-05	511,63	9,8229	0,605	5,73E-05	1253	11,229
0,11	5,03E-05	570,41	7,7612	0,61	5,78E-05	1242,8	11,869
0,115	5,19E-05	323,67	8,5642	0,615	5,82E-05	1205	10,237
0,12	5,44E-05	339,57	6,4007	0,62	5,87E-05	1220	8,9474
0,125	5,58E-05	602,59	10,188	0,625	5,91E-05	1231,3	11,739
0,13	5,55E-05	736,59	9,5775	0,63	5,95E-05	1211,6	12,346
0,135	5,54E-05	582,26	8,4514	0,635	5,98E-05	1173,3	10,37
0,14	5,54E-05	581,96	7,1892	0,64	6,02E-05	1200,8	8,9243
0,145	5,55E-05	764,85	10,558	0,645	6,04E-05	1194,2	11,81
0,15	5,56E-05	917,72	10,777	0,65	6,05E-05	1164,2	12,356
0,155	5,59E-05	823,19	8,5191	0,655	6,06E-05	1100,4	10,347
0,16	5,63E-05	849,95	7,5095	0,66	6,07E-05	1111,8	8,8512
0,165	5,66E-05	950,85	10,883	0,665	6,07E-05	1116,9	11,705
0,17	5,71E-05	1081,8	11,785	0,67	6,06E-05	1097,7	12,2
0,175	5,77E-05	1027,6	9,0022	0,675	6,04E-05	1055,7	10,114
0,18	5,83E-05	1053,3	8,552	0,68	6,03E-05	1055,7	8,5933
0,185	5,88E-05	1106,2	11,62	0,685	6,00E-05	1050,7	11,42
0,19	5,93E-05	1203,1	13,193	0,69	5,97E-05	1032,4	11,923
0,195	6,00E-05	1243,2	9,8694	0,695	5,94E-05	971,83	9,6839
0,2	6,05E-05	1304,3	9,7193	0,7	5,90E-05	973,5	8,2341
0,205	6,08E-05	1297	11,938	0,705	5,86E-05	992,68	10,89
0,21	6,12E-05	1325,3	13,99	0,71	5,81E-05	996,97	11,297
0,215	6,14E-05	1336,4	10,856	0,715	5,77E-05	925,89	9,2883
0,22	6,16E-05	1437,2	10,428	0,72	5,72E-05	914,81	7,8178
0,225	6,16E-05	1456,9	12,449	0,725	5,67E-05	944,32	10,317
0,23	6,16E-05	1461,8	14,095	0,73	5,63E-05	959,37	10,592
0,235	6,15E-05	1472	11,574	0,735	5,60E-05	887,59	8,7801
0,24	6,12E-05	1536,1	10,467	0,74	5,57E-05	867,25	7,3513
0,245	6,08E-05	1511,6	12,722	0,745	5,55E-05	882,82	9,7107
0,25	6,06E-05	1485	14,043	0,75	5,54E-05	894,36	9,9726
0,255	6,03E-05	1458,3	11,84	0,755	5,54E-05	785,27	8,3646
0,26	6,00E-05	1536,6	10,213	0,76	5,37E-05	762,68	7,0343
0,265	5,95E-05	1512,9	12,412	0,765	5,13E-05	794,25	8,9583
0,27	5,90E-05	1451,3	13,206	0,77	4,94E-05	792,24	9,0794
0,275	5,84E-05	1366,7	11,491	0,775	4,85E-05	675,07	7,8429
0,28	5,79E-05	1398,3	9,6901	0,78	4,83E-05	645,08	6,608
0,285	5,74E-05	1373	11,589	0,785	4,85E-05	661,54	8,3149
0,29	5,69E-05	1315,2	12,141	0,79	4,92E-05	652,83	8,2382
0,295	5,64E-05	1240,4	10,403	0,795	4,22E-05	542,34	7,295
0,3	5,60E-05	1218,1	8,6623	0,8	3,73E-05	524,21	6,252
0,305	5,57E-05	1157,9	10,464	0,805	3,28E-05	501,26	7,5189
0,31	5,54E-05	1091,8	10,682	0,81	2,95E-05	458,36	7,3736
0,315	5,33E-05	973,86	9,0089	0,815	2,87E-05	348,67	6,8308
0,32	5,18E-05	927,68	7,2392	0,82	2,59E-05	355,31	5,9182
0,325	5,05E-05	870,63	8,8811	0,825	2,49E-05	295,57	6,8797
0,33	4,93E-05	808,93	8,8073	0,83	2,64E-05	270,74	6,5489
0,335	4,86E-05	650,75	7,5846	0,835	2,21E-05	198,57	6,372
0,34	4,83E-05	567,96	6,0357	0,84	1,68E-05	257,83	5,7216
0,345	4,83E-05	551,17	7,6227	0,845	1,43E-05	186,83	6,3792
0,35	4,83E-05	586,89	7,4424	0,85	1,41E-05	227,5	6,124
0,355	4,85E-05	433,3	6,4004	0,855	1,23E-05	210,09	6,1916
0,36	4,91E-05	282,03	5,3827	0,86	6,66E-06	304,02	5,843
0,365	4,56E-05	301,57	6,5157	0,865	2,01E-06	211,79	6,2608
0,37	4,06E-05	395,97	6,6943	0,87	4,53E-06	232,62	6,0795
0,375	3,71E-05	227,6	6,2154	0,875	2,12E-06	296,75	6,4419
0,38	3,50E-05	244,27	5,5114	0,88	9,23E-06	332,55	6,0595
0,385	3,27E-05	300,24	6,7506	0,885	7,22E-06	314,72	6,5735
0,39	3,05E-05	475,66	6,5473	0,89	7,20E-06	367,35	6,3088
0,395	2,50E-05	391,92	6,8639	0,895	8,41E-06	372,44	6,686
0,4	1,66E-05	448,04	6,0777	0,9	9,55E-06	375,66	6,2712
0,405	6,74E-06	459,75	7,2859	0,905	1,05E-05	359,75	6,7428
0,41	4,04E-06	581,88	6,9054	0,91	1,56E-06	443,07	6,6716
0,415	4,56E-06	554,35	7,4286	0,915	7,62E-06	391,93	6,8339
0,42	7,23E-06	572,8	6,7347	0,92	7,39E-06	400,8	6,3315
0,425	7,28E-06	557,96	7,5458	0,925	1,37E-05	366,07	6,8933
0,43	1,01E-05	616,29	7,0802	0,93	1,78E-05	500,57	6,8514
0,435	9,98E-06	605,39	7,6647	0,935	2,80E-05	371,3	6,77
0,44	9,71E-06	587,81	6,8108	0,94	3,17E-05	358,51	6,0256
0,445	1,13E-05	561,66	7,5298	0,945	3,50E-05	344,43	6,9778
0,45	1,05E-05	568,6	7,0083	0,95	3,82E-05	491,08	6,9964
0,455	7,13E-06	550,89	7,4524	0,955	4,26E-05	310,9	6,597
0,46	8,18E-06	491,92	6,6023	0,96	4,59E-05	250,63	5,6201

0,465	7,14E-06	434,69	7,1503	0,965	4,86E-05	315,05	6,8955
0,47	3,30E-06	408,38	6,7146	0,97	4,83E-05	484,39	7,1698
0,475	7,58E-06	363,71	6,8749	0,975	4,83E-05	297,57	6,3925
0,48	1,09E-05	308,85	5,9946	0,98	4,86E-05	224,57	5,3059
0,485	1,77E-05	224,96	6,5569	0,985	4,94E-05	418,77	7,2905
0,49	2,49E-05	240,19	6,1796	0,99	5,03E-05	568,63	7,8335
0,495	2,49E-05	171,46	6,1121	0,995	5,16E-05	461,09	7,0259
0,5	2,55E-05	235,81	5,3472	1	5,36E-05	498,05	5,9916

3.2.4 Fatigue Life Analysis

As explained in 3.1.4, fatigue analysis of the structure was performed for the second feeder by applying the same method and technique.

Numerous important findings from the ANSYS fatigue life analysis provide light on the longevity and durability of the structure under cyclic stress scenarios.

The evaluation of the structure's anticipated life under cyclic loads is the main result. Engineers determine how many loading cycles a structure can sustain before fatigue failure, which aids in assessing a structure's dependability and durability.

The critical structural points most likely to experience fatigue damage are identified. This makes it easier for engineers to concentrate on mitigating techniques, such as better material selection or component redesigns, to maximize designs and guarantee structural integrity during the planned service life.

BURÇELİK said that this feeder broke down in about 1 month. In the Fatigue Life Analysis, we concluded that the first feeder broke at 10^4 cycles during use in the field, but the value of the second feeder, which we are currently analysing, at the same point was obtained at 10^6 cycles shown in Figure 3.54. This shows that, as we mentioned in the results, our feeder does not experience any problems considering the stress life graph.

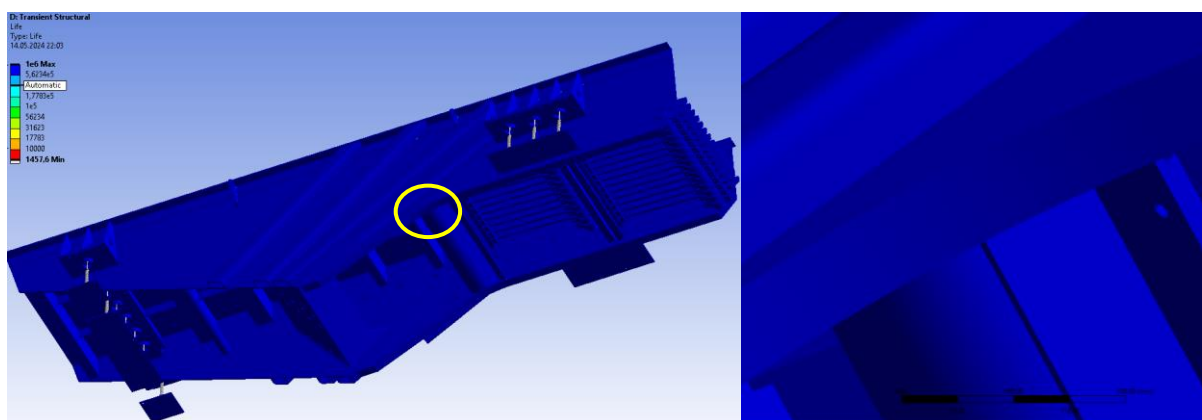


Figure 3.54: Result of transient structural – fatigue tool (life)

3.2.5 Effect of Feeder Meshing and Convergence Study on Analysis

As mentioned by Chandravanshi and Mukhopadhyay, 2017, in order to choose the right mesh number, meshes with different number of elements were created using the convergence principle and the maximum stress values obtained by static analysis were compared. The compared and obtained stress values were combined with the number of nodes and stress values, as stated in Figure 3.55, to obtain points of convergence and the network structure with the minimum number of nodes was selected.

The purpose of this study is to both obtain the correct mesh number and prevent excessive CPU times. If our systems operate at maximum efficiency, it may take days or even weeks to analyse a geometry with a high mesh structure.

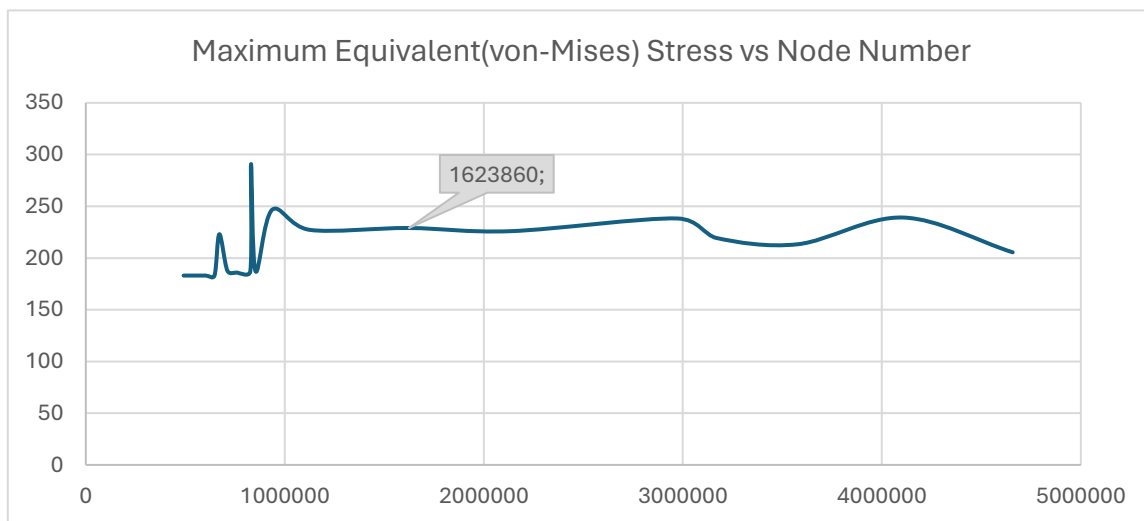


Figure 3.55: Graph of maximum stress (von-misses) vs number of nodes

As can be seen with the grey colour label in Figure 3.55, as a result of the analysis made on the object, the network structure with the lowest number of nodes in which linearity occurs in our graph was deemed sufficient for our mesh study. The number of nodes at this point is 1623860.

4 Result and Discussion

4.1 Conclusion of Thesis

The purpose of BURÇELİK's research was to examine two different feeder designs. As reported by the manufacturer, the first feeder became dysfunctional at the end of its life due to the breakage of its side plates, as shown in Figure 4.1. As a result, a revised second feeder was designed, different from the first feeder design. The differences in the feeders are shown in Figure 3.40 and Figure 3.41 In the second feeder, in addition to the first feeder, two different beams were added to the side outer walls, a radius transition was added instead of the hard transition in the broken area, and the wall thickness and radius of the cylindrical part under the gratings, which is the bridge between the two, was increased. Later, it was observed that the second feeder sent to the field by the company could operate without any distortion.



Figure 4.1: Broken area of the first feeder

The second feeder worked flawlessly. Four critical evaluations were performed to perform the necessary static and dynamic analyses: static analysis, modal analysis, dynamic analysis and fatigue analysis. To ensure the applicability and real-life usability of these analyses, error-free results had to be obtained. Many preparatory steps were meticulously implemented to ensure sensitive and near-accurate analyses, and analyses were carried out using existing data, information and documents provided by BURÇELIK.

There were two different results obtained during the static analysis. These are Total Deformation and Equivalent (von-Mises) Stress results. These results were used to compare two different feeders. Considering the total deformation results, it was observed that the first feeder had a minimum of 0 mm and a maximum of 49.557 mm, and a minimum of 0 mm and

a maximum of 58.395 mm for the second feeder. The reason why these results are so high is that the stretching amount of the springs is shown in the analysis. The minimum value being 0 in both feeders shows us that there is no deformation at those points or areas. The red and orange part in the first feeder in Figure 3.26 takes up more space than the red and orange part in the second feeder in Figure 3.49. Additionally, it was observed that there was less deformation on the back of the second feeder compared to the first feeder. Based on the above explanation, it has been concluded that the revision process on the second feeder is more effective than the old feeder. Considering the Equivalent (von-Mises) Stress results, in the first feeder in Figure 3.27 the lowest result was 0.00014889 MPa and the highest was 595.11 MPa, and in the second feeders in Figure 3.50 the lowest result was 4.98e-5 MPa and the highest was 557.74 MPa. First of all, the reason why the maximum values are so high is due to the loads on the springs. In the results obtained, there is no other part other than the springs that exceeds 230 MPa. If we talk about the difference between the two feeders, the stress distribution on the inside of the side walls of the first feeder is higher than that of the second feeder. The reason for this situation is interpreted as the beams added in the second feeder reducing this stress intensity from the walls and overlapping them. Additionally, considering the maximum values in the first and second feeders, a decrease of approximately 48 MPa was observed. In the first feeder, the max stress value of the broken area shown in Figure 4.2 was 142.38 MPa, and in the second feeder, the stress value was 84.495 MPa. The difference between these values shows that the optimization yielded successful results.

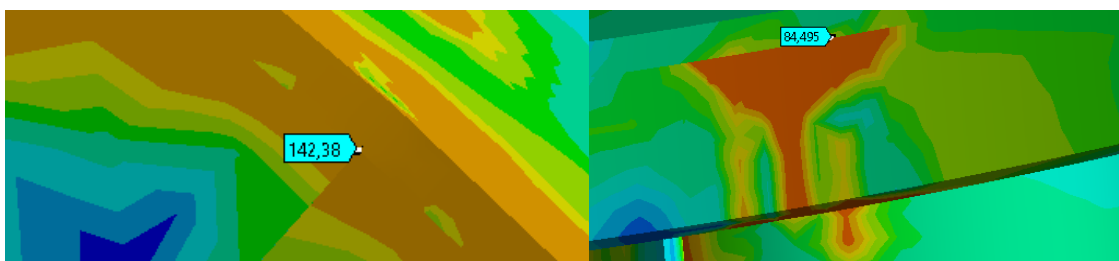


Figure 4.2: Max stress values in the fractured area (first feeder on the left, second feeder on the right).

In the modal analyses performed for both feeders, 10 mode results were obtained. The natural frequency values of the first feeder are between 5.141e-004 and 22.51 Hz. The natural frequency values of the second feeder are between 2.7525e-004 and 26.227 Hz. The results obtained reveal a critical natural frequency value in mode 7 for both feeders. The reason for this is that the operating frequency of the feeder is 15 Hz and the natural frequency values obtained in the results are close to the operating frequency. In addition, the values obtained are generally

within the frequency value range where the feeder can operate, which means that our feeder corresponds mode 1 to mode 6 natural frequency values from the moment it starts to work until it reaches 15 Hz. This means that if the feeder continues to operate at these six natural frequency values, it may cause the feeder to resonate and experience destructive effects. When we look at mode 7 in both feeders, we see a high deformation value at the very end of the grids. We think that the general natural frequency values of our feeder being close to the operating value may cause the damage to our feeder shown in Figure 4.1.

The boundary conditions in the dynamic analyses of both feeders are the same and the necessary information was provided to us by BURÇELİK. Static loads at boundary conditions are the same as in static analysis. Since dynamic loads change depending on time, table data of 200 steps and 1 second were prepared according to the vibro motor operating at 50 Hz. These data are shown in the Table. Dynamic loads were sorted according to the centrifugal force of the vibro motor, and the centrifugal force applied by each motor was transferred to ANSYS as 198996 N. These data are seen in Table 3.2 and Table 3.3. As a result of the simulation we obtained, the elliptical movement made by the feeders was approved by BURÇELİK and our consultant. In addition, it has been proven that the lengthening and shortening amounts of the springs are close to the real results. The equivalent (von-Mises) stresses obtained in the first feeder are as follows; For maximum values, the highest stress value is 1541.4 MPa and the lowest stress value is 80.306 MPa. For minimum values, the highest stress value is 4.6156e-005 MPa and the lowest stress value is 3.1879e-007 MPa. For the average stress value, the largest value is 16.919 MPa and the smallest value is 0.98827 MPa. In addition, it was observed that the springs changed 40 mm forward-backward and 90 mm up-down due to the movements resulting from the analysis. The results on the second feeder are as follows: For maximum values, 1536.6 MPa is the greatest stress value and 107.04 MPa is the lowest stress value. For minimum values, 1.5582e-006 MPa is the lowest stress value and 6.1637e-005 MPa is the highest stress value. According to the average stress values, 14.095 MPa is the highest value and 0.93728 MPa is the lowest value. It was also observed that the movements made in the analysis caused the springs to move 35 mm in both directions (left and right) and 120 mm up and down. It is thought that the biggest reason why these results are higher than static analyses is that the centrifugal force of vibro motors plays an important role in feeder movement. There are various factors that can contribute to differences in results, such as load application, time dependence, material behaviour, inertia effects, frequency effects. (Bathe, K.J., 2006) (Zienkiewicz, O.C. and Taylor, R.L., 2005)

Fatigue analysis performed on two feeders designated first feeder and second feeder gave opposite results. First feeder experienced structural failure after 14 days of operation, calculated in Title 3.1.4, due to cyclic loading accumulation that exceeded the fatigue strength limit of the feeder material. In contrast, second feeder exhibited an infinite fatigue life, i.e. a cycle of 10^6 .

While performing the analysis, as you can see in Figure 4.3, the analysis type we chose is stress life. In order to interpret the value, we obtained for the secondary feeder, the S-N diagram seen in Figure 4.4 shows us that the result of 10^6 we obtained gives the infinite life value. This shows the ability to sustain an indefinite number of load cycles without experiencing structural failure due to fatigue on the stress life graph. As a result of the analysis, the points where structural damage begins are seen in Figure 4.5.

Details of "Fatigue Tool"	
Domain	
Domain Type	Time
Materials	
Fatigue Strength Factor (Kf)	0,8
Loading	
Type	Fully Reversed
<input type="checkbox"/> Scale Factor	1,
Definition	
<input type="checkbox"/> Display Time	End Time
Options	
Analysis Type	Stress Life
Mean Stress Theory	Mean Stress Curves
Stress Component	Equivalent (von-Mises)
Life Units	
Units Name	cycles
1 cycle is equal to	1, cycles

Figure 4.3: Details of 'fatigue tool.'

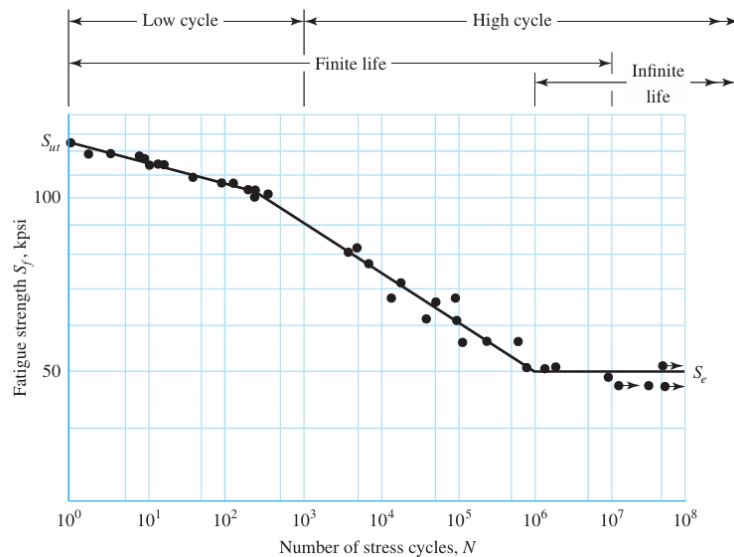


Figure 4.4: S-N diagram.

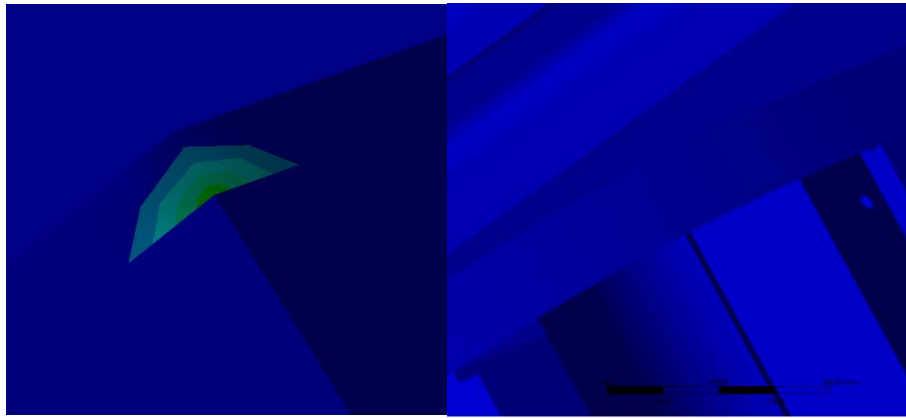


Figure 4.5: Fatigue life result values in the fractured area (first feeder on the left, second feeder on the right).

The different results observed in the fatigue analysis of first feeder and second feeder can be attributed to several factors. Differences in material properties, design considerations, operating conditions, maintenance practices, and manufacturing quality collectively affect the fatigue behaviour of mechanical components.

First feeder may be made of a material with lower fatigue strength compared to second feeder, leading to premature failure under cyclic loading conditions. In contrast, second feeder is likely to include design features that increase fatigue resistance and provide infinite fatigue life.

Operational parameters such as applied loads, cycle frequency and environmental factors can also affect fatigue behaviour. First feeder may have been exposed to more severe loading conditions or environmental influences that accelerated the accumulation of fatigue damage.

Proper maintenance practices and regular inspections can help detect and address potential fatigue-related problems, thereby extending the fatigue life of mechanical components. Additionally, manufacturing quality plays an important role in determining fatigue performance; higher quality standards result in increased fatigue resistance.

As a result, static analysis, modal analysis, transient structural analysis and fatigue life analysis were performed for both feeders. The project diagram can be seen in Figure 4.6. Comparisons were made in both design and analysis results for the two feeders, and necessary explanations were tried to be made for the differences in the results.

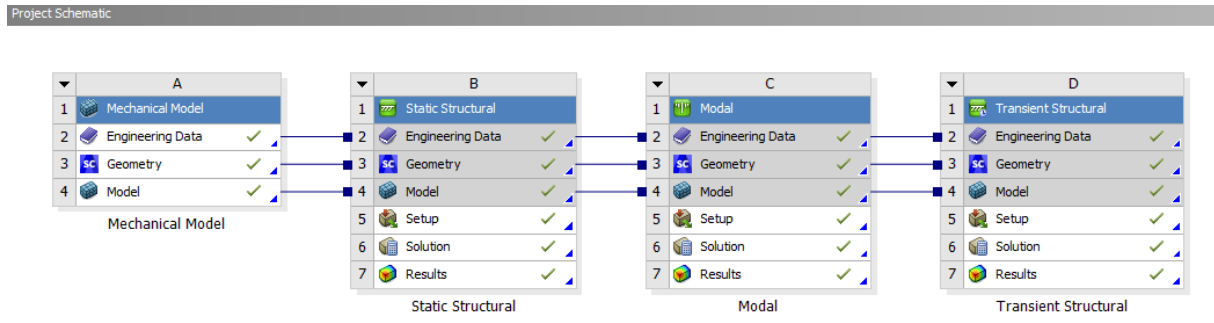


Figure 4.6: Project schematic of both feeders

4.2 Recommendations for Future Works

Enhanced Material Selection: A detailed review of the material selection process for vibrating feeder components should be conducted, taking into account analysis and factors such as strength, durability and fatigue resistance. To extend the life of the equipment, advanced materials or coatings that offer superior performance under operating conditions should be explored.

Refinement of Structural Design: Information obtained from analyses conducted on existing vibratory feeders should be leveraged to improve the structural design of future iterations. Particular attention should be paid to areas identified as prone to failure in the broken feeder, and design changes or reinforcements should be implemented to reduce stress concentrations and improve structural integrity, as in the second feeder.

Dynamic Analysis Optimization: To accurately capture the vibration behaviour of feeders under changing operating conditions, the dynamic analysis techniques used, such as modal and transient structural analysis, must be further optimized. This may include improving meshing strategies, boundary conditions, and load assumptions to improve the predictive capabilities of the analyses.

Integrated Fatigue Assessment: Fatigue assessment methodologies should be integrated into the design and analysis process to evaluate the long-term structural integrity of vibrating feeder components. Factors such as cyclic loading, material fatigue properties, and operational lifespan must be considered to proactively identify potential fatigue failure mechanisms and implement appropriate fatigue mitigation strategies.

Continuous Monitoring and Maintenance: For vibrating feeders in operation, a comprehensive monitoring and maintenance program should be implemented that includes condition monitoring techniques such as vibration analysis and thermography to detect early

signs of deterioration or failure. Proactive maintenance programs based on equipment usage and environmental factors should be developed to minimize the risk of unexpected malfunctions.

Validation Testing and Field Trials: Verification tests and field trials of revised vibrating feeder designs under real-world operating conditions should be conducted to verify the effectiveness of design improvements and analysis methodologies. Performance data and feedback should be collected from field trials to enable further improvements and adapt to end-user requirements.

Knowledge Transfer and Documentation: Facilitate knowledge transfer and documentation of lessons learned from the design, analysis and performance evaluation of vibrating feeders for future projects. A central repository of best practices, design guidelines, and failure analysis reports should be established to facilitate continuous improvement and dissemination of information throughout the organization.

Collaborative Research and Development: Collaborative research and development initiatives with industry partners, academic institutions, and research organizations should be encouraged to leverage expertise and resources in developing vibrating feeder technology. Opportunities for joint research projects, technology transfer agreements or consortium-based initiatives should be explored to accelerate innovation and address common challenges in the field.

By implementing these recommendations, future studies can build on the foundation established through the analysis and evaluation of vibrating feeders and ensure continuous improvement in design reliability, performance and longevity.

4.3 Evaluation of Current Work from MUDEK Perspective

4.3.1 Economic Analysis

The economic analysis of the vibrating feeders project indicates both positive and negative aspects. While the initial investment in conducting comprehensive analyses such as static, modal, transient structural, and fatigue analyses could be substantial, it proved to be beneficial in identifying critical issues and improving the design. However, the subsequent failure of one feeder on the 14th day suggests potential shortcomings in the initial design and analysis, leading to increased costs associated with repairs, downtime, and potential reputation damage. The

revised feeder, designed based on the analysis findings, showcases the economic benefits of investing in thorough engineering analyses to ensure product reliability and longevity. Overall, while there were initial costs, the long-term economic benefits of conducting in-depth analyses are evident through the infinite life of the revised feeder.

4.3.2 Real-Life Conditions

The real-life conditions under which the vibrating feeders operate play a crucial role in their performance and longevity. The failure of one feeder after only 14 days highlights the importance of accurately simulating real-world conditions during the analysis phase. Factors such as material properties, operating environment, vibration frequencies, and loading conditions must be carefully considered to develop a robust and reliable design. The revised feeder, which demonstrated infinite life under real-life conditions, indicates that the engineering analyses effectively accounted for these factors, resulting in a more resilient and durable product.

4.3.2.1 Producibility

Producibility refers to the ease and efficiency with which a product can be manufactured. In the case of the vibrating feeders, the engineering analyses should not only focus on performance but also on manufacturability. Complex designs or material requirements that are difficult to procure could hinder the producibility of the feeders, leading to increased manufacturing costs and potential delays. Therefore, it is essential to strike a balance between performance requirements and manufacturability constraints. The revised feeder, while meeting performance criteria, should also be evaluated from a manufacturability standpoint to ensure scalability and cost-effectiveness in production.

4.3.2.2 Constraints

Various constraints impact the design and analysis of vibrating feeders, including time, budget, material availability, and regulatory requirements. Meeting project deadlines while maintaining quality standards is often challenging, especially when conducting thorough engineering analyses. Additionally, budgetary constraints may limit the extent of analyses or the use of premium materials, potentially compromising the final product's performance and reliability. Regulatory requirements, such as safety standards, must also be adhered to throughout the design and analysis process to ensure compliance and mitigate risks. Balancing these constraints while delivering a reliable and cost-effective solution is essential for project success.

REFERENCES

1. Zhang, Y. L., Liu, X. P., & Hou, C. L. (2015). Key Technology Research on Dynamic Design of a Large Vibrating Screen. *Applied Mechanics and Materials*, 709, 9-14. <https://doi.org/10.4028/www.scientific.net/AMM.709.9>
2. Fanghella, P. (2021). Multibody modelling of a linear feeder for bulk materials. In *Multibody Mechatronic Systems: Papers from the MuSMe Conference in 2020* 7 (pp. 265-273). Springer International Publishing. https://doi.org/10.1007/978-3-030-60372-4_30
3. Li, L., Li, Y., Wang, J., & Ma, X. (2019). SIMULATION STUDY ON THE INFLUENCE OF VARIABLE FREQUENCY AND INPUT QUANTITY ON FEEDING ABILITY OF VIBRATORY FEEDER. *Academic Journal of Manufacturing Engineering*, 17(3).
4. Gitiaray, M., Taghvaei, S., & Hashemnia, K. (2023). DEM Study of the design parameters of a linear vibratory feeder in packaging black pepper seeds. *Granular Matter*, 25(2), 39. <https://doi.org/10.1007/s10035-023-01325-y>
5. Zhu, W., Wang, H., & Dong, L. (2012). 877. Design and performance analysis of dual vibrating motors self synchronous shaker with balanced elliptical motion. *Journal of Vibroengineering*, 14(4).
6. Singh, C., & Chandravanshi, M. L. (2023). Dynamic analysis and performance assessment of a vibratory feeder for different motor positions on trough. *Mechanics Based Design of Structures and Machines*, 51(11), 6453-6470. <https://doi.org/10.1080/15397734.2022.2047720>
7. Khoshdast, H., Jalilifard, S., & Khoshdast, H. (2021). Dynamic analysis of a dashpots equipped vibrating screen using finite element method. *Physicochemical Problems of Mineral Processing*, 57(1), 112-126. <https://doi.org/10.37190/ppmp/130001>
8. Wiendahl, H. P., & Ahrens, H. (1984). Design of vibratory feeders. *Assembly automation*, 4(4), 198-203. <https://doi.org/10.1108/eb004638>
9. Chandravanshi, M. L., & Mukhopadhyay, A. K. (2017). Dynamic analysis of vibratory feeder and their effect on feed particle speed on conveying surface. *Measurement*, 101, 145-156. <https://doi.org/10.1016/j.measurement.2017.01.031>
10. Dyrda, V., Kobets, A., Pukhalskyi, V., Kozub, Y., & Chernii, O. (2019). Dynamics of vibratory partitioned feeders for the uranium ore drawing and feeding (Doctoral dissertation, Інститут геотехнічної механіки ім. МС Полякова НАНУ). <https://doi.org/10.1051/e3sconf/20191090023>

11. Chandravanshi, M. L., & Mukhopadhyay, A. K. (2015). Experimental modal analysis of the vibratory feeder and its structural elements. International Journal of Applied Engineering Research, 10(13), 33303-33310.
12. Vaysman, V., Strunnikova, N., Chukurna, O., Dobrovolskyi, V., & Kassien, O. (2021, September). Improvement of the quality of the human environment by transporting and stabilizing sewage sludge for further processing. In Grabchenko's International Conference on Advanced Manufacturing Processes (pp. 445-454). Cham: Springer International Publishing. https://doi.org/10.1007/978-3-030-91327-4_44
13. Ramatsetse, B., Mpofu, K., & Makinde, O. (2017). Failure and sensitivity analysis of a reconfigurable vibrating screen using finite element analysis. Case studies in engineering failure analysis, 9, 40-51. <https://doi.org/10.1016/j.csefa.2017.04.001>
14. Guo, N. Q., Liu, W., & Huang, W. P. (2012). Finite Element Analysis of the Screen Box of the Combined Vibrating Screen Based on ANSYS. Applied Mechanics and Materials, 128, 1316-1320. <https://doi.org/10.4028/www.scientific.net/AMM.128-129.1316>
15. He, W. F., & Xian, A. M. (2013). Statics and modal analysis for large vibrating screen. Applied Mechanics and Materials, 380, 136-139. <https://doi.org/10.4028/www.scientific.net/AMM.380-384.136>
16. Xu, N., Wang, X., Yu, C., Gong, S., Lin, D., & Su, X. (2021). Structure optimization of vibrating feeder based on inertia release. Shock and Vibration, 2021, 1-13. <https://doi.org/10.1155/2021/8830882>
17. Chandravanshi, M. L., & Mukhopadhyay, A. K. (2017). Analysis of variations in vibration behavior of vibratory feeder due to change in stiffness of helical springs using FEM and EMA methods. Journal of the Brazilian Society of Mechanical Sciences and Engineering, 39, 3343-3362. <https://doi.org/10.1007/s40430-017-0767-z>
18. Oraon, S., Chandravanshi, M. L., & Bajpai, V. (2019). Diagnosis check in the Vibratory Feeder unit using FEA technique. Materials Today: Proceedings, 16, 329-335. <https://doi.org/10.1016/j.matpr.2019.05.098>
19. Yue-min, Z., Chu-sheng, L., Xiao-Mei, H., Cheng-Yong, Z., Yi-bin, W., & Zi-ting, R. (2009). Dynamic design theory and application of large vibrating screen. Procedia Earth and Planetary Science, 1(1), 776-784. <https://doi.org/10.1016/j.proeps.2009.09.123>
20. Yang, X., Wu, J., Jiang, H., Qiu, W., & Liu, C. (2019). Dynamic modeling and parameters optimization of large vibrating screen with full degree of freedom. Shock and Vibration, 2019. <https://doi.org/10.1155/2019/1915708>
21. Zhang, L. W., Yin, Z. J., Chen, B., Tang, Z. C., & Tian, Z. (2010). Dynamic Simulation and Experimental Modal Analysis of Large Vibratory Feeder. Advanced Materials

Research, 139, 2423-2426. <https://doi.org/10.4028/www.scientific.net/AMR.139-141.2423>

22. Li, C. L., He, F., Zhang, Y. Y., Gao, Y., & Gao, P. (2013). Failure analysis and structure improvement of beam of liner vibrating screen. Advanced Materials Research, 619, 69-73. <https://doi.org/10.4028/www.scientific.net/AMR.619.69>
23. Harat, R. O. (2020). Dynamic Investigation of Vibratory Screen Response in a Fem Environment. University of Pretoria (South Africa).
24. Chandravanshi, M. L. (2015). Modal Analysis of the Vibratory Feeder Unit and Its Structural Elements through Fem Technique. structure, 210, 0-3.
25. Nianqin, G., Sheng, G., & Leping, L. (2010, June). Modal characteristics and finite element analysis of screen box for ultra-heavy vibrating screen. In 2010 Third International Conference on Information and Computing (Vol. 4, pp. 284-287). IEEE. <https://doi.org/10.1109/ICIC.2010.343>
26. Peng, C. Y., & Su, R. H. (2011). Simulation applied to working frequency selection in large-scale vibrating screen's design. Journal of Coal Science and Engineering (China), 17, 439-442. <https://doi.org/10.1007/s12404-011-0416-6>
27. Ding, C. G., Song, F. Z., Song, B., & Men, X. H. (2012). The finite element analysis of vibrating screen. Applied Mechanics and Materials, 141, 134-138. <https://doi.org/10.4028/www.scientific.net/AMM.141.134>
28. Wang, Y. Y., Fu, X. H., Guo, T. T., Chen, L., & Mao, H. Q. (2010). Fatigue Life Analysis of Large-Scale Liner Vibration Screener Based on ANSYS. Applied Mechanics and Materials, 37, 466-470. <https://doi.org/10.4028/www.scientific.net/AMM.37-38.466>
29. Hou, Y. J., Fang, P., & Zeng, L. (2012). Finite element analysis of dual-frequency vibrating screen. Advanced Materials Research, 479, 2124-2128. <https://doi.org/10.4028/www.scientific.net/AMR.479-481.2124>
30. McMillan Jr, G. J. (2011). Analysis of Vibratory Equipment Using the Finite Element Method (Doctoral dissertation, University of Wisconsin--Stout).

APPENDICES

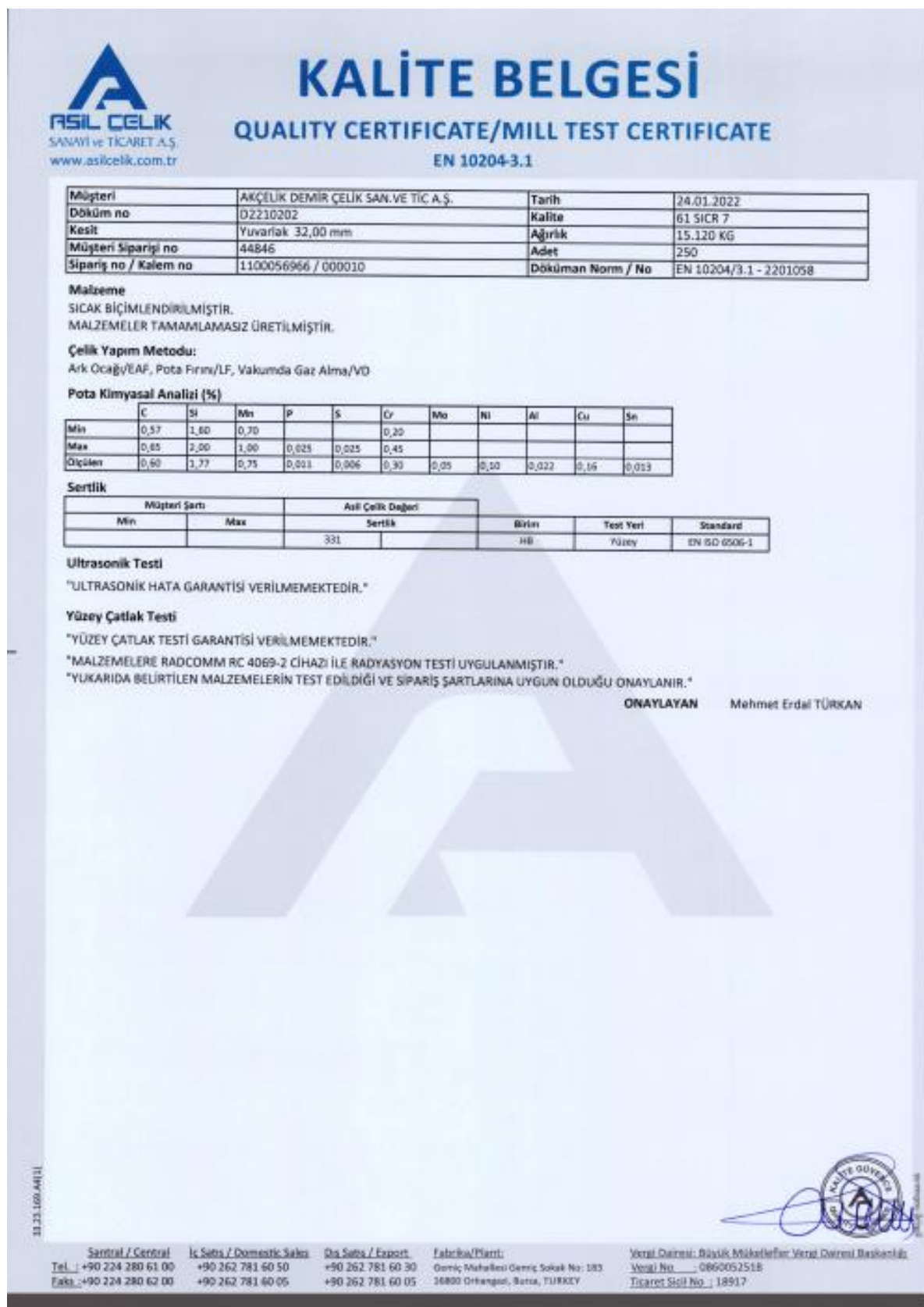


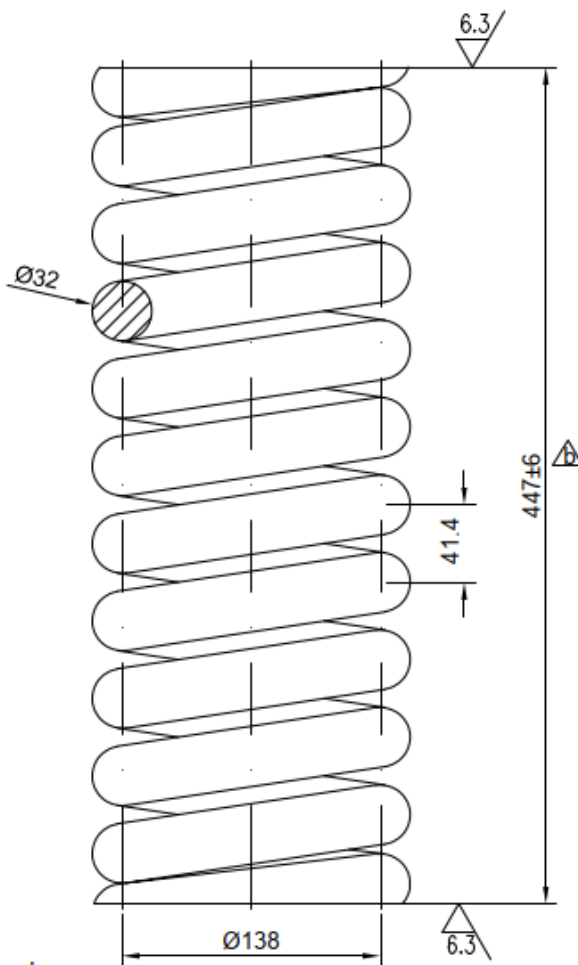
Figure A1: Quality certificate of springs

DOSYA NO.

İŞLENMİŞ YÜZELER İÇİN TOLERANS VERİLMEMİŞ ÖLÇÜLERDE MÜSAADE EDİLEBİLİR
SAPMALARI [DIN 7168-m]

ÖLÇÜ	0.5-3	3-6	6-30	30-120	120-400	400-1000	1000-2000	2000-4000	4000-8000
ML	-0.2	-0.2	-0.4	-0.6	-1.0	-1.6	-2.4	-4	-6
DELİK	+0.2	+0.2	+0.4	+0.6	+1.0	+1.6	+2.4	+4	+6
BOY	± 0.1	± 0.1	± 0.2	± 0.3	± 0.5	± 0.8	± 1.2	± 2	± 3

✓ (6.3)



NOT:
-İki Tarafı taşlanmış kapalı
-Kumlanmış
-if=9,5
-ig=11
C=422 Kg/cm

	05 / 2005	Toleranslar güncellendi.	18.04.2005	N.N.
REV.	EMİR NO.	DEĞİŞMELER	TARİH	İMZA
ÇİZEN	A.KORDE	16.12.2002		
KONTROL	S.ÖMER			
ÖLÇEK				
1/3				
EBADI:	MALZ.: SAE 9262	YAY	RS.NO. BT-12-0001-4b	TİPİ BT 140x1360
			NET Kg: 38	Brüt Kg:

Figure A2: Technical drawing of spring



ESTETİK YAY SAN. ve TİC. LTD. ŞTİ.



DENEY RAPORU

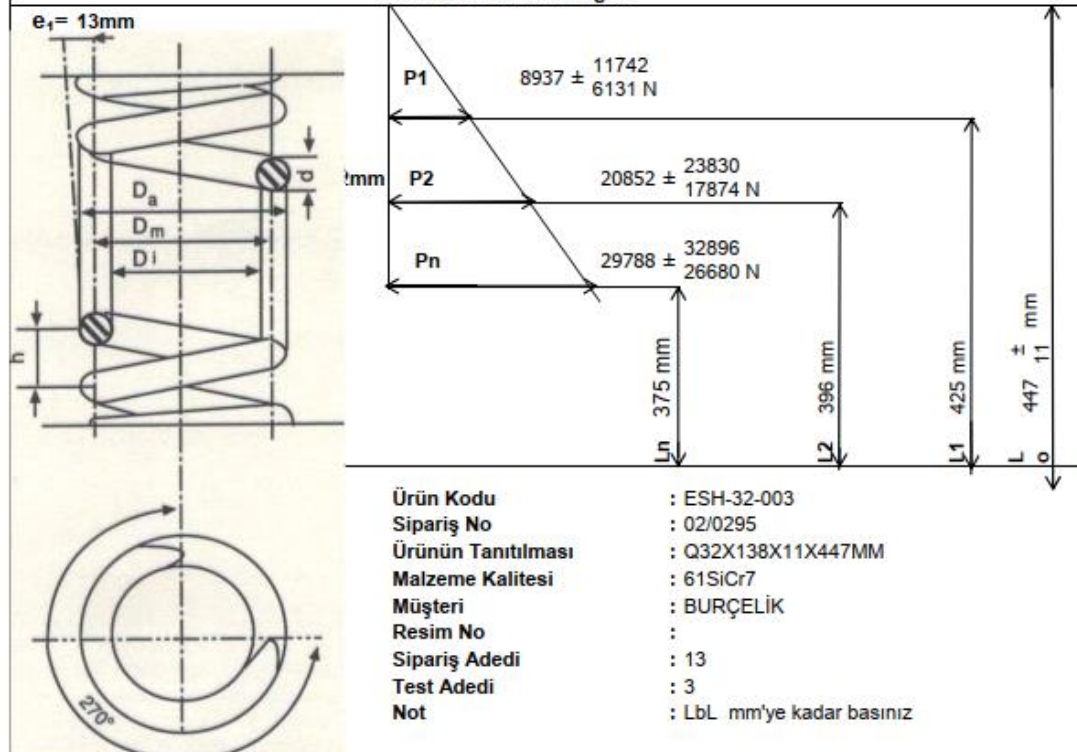
DENEY TARİHİ : 17.02.2023

DENEY STANDARTLARI :

TS 1441-1



Teorik karakteristik eğrisi



Sıra No	Yayının Çapı d mm	İç Yay Uz. Çapı Da mm	İç Yay İç Çapı Di mm	Toplam Sarım İğ	Serbest Boy Lo mm	Yüzey Sertliği H.R.C.	Statik O N	Dinamik Yük O N	Eksen kaçıklığı e1 mm	Yaylanma Miktari mm
1	32	171	107	11	449	44	9070	12	24,00	
2	32	171	107	11	451	45	10250	10	26,00	
3	32	171	107	11	451	46	9850	8	26,00	
Boya Kalınlığı :							Deney No :	T.02. 71		
Rapor Tarihi :			17.02.2023				İmza :	Tuna EZİM		
Adı ve Soyadı :				Muhsin AÇIKTEPE						

FR.08.49

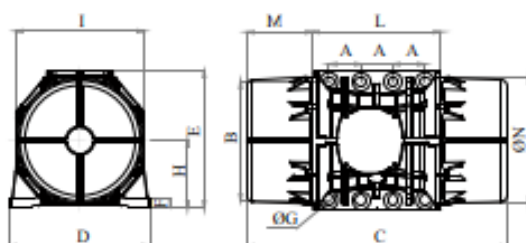
Figure A3: Experiment report of springs



MVE 19500/1E-105A0 [EE619500A5A08A0000]

3 PH - 6 kutup - 1000 d/d - 380-415 V [Delta] - 50 Hz

Çalışma momenti [Kg*cm]	Vibratör çekicileri [Kg*cm]	Santrifüj kuvveti [Kg]	Nominal voltaj [V]	Giriş gücü [kW]	Akım [A]	Güç faktörü	Ia/In
3.632	1.816	20.285	380-415 [Delta]	11,96	Δ 24	0,72	5,4



*Technical drawings are illustrative purposes only, please refer to 2D/3D drawing available on "YADEM" app. Contact us for more information.

TÜM EBATLAR [mm]													
Ağırlık [Kg]	A	B	G	Delik sayısı	C	D	E	F	H	I	L	M	N
768	140	480	45	8	1.060	570	542	48	268	510	560	250	490

TEKNİK ÖZELLİKLER							
Gres tipi			Yağlamasız	Vida	Pul	Sıkma torku [Nm]	Kablo tipi
Please refer to the label on the motorvibrator	Evet	M42	43 x 78 mm	2850	4G6 110°C	M32 110°C	

RULMAN ÖMÜR SAATLERİ				
Rulman modeli	Tip	100% Vurma Kuvveti	80% Vurma Kuvveti	50% Vurma Kuvveti
NJ 2322		6652	13996	67051

SERTİFİKASYON													
ATEX II 2 D Ex tb IIIC Tx Db IP66							IECEx Ex tb IIIC Tx Db IP66						
CLASS II DIV.2 GROUP F,G T4							IECEx						
Ex tb IIIC Tx Db IP66							IECEx						
[Tx Size Micro,10-30:100°C - Tx Size 40-91:135°C]							ETL						
CONFETO UL1004-3, UL1004-1,UL 60079-0,UL60079-31							Intertek						
CERT. CSA C22.2 No.100,CSA C22.2 No.77, CSA C22.2N.60079-0,CSA C22.2N.60079-31							CE						
T.Amb -20/+40°C							EAC						

REV.1-22/05/2019

Dimension with coarse degree of accuracy related to UNI 22768/1 Rights reserved to modify technical specifications.

Figure A4: Technical data of vibro motor

 SCAN QR CODE



ELECTRIC VIBRATORS MVE 1000 RPM OLI



> SCAN QR CODE
FOR MAINTENANCE
& INSTALLATION
DOCUMENTS

- Motors suitable for industry, chemicals, energy and environmental industries.
- From 53 kg and up to 25 T of centrifugal force.



We reserve the right to change specifications and dimensions without notice. * Working Moment = 2x static moment.

T R I P H A S E	MECHANICAL SPECIFICATIONS					ELECTRICAL SPECIFICATIONS			
	RPM	Model	Centrifugal Force	Static Moment *	Weight	Nominal Voltage	Maximal Current	Connector Type	Maximal Power
	50 Hz	Type/rpm	KG	N	kgmm	KG	V	A	Wye
1000	MVE 50/1	53	520	47,5	10	400	0,30	Y	0,12
	MVE 100/1	105	1030	94	11	400	0,30	Y	0,12
	MVE 200/1	187	1834	167,5	19	400	0,65	Y	0,15
	MVE 300/1	318	3120	284,5	26	400	0,67	Y	0,25
	MVE 500/1*	513	5033	459,5	34	400	1,22	Y	0,55
	MVE 800/1	767	7524	687	60	400	1,42	Y	0,75
	MVE 1100/1	1048	10281	938,5	78	400	1,42	Y	0,75
	MVE 1500/1	1590	15598	1424	84	400	1,80	Y	0,9
	MVE 1600/1	1673	16412	1498	90	400	2,40	Y	0,9
	MVE 2100/1	2083	20434	1865,5	105	400	3,00	Y	1,5
	MVE 2200/1	2239	21965	2005	107	400	3,00	Y	1,5
	MVE 2600/1	2610	25604	2337	146,5	400	4,10	Y	1,96
	MVE 3000/1	3017	29597	2701,5	155	400	4,50	Y	2,2
	MVE 3700/1	3797	37249	3512,5	159	400	4,50	Y	2,2
	MVE 3800/1	3799	37268	3402	216	400	5,50	Y	2,5
	MVE 4700/1	4681	45921	4191,5	220	400	6,50	Y	3,2
	MVE 5200/1*	5228	51287	4682	236	400	6,50	Y	3,2
	MVE 6500/1	6506	63824	5826	288	400	7,76	Y	4,3
	MVE 8000/1*	8018	78657	7180	309	400	12,60	Y	5,5
	MVE 9000/1*	8936	87662	8002	322	400	13,20	Y	6,2
	MVE 10000/1*	9986	97963	8942	374	400	14,00	Y	6,1
	MVE 11400/1	11485	112668	10284,5	404	400	13,00	Y	6,4
	MVE 13000/1*	12904	126588	11555	411	400	17,20	Y	8
	MVE 12000/1	12580	123410	11265	522	400	15,00	Y	8
	MVE 15000/1	14706	144266	13170	672	400	18,00	Y	10,1
	MVE 17500/1	17980	176384	16100	744	400	21,00	Y	11,9
	MVE 19500/1	20285	198996	18160	768	400	24,00	V	12
	MVE 22000/1	22711	222795	20335	916	400	28,00	Y	13,9
	MVE 25000/1	25532	250469	22860	994	400	28,00	Y	13,9

*These Models have several revisions to improve their performance that may explain the disparity with your own data.
Consult us directly if necessary.

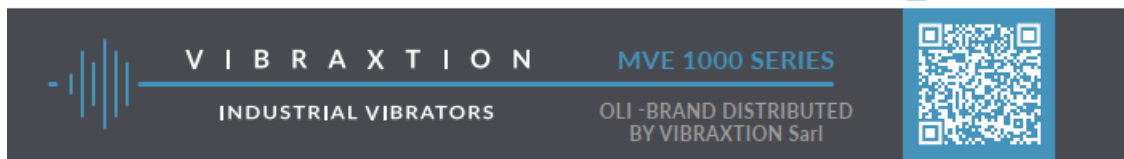
VIBRACTION SARL, 342 Chemin du Sermoraz 01700 BEYNOST - Tel. 04 37 86 12 09 - info@vibraxtion.fr

23

The technical information, diagrams and images present in this document are the exclusive property of Vibraxtion Sarl. Any reproduction is prohibited. This information is non-contractual.
Improper use of the equipment can cause damage or injury.

Figure A5: Technical data of vibro motor

 SCAN QR CODE



ELECTRIC VIBRATORS MVE 1000 RPM OLI

We reserve the right to change specifications and dimensions without notice.

Model	DIMENSIONS (mm)													Fig.
	A	B	C	D	E	F	ØG	H	I	L	M	N		
MVE 50/1	-	-	-	-	-	-	-	-	-	-	-	-	-	-
	80	110					11							
	90	125					13							
	124	110	274	150	173	15	11	79	150	166	52	134		1
MVE 100/1	80	110					11							
	90	125					13							
	124	110	304	150	173	15	11	79	150	166	67	134		1
	105	140	330	170	196	20	13	92	174	166	78	160		2
MVE 200/1	120	170	391	208	210	22	17	96	185	192	97	170		2
MVE 300/1	120	170	455	208	210	22	17	96	185	192	129	170		2
MVE 500/1*	120	170	455	230	260	26	17	124	240	218	112	222		2
MVE 800/1	140	190	446	230	260	26	17	124	240	218	134	222		2
MVE 1100/1	140	190	490	230	260	26	17	124	240	218	134	222		2
MVE 1500/1	140	190	566	230	260	26	17	124	240	218	172	222		2
MVE 1600/1	155	225	563	275	290	30	22	140	256	250	154	236		2
MVE 2100/1	155	225	623	275	290	30	22	140	256	250	184	236		2
MVE 2200/1	155	225	623	275	290	30	22	140	256	250	184	236		2
MVE 2600/1	155	255	692	304	314	30	23.5	147	285	277	205	265		2
MVE 3000/1	155	255	692	304	314	30	23.5	147	285	277	205	265		2
MVE 3700/1	155	255	734	304	314	30	23.5	147	285	277	226	265		2
MVE 3800/1	180	280	683	332	354	32	26	170	330	312	183	311		2
MVE 4700/1	180	280	733	332	354	32	26	170	330	312	208	311		2
MVE 5200/1*	180	280	733	332	354	32	26	170	330	312	208	311		2
MVE 6500/1	200	320	704	385	402	40	28	203	394	360	170	378		2
MVE 8000/1*	200	320	774	385	402	40	28	203	394	360	205	378		2
MVE 9000/1*	200	320	774	385	402	40	28	203	394	360	205	378		2
MVE 10000/1*	125	380	908	452	415	40	39	205	394	380	260	378		3
MVE 11400/1	125	380	908	452	415	40	39	205	394	380	260	378		3
MVE 13000/1*	125	380	948	452	415	40	39	205	394	380	280	378		3
MVE 12000/1	140	440	1020	530	484	37	45	232	446	470	275	424		4
MVE 15000/1	140	480	980	570	542	48	45	268	510	560	210	490		5
MVE 17500/1	140	480	1060	570	542	48	45	268	510	560	250	490		5
MVE 19500/1	140	480	1060	570	542	48	45	268	510	560	250	490		5
MVE 22000/1	140	520	1130	610	594	42	45	297	560	560	285	530		5
MVE 25000/1	140	520	1130	610	594	42	45	297	560	560	285	530		5

**These Models have several revisions to improve their performance that may explain the disparity with your own data.
Consult us directly if necessary.

The technical information, diagrams and images present in this document are the exclusive property of Vibraction Sarl. Any reproduction is prohibited. This information is non-contractual.
Improper use of the equipment cannot engage Vibraction Sarl.

Figure A6: Technical data of vibro motor

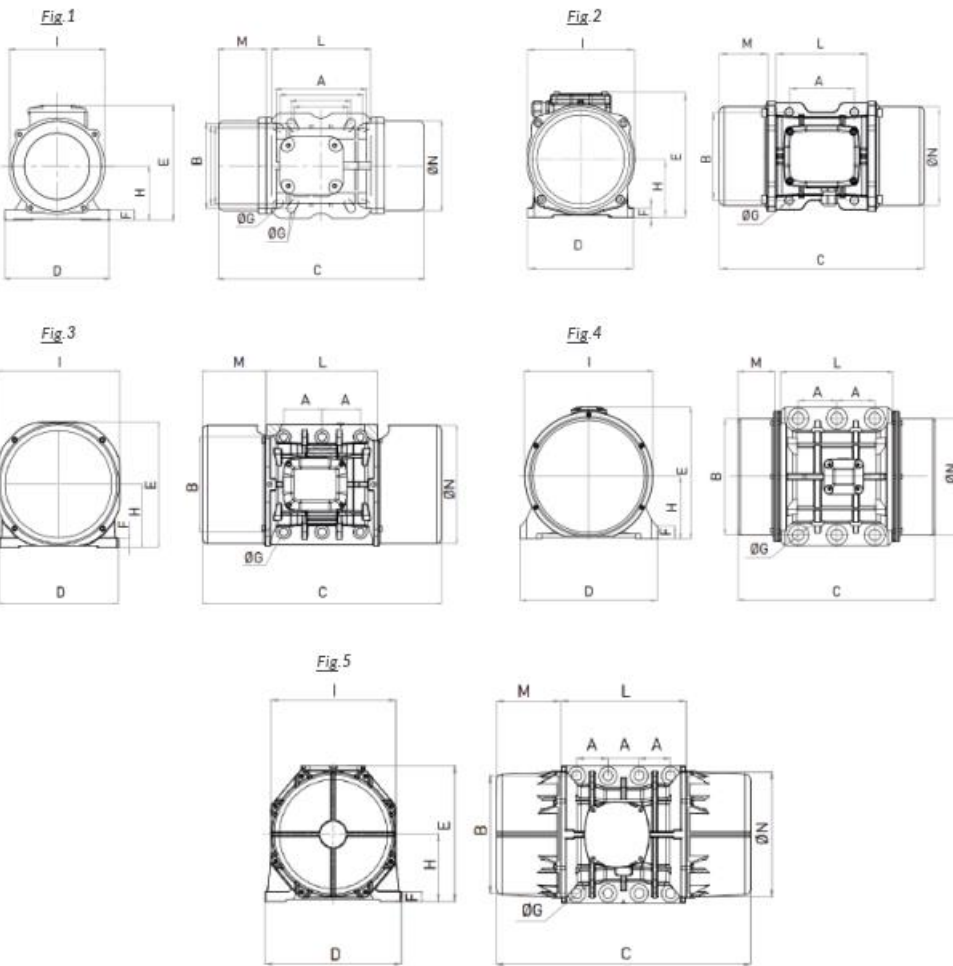
 SCAN QR CODE



VIBRAXTION
INDUSTRIAL VIBRATORS

MVE 1000 SERIES
OLI - BRAND DISTRIBUTED
BY VIBRAXTION Sarl

ELECTRIC VIBRATORS MVE 1000 RPM OLI



We reserve the right to change specifications and dimensions without notice.

VIBRAXTION SARL, 342 Chemin du Sermoraz 01700 BEYNOST - Tél. 04 37 86 12 09 -  info@vibraxtion.fr

25

The technical information, diagrams and images present in this document are the exclusive property of Vibraxtion Sarl. Any reproduction is prohibited. This information is non-contractual.
Improper use of the equipment can not engage Vibraxtion Sarl.

Figure A7: Technical data of vibro motor